GABRIELA TORRES DA SILVA

CARACTERIZAÇÃO MORFOANATÔMICA, TRANSCRIPTÔMICA E ESTUDO DA AQUISIÇÃO DE COMPETÊNCIA PARA A ORGANOGÊNESE *IN VITRO* DE ESPÉCIES DO GÊNERO *MELOCACTUS* (CACTACEAE)

Tese apresentada à Universidade Federal de Viçosa, como parte das exigências do Programa de Pós-Graduação em Fisiologia Vegetal, para obtenção do título de *Doctor Scientiae.*

VIÇOSA
MINAS GERAIS – BRASIL
2019

Ficha catalográfica preparada pela Biblioteca Central da Universidade Federal de Viçosa - Câmpus Viçosa

T
S586c
2019

Silva, Gabriela Torres da, 1988-
Caracterização morfoanatômica, transcriptômica e estudo da aquisição de competência para a organogênese *in vitro* de espécies do gênero *Melocactus* (Cactaceae) / Gabriela Torres da Silva. – Viçosa, MG, 2019.
xiv, 146 f. : il. (algumas color.) ; 29 cm.

Orientador: Wagner Campos Otoni.
Tese (doutorado) - Universidade Federal de Viçosa.
Inclui bibliografia.

1. Cactos - Propagação in vitro. 2. Tecidos vegetais - Cultura e meios de cultura. 3. Expressão gênica. I. Universidade Federal de Viçosa. Departamento de Biologia Vegetal. Programa de Pós-Graduação em Fisiologia Vegetal. II. Título.

CDD 22. ed. 583.56

GABRIELA TORRES DA SILVA

CARACTERIZAÇÃO MORFOANATÔMICA, TRANSCRIPTÔMICA E ESTUDO DA AQUISIÇÃO DE COMPETÊNCIA PARA A ORGANOGÊNESE *IN VITRO* DE ESPÉCIES DO GÊNERO *MELOCACTUS* (CACTACEAE)

Tese apresentada à Universidade Federal de Viçosa, como parte das exigências do Programa de Pós-Graduação em Fisiologia Vegetal, para obtenção do título de *Doctor Scientiae.*

APROVADA: 20 de fevereiro de 2019.

Aristéa Alves Azevedo

Diego Silva Batista

Lorena Melo Vieira

Lyderson Facio Viccini
(Coorientador)

Wagner Campos Otoni
(Orientador)

A minha mãe Rubi, que
"me deu ao mundo de maneira singular
me dizendo a sentença
para eu sempre pedir licença,
mas nunca deixar de entrar".
(Caetano Veloso)
Dedico

"Descobri como é bom chegar quando se tem paciência. E para chegar, onde quer que seja, aprendi que não é preciso dominar a força, mas a razão. É preciso, antes de tudo, querer."

(Amyr Klimk)

AGRADECIMENTOS

Ao Programa de Pós-Graduação em Fisiologia Vegetal da Universidade Federal de Viçosa (UFV) pela oportunidade de realizar desta especialização.

Ao Conselho Nacional de Desenvolvimento Científico e Tecnológico (CNPq) pela concessão da bolsa de doutorado. A Coordenação de Aperfeiçoamento de Pessoal de Nível Superior (CAPES) pela concessão da bolsa de doutorado sanduíche. A Fundação de Amparo à Pesquisa do Estado de Minas Gerais (FAPEMIG) pelo auxílio financeiro para realização deste trabalho.

Ao prof.º Wagner Campos Otoni pela orientação, paciência, compreensão e apoio. Por ter acolhido a proposta de trabalhar com cactos de braços abertos e por ter contribuído com seus conhecimentos. Obrigada pela confiança e por todos os ensinamentos.

Ao prof.º Lyderson Facio Viccini por disponibilizar o Laboratório de Genética e Biotecnologia (LGB) da Universidade Federal de Juiz de Fora para realização das análises de citometria de fluxo. Obrigada por ter acolhido a proposta, pela coorientação e por todas as contribuições.

A Dr. Andréa Dias Koehler pela coorientação, dedicação e apoio no delineamento e execução dos experimentos. Obrigada pelo acolhimento, pela parceria na adequação dos protocolos, e por todas as ideias que contribuiram muito para a qualidade deste trabalho.

A prof.ª Sheila Resende por ter um dia me apresentado aos cactos, pela coorientação e apoio. Obrigada por todos os ensinamentos de vida e profissionais, pela disponibilidade e palavras de incentivo.

Ao Dr. Diego Silva Batista por estar sempre disponível para tirar dúvidas, pelo auxílio nos delineamentos e apoio na execução das análises. Obrigada pelas palavras de incentivo e pelos conselhos.

A prof.ª Chelsea Dvorak Specht por ter acolhido a proposta de doutorado sanduíche, por ter disponibilizado o Specht Lab e se empenhado em encontrar os caminhos para a execução da montagem do transcriptoma na Universidade de Cornell.

A prof.ª Ana Maria Almeida por ter me apresentado ao prof.º Wagner Otoni e à prof.ª Chelsea Specht. Por todo apoio na realização da proposta do transcriptoma e pelo auxílio nas análises de expressão diferencial.

A RAPiD Genomics LLC, em especial ao Leandro Gomide, por disponibilizar todas as informações necessárias nas etapas que antecederam e sucederam o sequenciamento do RNA para o transcriptoma.

Ao Boyce Thompson Institute, e em especial a Dr.ª Susan Strickler, por ter armazenado os dados do sequenciamento em seus servidores e por todo o apoio na parte bioinformática da montagem, checagem da qualidade e análises de expressão diferencial do transcriptoma.

Ao Centro Nacional de Pesquisa em Energia e Materiais (CNPEM) e ao Laboratório Nacional de Nanotecnologia (LNNano) pela execução das análises de Microtomografia de Raio-X. Em especial, ao Dr. Caio Gomide Otoni pelo apoio na preparação das amostras e análises dos dados.

Ao Laboratório de Anatomia Vegetal da UFV por ter disponibilizado todo o material e equipamentos para a realização das análises anatômicas e testes histoquímicos. Em especial, a Aurora, Rosana, Miller, Luana e prof. ª Marília.

A todos que fazem ou já fizeram parte do Laboratório de Cultuda de Tecidos II da UFV nesses quatro anos de trabalho, pelos momentos de alegria e bom convívio. Em especial, a Duanny Caproni, Wellington Soares, Sérgio Felipe, Ludmila Correia, Tatiane Silva, Amanda Mendes, Evandro Fortin, Anyela Ríos, Daniele Vidal, Kamila Mota, Lorena Vieira, Kristiano Chagas e Ana Cláudia pelas contribuições e ensinamento. A dona Elci e dona Terezinha pelo apoio e pelas boas conversas.

A todos do LGB pelo auxílio nas análises. Em especial, ao Elyabe Matos pela enorme ajuda com as análises de citometria de fluxo, por cuidar das plantas, e pela acolhida nas minhas idas à Juiz de Fora.

Ao Laboratório de Cultura de Tecidos Vegetais da Universidade Federal da Bahia por ter concedido as primeiras plantas para o início dos experimentos, e por fornecer as

plantas germinadas em 2008 para a realização dos experimentos de citometria de fluxo.

Ao Irmão Delmar Alvim pela ajuda nas coletas de campo em Morro do Chapéu. Pelo seu papel como ativista ambiental, zelando pelo Parque Estadual de Morro do Chapéu. Obrigada pela gentileza e solicitude.

A todos os colegas da PPG em Fisiologia Vegetal pelos momentos de convívio e aprendizagem. Em especial, a Duanny Caproni e Vanessa Rosa pela amizade, apoio, carinho e atenção.

As(os) amigas(os) Bianca Nespoli, Camila Chagas, Cândia Paixão, Gabriela Lima e Victor Trafani que tornaram Viçosa um lugar muito além da UFV.

Ao Coral da UFV pela oportunidade de cantar, integrar e descontrair. Em especial a Andréa Bastos, Fred Augusto, Letícia Rocha e Marco Schiavo pela amizade, carinho e cuidado.

Ao Grupo de Estudos Budistas Bodisatva e Grupo de Estudos em Mindfulness do Departamento de Medicina e Enfermagem da UFV, em especial ao prof.º Leandro David, pelo acolhimento e apoio.

Ao Grupo Entre Folhas, em especial Alessandra Aziz, pelo apoio e por mostrar os novos caminhos. Ao Dr. Evandro Oliveira cujas palavras foram verdadeiros remédios.

Aos companheiros de casa, Andréa Bastos, Fred Augusto, Jônatas Pedro e Lola pelo companheirismo, bom convívio e momentos de descontração.

Aos amigos que me acompanharam na minha tragetória antes de chegar em Viçosa. Aos colegas da graduação Rafael Miranda, Camila Saraiva, Maíra Miele, Leonídia Serreti e Débora Santedicola pela presença forte em minha vida. A Cintia Régia e Sarah Diana pelo carinho e bons conselhos. Aos amigos de Porto Seguro Nathalie Serra, Qézia Cristina, Grazielle Lisandra, Patrícia Orrico, Joelma Brito, Edilson Dias e Marina Brito pelo apoio e cuidado.

Aos meus afilhados Júlia, Felipe e Theo por serem minha fonte de alegria e renovação de energia!

Por fim, aqueles que as palavras não conseguirão expressar toda a minha gratidão:

A família Torres pelo apoio e amor incondicional. Em especial as mulheres desta família, exemplos de força e perseverança: minha avó Dete, minha mãe, tia Ivana, tia Meyre, tia Neide e tia Rai. As minhas primas Mariana, Renata e Melissa. A minha cunhada Gabriela por ser sempre tão companheira e prestativa. Ao meu primo Francisco, a quem tenho muita admiração.

Ao meu irmão, Moiseis, pela parceria de vida, por compatilhar sonhos e ser uma presença viva mesmo com toda a distância. Obrigada por me ajudar nas coletas em Morro do Chapéu e também por ser tão criativo e prestativo com as imagens das pranchas.

A minha família Silva. Ao meu pai, que com seu exemplo de luta me inspira. A vó Berna e tio Renato. Minha família de São Paulo, tia Luci, Joyce e Sheila. Aos ausentes, que se foram antes de dividir comigo esta alegria, Tio Rai e Renatinho.

BIOGRAFIA

Filha de Ronaldo Batista da Silva e Rubenilde Marques Torres, natural de Salvador-BA. Ingressou na Universidade Federal da Bahia (UFBA) em 2007, onde obteve o título de Licenciada em Ciências Biológicas em 2011. Foi estagiária do Laboratório de Cultura de Tecidos Vegetais da UFBA de 2009 a 2014, atuando no Banco Ativo de Germoplasma (BAG) como responsável pela manutenção da coleção *ex vitro* e *in vitro* de espécies da família Cactaceae. Em 2012, ingressou no Programa de Pós-Graduação (PPG) em Genética e Biodiversidade da UFBA, onde desenvolveu trabalhos com marcadores moleculares de diversidade na caracterização do BAG *in vitro* e na micropopagação de espécies do gênero *Melocactus* (Cactaceae), obtendo o título de *Magister Scientiae* em 2014. Nesta mesma instituição, atuou como coordenadora da Semana de Biologia, da Semana de Seminários do PIBIC e como representante discente da PPG. Foi professora substituta do Departamento de Biologia Geral da UFBA de 2013 a 2014, onde ministrou aulas para turmas de Oceanografia, Educação Física e Medicina Veterinária. Em 2015, ingressou no Programa de Pós-Graduação em Fisiologia Vegetal, onde desenvolveu atividades de pesquisa no Laboratório de Cultura de Tecidos II (BIOAGRO), atuando na otimização da propagação *in vitro* de espécies do gênero *Melocactus.* Entre outubro de 2017 e abril de 2018 esteve em treinamento sanduíche, onde desenvolveu atividades na Universidade de Cornell (Ithaca, NY, EUA). Submeteu-se à defesa de tese no dia 20 de fevereiro de 2019.

SUMÁRIO

RESUMO

TORRES- SILVA, Gabriela, D.Sc., Universidade Federal de Viçosa, fevereiro de 2019. **Caracterização morfoanatômica, transcriptômica e estudo da aquisição de competência para a organogênese *in vitro* de espécies do gênero *Melocactus* (Cactaceae).** Orientador: Wagner Campos Otoni. Coorientadores: Andréa Dias Koehler, Lyderson Facio Viccini e Sheila Vitória Resende.

O Brasil é área prioritária na conservação da família Cactaceae por possuir grande número de espécies endêmicas. No entanto, fatores como degradação do habitat e coleta ilegal para comercialização como ornamental tem levado algumas espécies dessa família ao perigo de extinção, dentre estas espécies estão *Melocactus paucispinus* e *M. glaucescens*. Neste contexto, as técnicas de cultura de tecidos são uma importante ferramenta, pois permitem a propagação *in vitro* de material vegetal em larga escala, fornecendo uma alternativa à retirada dos indivíduos do seu habitat para a comercialização como ornamental. Contudo, a propagação *in vitro* de *Melocactus* apresenta alguns desafios, como o baixo número de brotos por explante, de brotos com variação morfológica e a ocorrência de variação somaclonal. Apesar do crescente interesse dos *Melocactus* como ornamental e da sua forma de propagação *in vitro* ser via cladódio, pouco se sabe sobre os aspectos morfofisiológicos relacionados à aquisição de competência para a organogênese *in vitro* dos membros deste gênero. Com o objetivo de aumentar o conhecimento sobre os processos da organogênese em espécies do gênero *Melocactus,* foi realizada a caracterização anatômica do cladódio de *M. glaucescens* e *M. paucispinus,* assim como a análise da ploidia das regiões do cladódio e a microtomografia de raio-X. As duas espécies de *Melocactus* estudadas apresentaram o mesmo padrão de organização dos tecidos e picos de ploidia, onde a periferia do cladódio e a medula apresentaram quatro picos de ploidia (2C, 4C, 8C e ~16C), as raízes são diploides e o córtex do cladódio apresentou um pico a mais de ploidia (~32C). A mixoploidia do cladódio foi atribuída ao programa de formação dos diferentes tecidos que compõem este órgão, o qual possui como uma das principais funções o armazenamento de água. As células com alta ploidia passaram por endociclos que aumentaram seus conteúdos de DNA, o que permite que o volume de armazenamento de água nos vacúolos seja maior para que assim possam desempenhar sua função de parênquima aquífero. A análise de microtomografia de raio-X mostrou que o diâmetro das células da região do córtex é maior do que na periferia e na medula

do cladódio, corroborando com os dados de ploidia. Para compreender as modificações anatômicas durante a organogênese de *M. glaucescens*, foi realizada a caracterização anatômica de explantes cultivados na ausência de regulador de crescimento e explantes cultivados na presença de 1,34 µM de ácido naftaleno acético (ANA), 17,76 µM de 6-benzilaminopurina (BA) e com as aréolas feridas. Além disso, foi realizada a análise de expressão do gene *SOMATIC EMBRYOGENESIS RECEPTOR-LIKE KINASE* (*MgSERK*-like) nos mesmos tratamentos. Foi observada a formação de brotações derivadas da ativação da região meristemática das aréolas, assim como de regiões mais internas do cladódio, sendo que mais meristemoides foram observados no córtex dos explantes que foram submetidos à ação de reguladores de crescimento e ferimento. Este tratamento também mostrou elevado número de brotações, ocorrência de variação morfológica e expressão do gene *MgSERK*-like em todos os períodos analisados da organogênese. Alterações no padrão de expressão durante a organogênese *in vitro* também foram observadas nas análises de expressão diferencial (ED) de explantes antes e após a indução de organogênese na presença de 1,34 µM de ANA, 17,76 µM de BA e com as aréolas feridas. A análise do transcriptoma mostrou que os explantes antes da indução da organogênese apresentavam o metabolismo mais comprometido com o metabolismo primário, principalmente com a fotossíntese, além da alta expressão do fator de transcrição TCP, o qual é responsável pela forte dominância apical nessa espécie que não apresenta ramificações laterais naturalmente. As análises no Gene Ontology, Kyoto Encyclopedia of Genes and Genomes, BiNGO e Plant Transcription Factor Database demonstram que o metabolismo nos explantes submetidos à organogênese é modificado e concentrado em genes relacionados com mitocôndria, parede celular, retículo endoplasmático, organização celular e biogênese, o que tem relação com o aumento da síntese de proteínas para dar suporte na divisão celular e formação de parede durante a regeneração. As análises de ED também indicam que os tecidos submetidos à organogênese apresentaram grande potencial na produção de compostos do metabolismo secundário, o que amplia as possibilidades de aplicação das culturas *in vitro* de *M. glaucescens.*

ABSTRACT

TORRES- SILVA, Gabriela, D.Sc., Universidade Federal de Viçosa, February, 2019. **Morphoanatomic characterization, transcriptomic and study of the acquisition of competence for the *in vitro* organogenesis of species of the genus *Melocactus* (Cactaceae).** Advisor: Wagner Campos Otoni. Co-advisors: Andréa Dias Koehler, Lyderson Facio Viccini and Sheila Vitória Resende.

Brazil is a priority area in the conservation of the Cactaceae family due its large number of endemic species. However, factors such as habitat degradation and illegal collection for commercialization as ornamental have taken some species of this family to the danger of extinction, among which are *Melocactus paucispinus* and *M. glaucescens*. In this context, tissue culture techniques are an important tool as they allow *in vitro* propagation of plant material on a large scale, providing an alternative to overharvesting for marketing as ornamental. However, the *in vitro* propagation of *Melocactus* presents some challenges, such as the low number of shoots per explant, shoots with morphological variation and the occurrence of somaclonal variation. Although the growing interest of *Melocactus* as ornamental and its *in vitro* propagation be via cladode, the knowledge about the morphophysiological aspects related to the acquisition of competence for the *in vitro* organogenesis in this species is limited so far. In order to increase the knowledge about organogenesis processes of *Melocactus* species, the anatomical characterization of *M. glaucescens* and *M. paucispinus* cladodium, as well as the ploidy of the cladode regions and X-ray micro-computed tomography (XRμCT) were performed. Both *Melocactus* species have the same pattern of tissue organization and ploidy peaks, where the cladode periphery and the pith presented four ploidy peaks (2C, 4C, 8C and ~16C), the roots are diploid and the cortex of the cladode showed an additional peak of ploidy (~32C). The mixoploidy of cladode was attributed to the formation program of the different tissues that compose this organ, which has as one of the main functions the water storage. The cells with higher ploidy passed through the endocycle, which increased their DNA contents, allowing the volume for water storage in the vacuoles to be larger so that they can perform their function as aquifer parenchyma. XRμCT analysis showed the cell lumen of the cortex region was larger than the periphery and pith of the cladode. In order to understand the anatomical changes during the organogenesis of *M. glaucescens*, anatomical characterization of explants cultivated in medium without plant growth regulator (PGR) and explants

cultivated in the presence of 1.34 μM naphthalene acetic acid (ANA), 17.76 μM 6-benzylaminopurine (BA) and wounded areolas. In addition, expression analysis of the *SOMATIC EMBRYOGENESIS RECEPTOR-LIKE KINASE* (*MgSERK-like*) gene was performed in the same treatments. The formation of shoots derived from the activation of the areolas meristematic region, as well as innermost regions of cladode, was observed, and more meristemoids were observed in the cortex of the explants that were submitted to PGR and wounding. This treatment also showed a higher number of shoots, morphological variation and expression of the *MgSERK-like* gene in all periods when the organogenesis was analyzed. Changes in the expression pattern during *in vitro* organogenesis were also observed in the analyses of differential expression (DE) of explants before and after the organogenesis induction in the presence of NAA 1.34 μM, BA 17.76 μM and wounded areolas. The differential transcriptome analysis showed that the metabolism of the explants before the organogenesis induction was compromised with the primary metabolism, mainly with the photosynthesis, besides the high expression of the transcription factor TCP, which is responsible for the strong apical dominance in this species, which does not have lateral branches naturally. Gene Ontology, Kyoto Encyclopedia of Genes and Genomes, BiNGO, and Plant Transcription Factor Database analyses demonstrate that metabolism in explants submitted to organogenesis is modified and concentrated in genes related to mitochondria, cell wall, endoplasmic reticulum, cell organization and biogenesis, which is related to the increase of protein synthesis to support cell division and formation of cell wall during regeneration. DE analyzes also indicate that tissues submitted to organogenesis present great potential in the production of secondary metabolism compounds, which increases the possibilities of application of *M. glaucescens in vitro* cultures.

INTRODUÇÃO GERAL

O Brasil representa o terceiro maior centro de diversidade da família Cactaceae, sendo considerada área prioritária de conservação, devido a singularidade que as espécies possuem em termos de gêneros e endemismo (Zappi et al. 2011).

O gênero *Melocactus* (L.) Link & Otto pertence à tribo Cereae e apresenta ampla distribuição, estendendo-se do oeste do México, em direção ao sul do Peru, através da Amazônia e o leste do Brasil (Das & Mohanty 2008). Das 37 espécies reconhecidas de *Melocactus,* o Brasil abriga 27 espécies e subspécies, das quais 26 espécies e subespécies ocorrem exclusivamente neste país, sendo 25 delas endêmicas do leste do Brasil (Taylor & Zappi 2004, Machado 2009).

O gênero *Melocactus* consiste principalmente em cactos de pequeno a médio porte e globosos, com caule altamente especializado chamado de cladódio. São invariavelmente plantas monocaules, uma vez que apresentam ramificações apenas se tiverem sofrido injúria (Das & Mohanty 2008, Machado 2009). O cladódio é dividido em costelas (Figura 1), com epiderme cutinizada (ácidos graxos polimerizados), e essa cutina é responsável pela cor glauco (verde-azulado, verde da cor do mar), esbranquiçada ou até azulada dos cladódios (Anderson 2001). O córtex representa a maior massa do cladódio, dividido em uma parte especializada na fotossíntese, o clorênquima, e outra parte que serve para reservatório de água, o parênquima aquífero (Anderson 2001).

Figura 1. *Melocactus paucispinus* G. Heimen & R. J. Paul (Cactaceae).

Em *Melocactus,* as gemas axilares desenvolvem um indumento com tricomas multicelulares que surgem do meristema axilar (aréola) e as folhas são transformadas em espinhos (Figura 1) (Mauseth 2017). As aréolas são geralmente em pouco número e bem espaçadas ao longo das costelas (Machado 2009). Todavia, a característica que mais distingue os *Melocactus* da maioria dos outros cactos é o cefálio, uma estrutura reprodutiva localizada no ápice do cladódio (Figura 1) (Das & Mohanty 2008, Machado 2009). Esta estrutura é responsável pelo nome vulgar "cabeça-de-frade" ou "coroa-de-frade" dado às espécies desse gênero (Machado 2009).

Atualmente, 14 espécies do gênero *Melocactus* aparecem nas principais listas de espécies ameaçadas de extinção (Zappi et al. 2011). Fatores como endemismo, degradação do habitat e coleta ilegal para comercialização como ornamental, têm levado algumas espécies desse gênero ao perigo de extinção (Zappi et al. 2011), entre as quais estão *Melocactus glaucescens* Buining & Brederoo e *M. paucispinus* G. Heimen & R. J. Paul.

Dentre as estratégias de conservação de espécies ornamentais, a cultura de tecidos se destaca por permitir a propagação *in vitro* de material vegetal em larga escala, com altas taxas de multiplicação em curto período, espaço reduzido e livre de patógenos, acelerando o crescimento das plantas (Malda et al. 1999, Rojas-Aréchiga & Vázquez-Yanes 2000). Esta estratégia possibilita uma alternativa à retirada dos indivíduos do seu habitat para a comercialização como ornamental e consequentemente reduz as pressões sobre as populações naturais (Malda et al. 1999, Estrada-Luna et al. 2008).

Contudo, a propagação *in vitro* de *Melocactus* apresenta alguns desafios. Torres-Silva et al. (2018), ao avaliarem os efeitos dos reguladores de crescimento ácido naftaleno acético (ANA) e 6-benzilaminopurina (BA), visando estabelecer um protocolo para a propagação de *M. glaucescens*, observaram que a presença do BA, apesar de ter favorecido um maior número de brotações, levou a formação de brotos com variação morfológica. Além disso, esses autores observaram variação somaclonal em brotos oriundos de explantes submetidos à organogênese na presença e ausência de reguladores de crescimento.

Apesar do crescente interesse dos *Melocactus* como ornamental e da sua forma de propagação *in vitro* ser via cladódio, existem poucos estudos que visam compreender a anatomia e citologia de seus tecidos. Atualmente existem somente três estudos anatômicos (Arruda et al. 2004, Arruda et al. 2005, Arruda & Melo-de-Pinna 2010) e três estudos citológicos das espécies desse gênero (Das et al. 1998a, Das et al. 1998b, Assis et al. 2003).

Além da falta de conhecimento sobre a organização dos tecidos de *Melocactus,* pouco se sabe sobre os eventos morfofisiológicos que estão envolvidos na aquisição de competência para a produção de brotos nas suas espécies. A propagação *in vitro* de espécies desse gênero, assim como para a maioria das Cactaceae, ocorre pela ativação do meristema axilar, processo chamado de ativação areolar (Pérez-Molphe-Balch et al. 2015, Lema-Rumińska and Kulus 2014). As aréolas são reconhecidas por possuirem tecido meristemático capaz de regenerar plantas inteiras através da ativação de suas células somente pelo corte ou pela adição de reguladores de crescimento nos meios de cultura (Pérez-Molphe-Balch et al. 2015, Lema-Rumińska and Kulus 2014).

Apesar da ativação areolar ser uma técnica relativamente simples, poucas espécies de cactos possuem protocolos de propagação *in vitro* bem estabelecidos, além de existirem poucos trabalhos que exploraram os aspectos anatômicos e moleculares relacionados à regeneração *in vitro* de cactos (Pérez-Molphe-Balch et al. 2015). Contudo, a ativação areolar pode ser mais complexa do que a mera aquisição de competência de células meristemáticas. Sánchez et al. (2015), por exemplo, observaram que a morfogênese de flores e brotos em *Echinocereus* ocorre em regiões internas do cladódio, como resultado do enrolamento e *looping* do meristema da aréola, causado pela camada de periderme que sela e interrompe seu crescimento.

Essa falta de informação sobre a morfogênese de espécies da família Cactaceae contribui para que ainda existam desafios básicos na propagação *in vitro* de *Melocactus*, como número reduzido de brotos por explante, alta proporção de brotos com variação morfológica e ocorrência de variação somaclonal (Torres-Silva et al. 2018). A compreensão dos eventos moleculares fundamentais na aquisição de competência na ativação areolar dos cactos pode guiar a melhoria dos protocolos de propagação de membros dessa família.

Uma abordagem útil para entender a regeneração *in vitro* é a busca de genes que podem ser marcadores de aquisição de competência. Os trabalhos mais recentes de avaliação da expressão do gene *somatic embryogenesis receptor-like kinase* (*SERK*) indicam uma ligação entre a aquisição de competência celular e a sua expressão durante a organogênese, sugerindo que esse gene seja um amplo marcador de pluripotência e um bom candidato para compreender os processos de regeneração em plantas (Sharma et al. 2008).

Outra abordagem que aumenta sobremaneira o conhecimento dos processos fisiológicos e moleculares de um organismo é o sequenciamento do conjunto completo dos seus transcritos, o transcriptoma (Xiao et al. 2013, Nadiyra et al. 2018). Os dados do transcriptoma fornecem um recurso notável para a rápida elucidação de vias biossintéticas e seu mapeamento com diagramas gráficos, além da identificação de fatores de transcrição, microRNAs, transportadores e outros (Pal et al. 2018). Além disso, o transcriptoma é uma ferramenta útil no estudo do conteúdo genético de organismos que não possuem genoma sequenciado, como é o caso da espécie não-modelo *M. glaucescens.*

Sendo assim, esta tese é composta de três capítulos que se propõem em caracterizar a morfoanatomia e estudar a aquisição de competência para a organogênese *in vitro* de espécies do gênero *Melocactus.* Para tal, foi realizada a caracterização do cladódio de duas espécies do gênero *Melocactus,* e também dos explantes de *M. glaucescens* que foram submetidos à organogênese. A aquisição da competência foi estudada com a hibridização *in situ* do putativo gene *SERK* em explantes submetidos à organogênese na ausência e presença de regulador de crescimento e ferimento. E as modificações das vias biossintéticas relacionadas à aquisição de competência para a organogênese *in vitro* de *M. glaucescens* foram acessadas com a montagem e caracterização comparativa de seu transcriptoma.

REFERÊNCIAS

Anderson, E. F. (2001). The cactus family. Timber Press, Portland, Oregon, 768p.

Arruda, E.C.P.; Alves, M.; Melo-de-Pinna, G. F. (2004). Elementos traqueais de cinco táxons de Cactaceae da caatinga pernambucana, Brasil. Acta Bot Brasilica, 18(4): 731–736. doi: 10.1590/S0102-33062004000400004

Arruda, E.; Melo-de-Pinna, G.F.; Alves, M. (2005). Anatomia dos órgãos vegetativos de Cactaceae da caatinga pernambucana. Rev Bras Bot, 28(3): 589–601. doi: 10.1590/S0100-84042005000300015

Arruda, E.; Melo-de-Pinna, G.F. (2010). Wide-band tracheids (WBTs) of photosynthetic and non-photosynthetic stems in species of Cactaceae. J Torrey Bot Soc, 137(1):16–29.

Assis, J.G.A.; Oliveira, A.L.P.C.; Resende, S.V.; Senra, J.F.V.; Machado, M. (2003). Chromosome numbers in Brazilian *Melocactus* (Cactaceae). Bradleya, 21: 1–6. doi: 10.25223/brad.n21.2003.a2

Das, A. B.; Mohanty, S.; Das, P. (1998a). Variation in karyotype and 4C DNA content in six species of *Melocactus* of the family Cactaceae. Cytologia, 63:9–16. doi: doi.org/10.1508/cytologia.63.9

Das, A.B.; Mohanty, S.; Das, P. (1998b). Interspecific variation in DNA content and chromosome analysis in *Melocactus*. Cytologia, 63: 239–247. doi: 10.1508/cytologia.63.239

Das, A. B.; Mohanty, S. (2008). Preliminary study on genetic relationships of *Melocactus* Link & Otto of the family Cactaceae revealed through karyotype, DNA content and RAPD analysis. Caryology, 61(1): 1-9. doi: 10.1080/00087114.2008.10589604

Estrada-Luna, A. A.; Martínez-Hernández, J. J.; Torres-Torres, M. E.; Chablé-Moreno, F. 2008. *In vitro* micropropagation of the ornamental prickly pear cactus *Opuntia lanigera* Salm–Dyck and effects of sprayed GA_3 after transplantation to *ex vitro* conditions. Sci Hortic, 117: 378-385. doi: 10.1016/j.scienta.2008.05.042

Lema-Rumińska, J.; Kulus, D. (2014). Micropropagation of cacti – a Review. Haseltonia, 18: 46–63. doi: 10.2985/026.019.0107

Machado, M. C. (2009). The genus *Melocactus* in eastern Brazil: part I - an introduction to *Melocactus*. British Cact Succ J, 27: 1-16.

Malda, B. G.; Backhaus, R. A.; Martin, C. (1999). Alterations in growth and crassulacean acid metabolism (CAM) activity of *in vitro* cultured cactus. Plant Cell Tissue Organ Cult, 58: 1-9. doi: 10.1023/A:1006377206855

Mauseth, J.D. (2017). An introduction to cactus areoles part II. British Cact Succ J, 89(5):219-229. doi: doi.org/10.2985/015.089.0503

Pal, T.; Padhan, J.K.; Kumar, P.; Sood, H.; Chauhan, R.S. (2018). Comparative transcriptomics uncovers differences in photoautotrophic versus photoheterotrophic modes of nutrition in relation to secondary metabolites biosynthesis in *Swertia chirayita*. Mol Biol Rep, 45:77–98. doi: nb10.1007/s11033-017-4135-y

Pérez-Molphe-Balch, E.; Santos-Díaz, M.S.; Ramírez-Malagón, R.; Ochoa-Alejo, N. (2015). Tissue culture of ornamental cacti. Sci Agric 72(6):540–561. doi: 10.1590/0103-9016-2015-0012

Rojas-Aréchiga, M. & Vázquez-Yanes, C. (2000). Cactus seed germination: a review. J Arid Environ, 44: 85-104. doi: 10.1006/jare.1999.0582

Sánchez, D.; Grego-Valencia, D.; Terrazas, T.; Arias, S. (2015). How and why does the areole meristem move in *Echinocereus* (Cactaceae)? Ann Bot, 115: 19-26. doi:10.1093/aob/mcu208

Sharma, S.K.; Millam, S.; Hein, I.; Bryan, G.J. (2008). Cloning and molecular characterisation of a potato *SERK* gene transcriptionally induced during initiation of somatic embryogenesis. Planta, 228:319-330. doi: 10.1007/s00425-008-0739-8

Taylor, N. P.; Zappi, D. C. (2004). Cacti of Eastern Brazil. Richmond, Surrey, UK: Royal Botanic Gardens, Kew.

Torres-Silva, G.; Resende, S.V.; Lima-Brito, A.; Bezerra, H.B.; D, de Santana, J.R.F.; Schnadelbach, A.S. (2018). *In vitro* shoot production, morphological alterations and

genetic instability of *Melocactus glaucescens* (Cactaceae), an endangered species endemic to eastern Brazil. S Afri J Bot, 115:100–107. doi: 10.1016/j.sajb.2018.01.001

Xiao, M.; Zhanga, Y.;Chenc. X.; Lee, E-J. et al. (2013). Transcriptome analysis based on next-generation sequencing of non-model plants producing specialized metabolites of biotechnological interest. J Biotechnol, 166(3):122-134. doi: 10.1016/j.jbiotec.2013.04.004

Zappi, D.; Taylor, N. P.; Silva, S. R.; Machado, M. C.; Moraes, E. M.; Calvente, A.; Cruz, B.; Correia, D.; Larocca, J.; Assis, J. G.; Aona, L.; Menezes, M. O. T.; Melado, M.; Marchi, M. N.; Bellintani, M.; Coelho, P.; Nahoum, P.; Resende, S. (2011). Plano de Ação Nacional para a Conservação da Cactaceae. In: Silva, S. R.; Zappi, D.; Taylor, N.; Machado, M. C. (Orgs.). Brasília: Instituto Chico Mendes de Conservação da Biodiversidade. Série Espécies Ameaçadas, n.24, 112p.

CHAPTER 1

Tissue organization and ploidy distribution in *Melocactus* species as revealed by flow cytometry, anatomy and x-ray micro-computed tomography

ABSTRACT

Cacti have a high specialized stem (cladode) that confers the capability to survive in extended dry periods. Despite the ornamental value of cacti and the main source of explants used in tissue culture techniques be the cladode, there are no studies until now that investigate their morpho-anatomical and cytological characteristics. The occurrence of mixed ploidy cell in cacti tissues and the recurrent report of morphological alteration during the cacti *in vitro* shoot production, drive this investigation to understand if *Melocactus* tissues are mixoploid, how mixoploidy is distributed throughout their tissues, and if the pattern of ploidy changes after long periods of *in vitro* culture. In order to investigate the ploidy pattern through tissues, plant of *M. glaucescens* and *M. paucispinus* germinated and cultivated *in vitro* were analyzed. Samples of topophysical longitudinal region of cladode (apical, medial and basal), and from different regions (periphery, cortex, and pith of cladode and root apexes) and ages (four and ten years of *in vitro* culture) were analyzed. Anatomical and histochemical (toluidine blue, Xylidine Ponceau, Periodic Acid Schiff, ruthenium red, and acid floroglucin), and X-ray micro-computed tomography analyzes were performed. *M. glaucescens* and *M. paucispinus* exhibit the same pattern of cell ploidy in all topophysical regions and ages and different ploidy throughout the regions. The consequence of endoreduplication in *Melocactus* cladodes is the increase of volume cell, which is observed by X-ray micro-computed tomography analysis. The low presence of support elements (i. e. sclereids and fibers) indicates that epidermis, collenchyma, wide-band tracheid presents on vascular bundles and pith, and the water stored on aquifer parenchyma are responsible for the cladode physical support. Thus, the extreme specialization of cladode allowed the cacti to use the aquifer parenchyma not just to water-storage but also to maintain the cladode shape. As revealed by flow cytometry, anatomy, and X-ray microtomography, the mixoploidy in both *Melocactus* species is not related to the age of culture, but is a developmental program characteristic, where endoclycle promote cell differentiation to perform a valuable function of accumulating water, the most restricted natural resource in the ambient where these plants occur.

Keywords: cacti, endoclycle, endoreduplication, genome size, mixoploidy.

1. INTRODUCTION

Cacti are species highly adapted to xeric environments (Anderson 2001). The vegetative body, namely cladode, is covered by a thick waxy layer of polymerized fatty acids that restrict water loss. The large substomatal chambers, which ensure gaseous exchanges shortly after the stomata opening, increasing the gas exchange efficiency (Arruda et al. 2004). The mucilage secretory structure secretes a polysaccharide which retains water, increasing the cell volume and providing the water-storage (Ventura-Aguilar et al. 2017). A significant part of the cladode consists mostly of aquifer parenchyma, which is water-storage specialized tissues (Anderson 2001, Arruda et al. 2004, Ventura-Aguilar et al. 2017).

The cladodes play an important role in taxonomy, as their colors and shapes are characteristics that distinguish cacti subfamilies and genera (Anderson 2001). Moreover, the cladode is the mostly used propagule in the vegetative propagation, which can be performed by removing their branches, or using their parts as explants in tissue culture techniques (Lema-Rumińska and Kulus 2014, Pérez-Molphe-Balch et al. 2015).

The high ornamental value of Cactaceae species has stimulated overharvesting individuals from wild populations (Pérez-Molphe-Balch et al. 2015, Goettsch et al. 2015). *Melocactus glaucescens* Buining & Brederoo and *Melocactus paucispinus* G. Heimen & R. J. Paul are endemic to Bahia state, eastern Brazil, and are listed as endangered in the Convention on International Trade in Endangered Species of Wild Fauna and Flora (CITES 2018) and in the IUCN Red List of Threatened Species (IUCN 2018).

This scenario led to the development of conservation strategies, in which *in vitro* propagation protocols have been proposed for *Melocactus* species (Resende et al. 2010, Torres-Silva et al. 2018). Tissue culture techniques represent an alternative to the conventional propagation of this genus, even though the slow growth, requiring about ten years to reach reproductive phase (Machado 2009, Lema-Rumińska and Kulus 2014, Pérez-Molphe-Balch et al. 2015).

Melocactus cladodes consist mainly of small to medium-sized stem, with globular shape and without branches (Das & Mohanty 2008, Machado 2009). For *in*

vitro shoot production of *M. glaucescens*, apical cladode segments are removed and posteriorly sectioned transversally, generating explants in disc format (Torres-Silva et al. 2018). Shoots arise from areola region in *M. glaucescens* cladode grown in culture medium with and without plant growth regulators (PGRs), which is named areola activation, being the main form of cacti propagation (Lema-Rumińska and Kulus 2014, Pérez-Molphe-Balch et al. 2015, Torres-Silva et al. 2018).

Despite the growing interest for cacti in the ornamental industry and the main form of propagation being via cladode, there are few studies focused on better understanding the tissue anatomical and cytological organization. For *Melocactus*, few studies of anatomy (Arruda et al. 2004, Arruda et al. 2005, Arruda and Melo-de-Pinna 2010), and cytogenetic are available (Das et al. 1998a, Das et al. 1998b, Assis et al. 2003).

Furthermore, a recent protocol for *in vitro* shoot production of *M. glaucescens* revealed the occurrence of morphological and genetic variation in shoots derived from culture media with and without PGRs (Torres-Silva et al. 2018). But the lack of correlation between shoots with morphological alteration and shoots with genetic variation shows the need to better understand the cytological organization of *Melocactus* cladodes. The more recent cytological characterization of cacti was performed with different tissues of *Copiapoa tenuissima*, where Lema-Rumińska (2011) revealed the occurrence of cells with mixed ploidy, which the level of ploidy increasing following the tissue specialization, results that were attributed to age and use of PGR in culture medium.

The characteristic to retain cells with various DNA contents in the somatic tissues is called mixoploidy, and this phenomenon is common in tissues of succulents and cacti (Lee et al. 2009, Lema-Rumińska 2011, Scholes and Paige 2015). DNA content of 2C, 4C, 8C, and 16C were reported before to other Cactaceae species as *Copiapoa tenuissima*, *Consolea corallicola, Consolea picardea, Consolea moniliformis, Mammillaria san-angelis*, *M. albilanata*, *M. crucigera*, *M. dixanthocentron*, *M. flavicentra*, *M. haagena*, *M. huitzilopochtl*, *M. supertexta, Opuntia heliabravoana*, *O. joconostle*, *O. matudae*, *O. oligacantha*, *O. hyptiacantha*, and *O. tomentosa,* (Palomino et al. 1999, Negrón-Ortiz 2007, Angel et al. 2006, Lema-Rumińska 2011, Palomino et

al. 2016). However, there are few studies so far investigating how this mixoploidy can be distributed along the cacti tissues (Lema-Rumińska 2011).

Cells with mixed ploidy are produced as a result of the repetition of endocycles, in which there is an increase in the ploidy level without the occurrence of cytokinesis (Lema-Rumińska 2011). The biological function of endocycles is related to the forming of specialized cell types as trichomes and vascular elements; cells with higher metabolic activity such as embryo-associated cells; and tissues for stock as cotyledonary and aquifer parenchyma cells, which occur through different plant organs (de Rocher et al. 1990, Palomino et al. 1999, Lee et al. 2009, Bourge et al. 2018).

Endoclycle is reported to occur as a result of a complex genetic regulation that confers specialization for a given species, an organ, and a development step. The difference in DNA content of cells, organs and species is widely reveled by flow cytometry, an easy approach technique that provides fast and precise genome size estimation (Bourge et al. 2018). Recent studied using flow cytometry to access ploidy level of cells from different tissues of the same individual revels that this is a technique capable of distinguish genome size in intra-specific samples (Nagymihály et al. 2017, Bateman et al. 2018).

This work aimed to gather cytological, histochemical and anatomical information in order to understand if *Melocactus* tissues are mixoploids, how this mixoploidy is distributed through the regions of cladode and the alterations in the pattern of ploidy after long periods of *in vitro* culture. This study brings information that will contribute to better understand the morphological and genetic alterations during the *in vitro* propagation in *Melocactus* species.

2. MATERIALS AND METHODS

Plant material

Seeds were collected in Morro do Chapéu city (Bahia State, eastern Brazil) from natural populations located in 11°29′38.4′S; 41°20′22.5′W (*Melocactus glaucescens*) and 11°33′52.0′S; 41°10′38.8′W (*Melocactus paucispinus*).

For establishing the *in vitro* cultures, the seeds were surface-sterilized by immersion in ethanol 96% for 1 min, commercial bleach (SuperGlobo®) at 2% for 10 min, and subsequently washed thrice in sterile water under aseptic conditions. Afterwards, seeds were germinated in flasks containing 50 mL of MS culture medium (Murashige and Skoog 1962) at quarter-strength salt concentration. After germination, the plants were subcultured periodically in flasks containing 50 mL of MS culture media at half-strength salt concentration.

All culture media were supplemented with 15 g L^{-1} sucrose and solidified with 7 g L^{-1} agar (PhytoTecnology Lab®), with pH was adjusted to 5.7 before autoclaving. The media were autoclaved for 20 min at 120ºC. Cultures were maintained at 25±2°C under two fluorescent lamps with photosynthetically active radiation levels of 60 µmol m^{-2} s^{-1} and a 16/8-h light/dark photoperiod. The samples for all experiments were selected from the germplasm collection of the Laboratory of Plant Tissue Culture II (BIOAGRO) on Federal University of Viçosa (Brazil) to perform the analyses.

Flow cytometry

In order to investigate how the different ploidy occurs through the *Melocactus* cladode, two experiments were performed. In the first experiment, the cladodes were sectioned transversally producing three topophysical regions (apical, medial and basal) (Figure 1). Three plants of *M. glaucescens* and three plants of *M. paucispinus* with age of ten years were analyzed.

The second experiment analyzed four regions and two ages of *in vitro* culture. The regions of cladode were manually separated, generating three samples: the outermost region of cladode (named periphery), the cortex region of cladode, and the

pith (Figure 1). The root apexes were also analyzed. Plants with ten and four years of *in vitro* culture were used.

For the flow cytometry analyzes, approximately 20–30 mg of fresh tissue was chopped with a disposable steel razor blade in 1 mL WPB buffer to release nuclei (Loureiro et al. 2007). *Solanum lycopersicum* (2C DNA content = 1.96 pg) was used as an internal reference standard (Doležel et al. 1998). Previously macerated tissues were filtered with 50 µM nylon mesh, and collected in a polystyrene tube. The filtrate was stained with 25 µL propidium iodide solution (1 mg/mL; Sigma Chemical Company, USA). Samples were incubated at 4ºC in the dark and examined after 30 min. At least 10,000 nuclei were analyzed in each sample thrice.

Analyzes were performed using a CytoFLEX (Beckman Coulter, CA, EUA) at the Institute of Biological Sciences (ICB) of the Federal University of Juiz de Fora (UFJF). Cytometric histograms were generated and analyzed using the software CytExpert 2.0.1. Nuclear DNA content (pg) was estimated by the follow equation (Doležel and Bartoš 2005):

$$\text{Sample (2C DNA)} = \frac{\text{G1 peak channel of sample}}{\text{G1 peak channel of } S.\ lycopersicum \times 1.96\text{pg } (S.\ lycopersicum \text{ DNA content})}$$

Anatomy

For anatomical characterization of *Melocactus* stem, samples from the medial region of cladode were collected from five plants of *Melocactus glaucescens* and five plants of *M. paucispinus*. The samples were fixed in Karnovsky 0.1M solution (Karnovsky 1965) under -250 mmHg of vacuum for 1 h. The material was stored in this solution until handling, when the material was dehydrated in ethanol series and submitted to -250 mmHg of vacuum. The samples were then embedded in methacrylate resin (Historesin, Leica®, US). After the inclusion, transversal and longitudinal sections (average 5 µm in thickness) were made with a rotary microtome (RM 2155 - Leica®). The sections were disposed in slides and stained with 0.05% (v/v) toluidine blue pH 4.4 for 10 min (O'Brien and McCully 1981).

The slides were also submitted to histochemical analyses in Xylidine Ponceau (XP) solution to evidence protein, Periodic Acid Schiff (PAS) reaction for the detection of polysaccharides, ruthenium red to analyze pectin, and acid floroglucin for the observation of lignin (Johansen 1940).

The material was observed in microscope (AX70TRF, Olympus Optical, Tokyo, Japan). Pictures were made with a digital camera (Spot Insightcolour 3.2.0, Diagnostic Instruments Inc.) using the Spot Basic Image software. The scales were projected in the same optical conditions.

X-ray micro-computed tomography (XRμCT)

To investigate how much increased ploidy affected cell size relative to cladode regions, X-ray images have been performed. Lyophilized samples of *Melocactus glaucescens* and *M. paucispinus* were submitted to high-resolution XRμCT projections. The images were acquired on a SKYSCAN 1272 (BrukermicroCT, Kontich, Belgium) scanner at Brazilian Nanotechnology National Laboratory (LNNano), Brazilian Center for Research in Energy and Materials (CNPEM), operating at source voltage of 20 kV and current of 175 μA. The NRecon software, version 1.6.10.4 (BrukermicroCT), was used to reconstruct projections into three-dimensional images, which were processed using the CTVox software, version 3.3 (BrukermicroCT), for 3D viewing and cutting. Two-dimensional images were processed using the DataViewer software, version 1.5.6.2 (BrukermicroCT). At least 200 undamaged cells selected from the periphery and cortex of cladode, in at least four cross-sectional layers within sample height, had their equatorial diameters (in case on round-shaped cells) or maximum Feret diameters (for irregular-shaped cells, probably resulting from drying artefacts) determined using ImageJ software, version 1.52a.

Statistical analyzes

The data were submitted to analysis of variance (ANOVA) in Minitab® 17 statistical software (Minitab 2010) to detect differences between topophysical regions of cladode, as well as between regions of cladode and ages. The data from different

regions of cladode and ages was arranged in a factorial scheme (four regions × two ages). The means were compared with Tukey's test with 5% level of probability.

3. RESULTS

Flow cytometry

Flow cytometry analysis revealed that plants of *Melocactus glaucescens* and *M. paucispinus* have four peaks of ploidy (2C, 4C, 8C, and 16C) on all analyzed topophysical regions of the cladode (Tables 1 and 2). For *M. glaucescens*, the nuclear content varied from 2.97 pg (2C) to 23.56 pg (~16C) of DNA (Table 1).

M. paucispinus, by its turn, showed cells with higher nuclear content, ranging from 6.06 pg (2C) to 48.93 pg (~16C) of DNA (Table 2). There was no statistical difference in the nuclear content of cells from apical, medial and basal regions of the cladode in both species (Tables 1 and 2).

Since these first analyzes were done with ten years of culture plants, another experiment was performed to identify if these cells with mixed ploidy were due to the time of cultivation or characteristics of the species.

Mixoploidy was observed in different regions of cladode and ages of both species (Tables 3 and 4). No interaction was observed between the regions of cladode and ages, also the ploidy levels between ages did not differ statistically ($P<0.01$) for *M. glaucescens* (Table 3). Although, ploidy level among the regions of cladode differed statistically ($P<0.01$). One more peak of ploidy was observed in cortex region with approximately 47 pg of DNA (~32C). Roots were not mixoploids, presenting two peaks of ploidy (2C and 4C).

A similar pattern of ploidy was observed in *M. paucispinus*. There was no interaction between regions of cladode and ages, and the ploidy level between ages did not differed statistically ($P<0.01$) (Table 4). As observed in *M. glaucescens*, the cortex region showed one more peak of ploidy in *M. paucispinus* with approximately 95 pg of DNA (~32C). The roots of *M. paucispinus* also are diploid, with two peaks of ploidy (2C and 4C).

Anatomy

Melocactus glaucescens and *M. paucispinus* dermal system consists of a flat and uniseriate epidermis with round, compact, and small cells. Stomata are located at the same level as the other epidermal cells substomatal cavities of varied depths (Figure 2.A; Figure 3.A).

The ground system is formed by a subepidermal periderm, which showed irregular wall thickening. Collenchyma cells are bigger than epidermal cells. The cortical region is composed of aquifer and chlorophyll parenchyma with vascular bundles (Figure 2-B). These tissues presented cells with nuclei of different sizes, as well as the biggest nuclei observed in the cladode cells (Figure 2.B; Figure 3.B).

The vascular system is organized in circle. The bundles showed collapsed primary phloem with sieve tube element and parenchyma. Xylem presents tracheids and parenchyma cells, with few vessel elements and fibers. The tracheids showed secondary wall with helical thickening, called wide-band tracheid (WBT) (Figure 2.B; Figure 3.B).

In both species, XP test colored protein corpuscles close to cortical vascular bundles (Figure 2.D). The ruthenium red test showed that the first layers of cell of cladode present more pectin content, for both species (Figure 2.E; Figure 3.E). PAS test indicates more polysaccharides content in periphery region of cladode. For both species, PAS reacted more in the epidermis and collenchyma (Figure 2.H; Figure 3.H). For both species, the acid floroglucin test was positive just in spine region and for the secondary wall with helical thickening of WBT.

X-ray micro-computed tomography (XRμCT)

Two- and three-dimensional images indicate that the cortical cells are bigger than epidermal and collenchyma ones (Figure 4). The two-dimensional images of both species revealed that the cell diameter increases from the periphery (epidermis and collenchyma) to the inside (aquifer parenchyma) of the cladode. Size distribution of the diameters of cells of *M. glaucescens* and *M. paucipinus* in periphery (57 ± 25 and 58 ± 27 μm, respectively) and cortex of cladode (150 ± 54 and 135 ± 56 μm, respectively) exhibited differences, which periphery cells have lower lumen size than cortex cells (Figure 5). Cortex cells presented almost 3x (*M. glaucescens*) and approximately 2x of (*M. paucispinus*) size than periphery cells.

4. DISCUSSION

The species studied here are from the same genus and present the same patterns of ploidy peaks, but differ in 2C DNA content. *M. glaucescens* has approx. 3 pg of DNA (2C), which corresponds to 2,934 Mbp (1 pg = 978 Mbp, Doležel et al. 2007). This value is very close to the DNA content of other cacti species, as seven *Mammillaria* species (average of 3.13 pg) and *Copiapoa tenuissima* (2,87 pg) (Del Angel et al. 2006, Lema-Rumińska 2011). This nuclear DNA content is indication of small genome size, and 2C value of *M. glaucescens* is one of the smallest values reported in comparison to the genome size of others cacti species.

M. paucispinus has approx. 6 pg of DNA (2C), corresponding to 5,868 Mbp, which is close to six species of *Opuntia* (average of 6.51 pg) analyzed by Palomino et al. (2016). As observed by Das et al. (1998b), *Melocactus* genus presents DNA amount that differ significantly at species level. The remarkable differences of DNA content between species turns the flow cytometry a useful technique to identify species of *Melocactus* genus with doubt of identification in natural population and Germplasm Banks.

The differences on ploidy level between species are related to loss or addition of many repeats in genome through alteration of micro- and macro-environment during evolution (Das et al. 1998b). For this reason, for many years, the studies that investigate ploidy level were restricted to systematic and evolution approach (Bateman et al. 2018).

Only recently the potentiality of the consequences of duplication events affecting only specific cells or tissues have been recognized, and other insights have emerged from the homogenized tissues necessary for flow cytometric analysis (Bateman et al. 2018). The choice of flow cytometry to the cytological characterization of *M. glaucescens* and *M. paucispinus* cladodes allowed observing that these species have cells with mixed ploidy (mixoploidy), with DNA content of 2C, 4C, 8C, ~16C, and ~32C. The DNA content was not exactly the values corresponding to 16C and 32C, which may be due to the loss of some DNA sequencing during endocycles, which was reported before for other cacti species (Palomino et al 2016).

Karyotype of *M. glaucescens* and *M. paucispinus* were previously documented by Assis et al. (2003) in a cytogenetic study of the apex of roots, which reveled 2n = 44

as the chromosome numbers of both species. Roots of *M. glaucescens* and *M. paucispinus* are diploid, showing just two peaks of ploidy (2C and 4C), as reported by Assis et al. (2003) (Figure 1).

The cells with lower DNA content (2C), as observed in roots of these species, have the benefit from rapid genome replication and cell division (Scholes and Paige 2015). Considering the arid natural habitat that cacti occur, cells with rapid growth is a remarkable advantage to root rapid recover and proliferation during the sporadic and rapid rain season.

Small genomes also confer to the cell the capability of many rounds of endoreduplication, which generate cells with higher DNA content and specialization (Bateman et al. 2018). The higher ploidy level of *M. glaucescens* and *M. paucispinus* cortex cells can be related to the presence of aquifer parenchyma, which is formed by cells that reasonably reach high level of ploidy to turn itself large-volume cells with high capability to water-storage (de Rocher et al. 1990). For this reason, endoreduplication is associated to adaptation to extremely dry environment condition and temperature (Lema-Rumińska 2011, Scholes and Paige 2015).

In order to become larger, the cells proceed discrete periods of S-phase and G-phase, without cytokinesis (endocycle), resulting in cells with a single polyploid nucleus (Lee et al. 2009, Scholes and Paige 2015). The increase of nucleus volume is often correlated to increasing in cell size, due to the functional surface-to-volume ratio, and for this reason endoreduplication also offers an efficient strategy for plant growth (Kondorosi et al. 2000, Lee et al. 2009).

In cacti, the growth caused by endoreduplication is related to the capability of parenchyma cells expand to water-storage. The movements of swelling and contraction occur naturally during the day. Due to Crassulaceae Acid Metabolism (CAM), at night stomata are open and the transpiration causes reductions of stem water potential, occurring stem contractions (Wai et al. 2017). In the vacuole of parenchyma cells, the nocturnal accumulation of malic acid by CAM and the daily synthesis of carbohydrates increase its osmotic pressure, driving water into the parenchyma cells and resulting in cladode swelling during the day (Scalisi et al. 2016, Wai et al. 2017).

Parenchyma cells have a high capacity for cell expansion when water is available and this tissue occupy from 50 to 70 % of the cortex volume of cacti (Barcikowski and Nobel 1984). In periods of drought, the cells also accumulate in vacuole secondary metabolites (such as phenolic compound and betalain) and polymerized sugars to reduce the water loss and prevent cellular damages caused by drought (Jain and Gould 2015, Ventura-Aguilar et al. 2017). The volume of cladode decrease during the dry period, and *Melocactus curvispinus* plantlets could survive eight months using water stored in their body to satisfy its hydric demands and to keep photosynthesis going to reduce the probability of carbon starvation (Lina and Eloisa 2018).

The capability of expansion and contraction of parenchyma cells is related to the highlight content of mucilage and pectin over lignin, as observer here in ruthenium red, PAS and acid floroglucin tests for both species (Figures 2 and 3). Soluble fibers allow setting up a colloidal system, attracting water and filling the aquifer parenchyma cells, which makes them hard but flexible (Ventura-Aguilar et al. 2017).

The strategy of storage mucilage and pectin is widespread in Cactaceae. In *Opuntia ficus-indica*, mucilage constitutes approx. 14 % of the dry weight of the cladodes, and can hold more than 30% of the total water of the aquifer parenchyma (Ventura-Aguilar et al. 2017). Soluble fibers added with large volume of vacuoles caused by endoreduplicated cells provide a huge system of water-storage.

Therefore, *Melocactus* species present both strategies for rapid growth response. The roots have small genomes, which provide fast division of genome and rapid recover and proliferation of the cell during rain period. On other hand, most part of cladode (aquifer parenchyma) present a more economically metabolic growth strategy: endoreduplication. In situations where basic sources (such as water or energy) are limiting and rapid growth is necessary, increasing cell size without cell division may be more advantageous, since cell division can be slower and require more energy than simply increasing the volume of a single cell (de Rocher et al. 1990, Lee et al. 2009, Lema-Rumińska 2011, Bateman et al. 2018).

Even though endoreduplication is a growth strategy observed in most of the cacti vegetative body, endoclycle is a tissue-specific pathway exclusive to specialized

cell types with specific biological functions, which confers a mechanism to control cell size, not being universal to the organism (Lee et al. 2009). In a study of mixoploidy in the complex labellum of sexually deceptive bee orchids, Bateman et al. (2018) suggest that endoclycle determine the final size and shape of the affected cell, which can occur in a single tissue of a single organ, indicating remarkable subtle and sophisticated genetic and/or epigenetic control of development.

Endoreduplication has been investigating in recent years and it is attributed to ontogenetic program and response to external factors (Scholes and Paige 2015). The fact of *M. glaucescens* and *M. paucispinus* exhibit the same pattern of cell ploidy in all topophysical (apical, medial and basal) regions and ages analyzed, and different ploidy throughout tissues, allows concluding that mixoploidy is a developmental characteristic of the cladode of these species.

Four and ten years of PGR-free *in vitro* culture of *Melocactus* species exhibited similar pattern of ploidy peaks, likewise the peaks funded by Lema-Rumińska (2011) in different tissues of *C. tenuissima.* Similarly with the results with *Melocactus* species, long-term cultures of *Mammillaria san-angelis* and *Beta vulgaris* did not show ploidy pattern modifications (Palomino et al. 1999, Sliwinska and Lukaszewska 2005).These data reinforce the indication that endoreduplication may be linked to the process of cellular differentiation that yields different types of cells not being exclusively linked to age (de Rocher et al. 1990).

Long-term cultures of *M. glaucescens* and *M. paucispinus*, as well as *C. tenuissima* and *M. san-angelis*, showed the maximum ploidy of ~32C (Palomino et al. 1999, Lema-Rumińska 2011). The constancy of an endopolyploidy pattern in cacti tissues, despite the age of culture, is another indication that the endoreduplication cycles in plants are genetically regulated to drive cell differentiation, and is a fine-tooled response during organismal development (Cebolla et al. 1990, Nagymihályet al. 2017, Bateman et al. 2018).

Not just only endoreduplicated cells occur in cortical region (Tables 2 and 3), this is caused by the fact of diploid cells, even after differentiation, also occurs in the cortex region, as phloem companion cells, which serve highly specialized function that would possibly be disrupted by increasing ploidy (Barow 2006, Schole and Paige 2015).

The consequence of endoreduplication in *Melocactus* cladodes is the increase of volume cell, which is observed by XRμCT analyses. In 2D and 3D images it is possible recognize the cellular lumen, which increase the diameter from periphery (epidermis and collenchyma) to cortex region (Figure 4). The larger cells are located on the cortical region, the same region that occurred the high level of ploidy and where the aquifer parenchyma, turning evident the high water-storage capability of this tissue.

The main elements which confer cellular support properties to succulent plants are present in the peripheral region of the cladode, evident in PAS and ruthenium red tests (Figure 2.E-G and Figure 3.E-G). As observed by Ventura-Aguilar et al. (2017) in *O. ficus-indica* cladodes, the collenchyma cell walls are eight-fold thicker that of C3 and C4 plants, providing structural support to the cells of this tissue. However, floroglucin test revealed the presence lignin just in spines and in the helical thickening walls of WBT.

WBT is a special type of tracheid, which shows absence of perforations on its walls and presence of rigid secondary thickening bands (Mauseth 1999). WBT were reported before to several species of cacti, including in *Melocactus zehntner* and *M. bahiensis* (Mauseth et al. 1995, Mauseth and Plemons-Rodriguez 1997, Mauseth 1999, Stone-Palmquist and Mauseth 2002, Arruda et al. 2004, Mauseth 2004, Arruda et al. 2005, Mauseth 2006, Melo-de-Pinna et al. 2006, Vázquez-Sánchez et al. 2007, Arruda and Melo-de-Pinna 2010, Terrazas et al. 2016, Reyes-Rivera et al 2018). The low presence of support elements (i. e. sclereids and fibers) indicates that epidermis, collenchyma, WBT present on vascular bundles and pith, and the water stored on aquifer parenchyma are responsible for the support of the cladode. Thus, the extreme specialization of cladode allowed cacti to use the aquifer parenchyma not just to water-storage but also to use the stored water as support the cladode shape.

The morphological and genetic variations observed in *M. glaucescens in vitro* shoot production can be related to the rounds of endoreduplication that occurs in cells of cladode. There are recent evidences that shoot organogenesis in *M. glaucescens* occurs not just in the meristematic region of areola, but also around the vascular bundle (*data not published – see chapter 2*). In expanding mixoploid tissues, growth of neighboring cells must be tightly coordinated in order to avoid local distortions of tissue (Traas et al.

1998), which can affect the initial formation process of meristemoids that occurs in regions with cell with high ploidy.

5. CONCLUSIONS

This study brings important information to understand the tissue organization and ploidy distribution on cladode of *Melocactus* species. As revealed by flow cytometry, anatomy, and X-ray micro-computed tomography, the mixoploidy observed in both *Melocactus* species is not related to age of culture, but is a characteristic of the developmental program, where endoclycle promote cell differentiation to perform a valuable function of accumulating water, the most restricted natural resource in the ambient where these plants live.

Melocactus has a strategy to trigger a rapid response to growth when the water is available: small genome in the roots that provides rapid cell division cycles and endoreduplication in the cortex cells, which are capable of a huge expansion to optimize water-storage.

6. ACKNOWLEDGMENTS

We thank Delmar Lopes Alvim for help during field works, the Laboratory of Genetic and Biotechnology (LGB) of Federal University of Juiz de Fora (UFJF) for performing the flow cytometer analyses, and Brazilian Nanotechnology National Laboratory (LNNano) at Brazilian Center for Research in Energy and Materials (CNPEM) for performing the X-ray micro-computed tomography analyses.

7. FUNDING

This work was supported by the Conselho Nacional de Desenvolvimento Científico e Tecnológico (CNPq), Fundação de Amparo à Pesquisa do Estado de Minas Gerais (FAPEMIG), and Coordenação de Aperfeiçoamento de Pessoal de Nível Superior (CAPES).

8. REFERENCES

Anderson, E.F. (2001). The cactus family. Timber Press, Portland, Oregon, 768p.

Arruda, E.C.P.; Alves, M.; Melo-de-Pinna, G. F. (2004). Elementos traqueais de cinco táxons de Cactaceae da caatinga pernambucana, Brasil. Acta Bot Brasilica, 18(4): 731–736. doi: 10.1590/S0102-33062004000400004

Arruda, E.; Melo-de-Pinna, G.F.; Alves, M. (2005). Anatomia dos órgãos vegetativos de Cactaceae da caatinga pernambucana. Rev Bras Bot, 28(3): 589–601. doi: 10.1590/S0100-84042005000300015

Arruda, E.; Melo-de-Pinna, G.F. (2010). Wide-band tracheids (WBTs) of photosynthetic and non-photosynthetic stems in species of Cactaceae. J Torrey Bot Soc, 137(1):16–29.

Assis, J.G.A.; Oliveira, A.L.P.C.; Resende, S.V.; Senra, J.F.V.; Machado, M. (2003). Chromosome numbers in Brazilian *Melocactus* (Cactaceae). Bradleya, 21: 1–6. doi: 10.25223/brad.n21.2003.a2

Barcikowski, W.; Nobel, P.S. (1984). Water relations of cacti during desiccation: distribution of water in tissues. Bot Gaz, 145(1):110–115. doi: 10.1086/337433

Barow, M. (2006). Endopolyploidy in seed plants. Bioessays, 28(3): 271–281. doi: 10.1002/bies.20371

Bateman, R.M.; Guy, J.J.; Rudall, P.J.; Leitch, I.J.; Pellicer, J.; Leitch, A.R. (2018). Evolutionary and functional potential of ploidy increase within individual plants: somatic ploidy mapping of the complex labellum of sexually deceptive bee orchids. Ann Bot, 122(1):133–150. doi: 10.1093/aob/mcy048

Bourge, M.; Brown, S.C.; Siljak-Yakovlev, S. (2018). Flow cytometry as tool in plant sciences, with emphasis on genome size and ploidy level assessment. Gen Appl, 2(2):1–12. doi: 10.31383/ga.vol2iss2pp1-12.

Cebolla, A.; Vinardell, J.M.; Kiss, E.; Oláh, B.; Roudier, F.; Kondorosi, A.; Kondorosi, E. (1999). The mitotic inhibitor *ccs52* is required for endoreduplication and ploidy-dependent cell enlargement in plants. EMBO J, 18(16):4476–4484. doi: 10.1093/emboj/18.16.4476

CITES (2018).Convention on international trade in endangered species of wild fauna and flora. Apêndice 1. [on line] URL, http: //www.cites.org/eng/app/index.shtml. Accessed in December 20th, 2018.

Das, A. B.; Mohanty, S.; Das, P. (1998a). Variation in karyotype and 4C DNA content in six species of *Melocactus*of the family Cactaceae. Cytologia, 63:9–16. doi: doi.org/10.1508/cytologia.63.9

Das, A.B.; Mohanty, S.; Das, P. (1998b). Interspecific variation in DNA content and chromosome analysis in *Melocactus.* Cytologia, 63: 239–247. doi: 10.1508/cytologia.63.239

Das, A.B.; Mohanty, S. (2008). Preliminary study on genetic relationships of *Melocactus* Link & Otto of the family Cactaceae revealed through karyotype, DNA content and RAPD analysis. Caryology, 61(1): 1–9. doi: 10.1080/00087114.2008.10589604

deRocher, J.; Harkins, K. R.; Galbraith, D.W.; Bohnert, H. J. (1990). Developmentally regulated systemic endopolyploidy in succulents with small genomes. Science, 250(4977): 99–101. doi: 10.1126/science.250.4977.99

Del Angel, C.; Palomino, G.; García, A.; Méndez, I. (2006). Nuclear genome size and karyotype analysis in *Mammillaria* species (Cactaceae). Caryologia, 59(2):177–186. doi: 10.1080/00087114.2006.10797914

Doležel J.; Bartoš J. (2005). Plant DNA flow cytometry and estimation of nuclear genome size. Ann Bot 95:99–110. doi:10.1093/aob/mci005

Doležel, J.; Greilhuber, J.; Lucretti, S.; Meister, A.; Lysak, M.A.; Nardi, L.; Obermayer, R. (1998). Plant genome size estimation by flow cytometry: Inter-laboratory comparison. Ann Bot, 82(Suppl. A):17-26. doi: 10.1093/oxfordjournals.aob.a010312

Goettsch, B., et al. (2015). High proportion of cactus species threatened with extinction. Nat Plants, 1:15142. doi: 10.1038/NPLANTS.2015.142

IUCN (2018).IUCN Red List of Threatened Species.Version 2013.2. [on line] URL, http://www.iucnredlist.org. Accessed in December 20th, 2018.

Jain, G.; Gould, K.S. (2016). Are betalain pigments the functional homologues of anthocyanins in plants? Environ Exp Bot, 119:48–53. doi: 10.1016/j.envexpbot.2015.06.002

Johansen, D. A. (1940). Plant microtechnique. McGraw-Hill Publishing Company Ltd., London, pp.523 pp.

Karnovsky, M.J. (1965). A formaldehyde-glutaraldehyde fixative of high osmolality for use in electron microscopy. J Cell Biol, 27(2):1–149A.

Kondorosi, E.; Roudier, F.; Gendreau, E. (2000). Plant cell-size control: growing by ploidy? Curr Opin Plant Biol, 3(6):488–492. doi: 10.1016/S1369-5266(00)00118-7

Lee, H. O.; Davidson, J. M.; Duronio, R. J. (2009). Endoreplication: polyploidy with purpose. Genes Dev, 23:2461–2477. doi: 10.1101/gad.1829209

Lema-Rumińska, J. (2011). Flow cytometric analysis of somatic embryos, shoots, and calli of the cactus *Copiapoa tenuissima* Ritt. *formamonstruosa*. Plant Cell Tissue Organ Cult, 106: 531–535. doi: 10.1007/s11240-011-9941-7

Lema-Rumińska, J.; Kulus, D. (2014). Micropropagation of cacti – a Review. Haseltonia, 18: 46–63. doi: 10.2985/026.019.0107

Lina, A.; Eloisa, L. (2018). How do young cacti (seeds and seedlings) from tropical xeric environments cope with extended drought periods? J Arid Environ, 154:1–7. doi: 10.1016/j.jaridenv.2018.03.009

Loureiro, J., Rodriguez, E., Doležel, J., Santos, C. (2007). Two new nuclear isolation buffers for plant DNA flow cytometry: A Test with 37 Species. Ann Bot, 100(4), 875–888. doi:10.1093/aob/mcm152

Machado, M.C. (2009). The genus *Melocactus* in eastern Brazil: part I - an introduction to Melocactus. British Cact Succ J, 27:1–16.

Mauseth, J.D.; Uozumi, Y.; Plemons, B.J.; Landrum, J.V. (1995).Structural and systematic sudy of an unusual tracheid type in cacti. J Plant Res, 108: 517–526. doi: 10.1007/BF02344242

Mauseth, J.D. (1999). Comparative anatomy of *Espostoa*, *Pseudoespostoa*, *Thrixanthocereus* and *Vatricania*. Bradleya 17: 27–37. doi:10.25223/brad.n17.1999.a2

Mauseth, J.D. (2004). Wide-band tracheids are present in almost all species of Cactaceae. J Plant Res, 117(1):69–76. doi: 10.1007/s10265-003-0131-5

Mauseth, J.D. (2006). Wood in the cactus subfamily Opuntioideae has extremely diverse structure. Bradleya, 24:93–106. doi: 10.25223/brad.n24.2006.a10

Mauseth, J.D.; Plemons-Rodriguez, B.J. (1997). Presence of paratracheal water storage tissue does not alter vessel characters in cactus wood. Am J Bot, 84(6): 815–822. doi: 10.2307/2445817

Melo-de-Pinna, G.F.; Arruda, E.; Abreu, D.D. (2006). Wide-band tracheids in Brazilian cacti. Bradleya, 24:53–60. doi: 10.25223/brad.n24.2006.a4

Minitab (2010). Minitab Statistical Software [Computer software]. State College, PA: Minitab, Inc. (www.minitab.com)

Murashige, T., Skoog, F. (1962).A revised medium for rapid growth and bio assays with tobacco tissue cultures. Physiol Plant, 15:473–497. doi:10.1111/j.13993054.1962.tb08052.x

Nagymihály, M.; Veluchamy, A.; Györgypál, Z.; Ariel, F.; Jégu, T.; Benhamed, M.; Szűcs, A.; Kereszt, A.; Mergaert, P.; Kondorosi, E. (2017). Ploidy-dependent changes in the epigenome of symbiotic cells correlate with specific patterns of gene expression. PNAS. doi: 10.1073/pnas.1704211114

O'Brien, T.P.; McCully, M.E. (1981). The study of plant structure: principles and selected methods. Melbourne, Vic., Australia: Termacarphi Pty Ltd.

Palomino, G.; Doležzel, J.; Cid, R.; Brunner, I.; Méndez, I.; Rubluo, A. (1999). Nuclear genome stability of *Mammillaria san-angelensis* (Cactaceae) regenerants induced by auxins in long-term in vitro culture. Plant Sci, 141:191–200. doi: 10.1016/S0168-9452(98)00216-7.

Palomino, G.; Martínez, J.; Méndez, I.; Muñoz-Urías, A.; Cepeda-Cornejo, V.; Pimienta-Barrios, E. (2016). Nuclear genome size, ploidy level and endopolyploidy

pattern in six species of *Opuntia* (Cactaceae). Caryologia, 69(1):82–89. doi: 10.1080/00087114.2015.1109956

Pérez-Molphe-Balch, E.; Santos-Díaz, M.S.; Ramírez-Malagón, R.; Ochoa-Alejo, N. (2015). Tissue culture of ornamental cacti. Sci Agric 72(6):540–561. doi: 10.1590/0103-9016-2015-0012

Resende, S. V.; Brito, A. L.; de Santana, J. R. F. (2010). Influência do substrato e do enraizamento na aclimatização de *Melocactus glaucescens* Buining & Brederoo propagados *in vitro.* Rev Ceres, 57(6):803–809. doi: 10.1590/S0034-737X2010000600016

Reyes-Rivera, J.; Soto-Hernández, M.; Canché-Escamilla, G.; Terrazas, T. (2018). Structural characterization of lignin in four cacti wood: implications of lignification in the growth form and succulence. Front Plant Sci, 9:1538. doi: 10.3389/fpls.2018.01518

Scalisi, A.; Morandi, B.; Inglese, P.; Lo Bianco, R. (2016). Cladode growth dynamics in *Opuntia ficus-indica* under drought. Environ Exp Bot, 122:158–167. doi: 10.1016/j.envexpbot.2015.10.003

Scholes, D.R.; Paige, K.N. (2016). Plasticity in ploidy: a generalized response to stress. Trends Plant Sci, 20(3):165–175. doi: 10.1016/j.tplants.2014.11.007

Sliwinska E.; Lukaszewska E. (2005). Polysomaty in growing *in vitro* sugar-beet (*Beta vulgaris* L.) seedlings of different ploidy level. Plant Sci, 168:1067–1074. doi:10.1016/j.plantsci.2004.12.003

Stone-Palmquist, M. E.; Mauseth, J. D. (2001). The structure of enlarged storage roots in cacti. Int J PlantSci, 163(1):89–98. doi: 10.1086/324551

Terrazas, T.; Escamilla-Molina, R.; Vázquez-Sánchez, M. (2016). Variation in the tracheary elements in species of *Coryphantha* (Cacteae-Cactoideae) with contrasting morphology: the bottleneck model. Braz J Bot, 39(2):669–67. doi: 10.1007/s40415-016-0249-z

Torres-Silva, G.; Resende, S.V.; Lima-Brito, A.; Bezerra, H.B.; D, de Santana, J.R.F.; Schnadelbach, A.S. (2018). *In vitro* shoot production, morphological alterations and

genetic instability of *Melocactus glaucescens* (Cactaceae), an endangered species endemic to eastern Brazil. S Afri J Bot, 115:100–107. doi: 10.1016/j.sajb.2018.01.001

Traas, J.; Hülskamp, M.; Gendreau, E.; Höfte, H. (1998). Endoreduplication and development: rule without dividing? Curr Opin Plant Biol, 1:498–503.

Vázquez-Sánchez, M.; Terrazas, T.; Arias, S. (2007). Morphology and anatomy of the *Cephalocereus columna-trajani* cephalium: why tilting? Plant Syst Evol, 265:87–99. doi: 10.1007/s00606-007-0520-7

Ventura-Aguilar, R.I.; Bosquez-Molina, E.; Bautista-Baños, S.; Rivera-Cabrera, F. (2017). Cactus stem (*Opuntia ficus-indica* Mill): anatomy, physiology and chemical composition with emphasis on its biofunctional properties. J Sci Food Agric, 97(15): 5065–5073. doi: 10.1002/jsfa.8493

Wai, C. M.; Van Buren, R.; Zhang, J.; Huang, L.; Miao, W.; Edger, P.P.; Yim, W.C.; Priest, H.D.; Meyers, B.C.; Mockler, T.; Smith, J.A.C.; Cushman, J.C.; Ming, R. (2017). Temporal and spatial transcriptomic and microRNA dynamics of CAM photosynthesis in pineapple. Plant J, 92(1):19–30. doi: 10.1111/tpj.13630

9. TABLES, FIGURES, AND LEGENDS

Table 1. Nuclear content (pg) from different topophysical regions of *Melocactus glaucescens* cladodes.

	2C	4C	8C	~16C
Apical	3.06 a	6.06 a	12.06 a	23.56 a
Medial	2.98 a	5.85 a	11.53 a	22.46 a
Basal	2.97 a	5.81 a	11.52 a	22.40 a

Means followed by the same letter in the same columns do not differ by the Tukey's test ($P<0.01$).

Table 2. Nuclear content (pg) from different topophysical regions of *Melocactus paucispinus* cladodes.

	2C	4C	8C	~16C
Apical	6.24 a	12.44 a	24.90 a	48.93 a
Medial	6.34 a	12.66 a	25.01 a	48.89 a
Basal	6.06 a	12.15 a	24.01 a	47.97 a

Means followed by the same letter in the same columns do not differ by the Tukey's test ($P<0.01$).

Table 3. Nuclear content (pg) of perifery, cortex and pith of cladode and root apices of *Melocactus glaucescens* with ten and four years of *in vitro* culture.

	2C	**4C**	**8C**	**~16C**	**~32C**
Ten-years plants					
Periphery	3.17	6.06	13.06	24.97	-
Cortex	3.06	5.85	12.09	23.66	46.79
Pith	3.12	5.81	12.48	24.22	-
Root	3.06	6.06	-	-	-
Four-years plants					
Periphery	3.10	6.01	12.62	24.24	-
Cortex	3.11	5.95	12.22	24.00	47.56
Pith	3.26	5.91	12.65	24.50	-
Root	3.04	6.03	-	-	-

Peaks exhibited the same pattern in ten- and four-years plants, and different peaks pattern in cortex and roots tissue by the Tukey test ($P<0.01$).

Table 4. Nuclear content (pg) of periphery, cortex and pith of cladode and root apices of *Melocactus paucispinus* with ten and four years of *in vitro* culture.

	2C	**4C**	**8C**	**~16C**	**~32C**
Ten-years plants					
Periphery	6.17	12.06	25.06	47.97	-
Cortex	6.06	12.85	24.09	46.66	94.79
Pith	6.12	12.81	24.48	48.22	-
Root	6.06	12.06	-	-	-
Four-years plants					
Periphery	6.15	12.36	25.10	47.23	-
Cortex	6.09	12.15	24.02	46.62	95.24
Pith	6.22	12.1	24.13	48.13	-
Root	6.16	12.19	-	-	-

Peaks exhibited the same pattern in ten- and four-years plants, and different peaks pattern in cortex and roots tissue by the Tukey test (P<0.01).

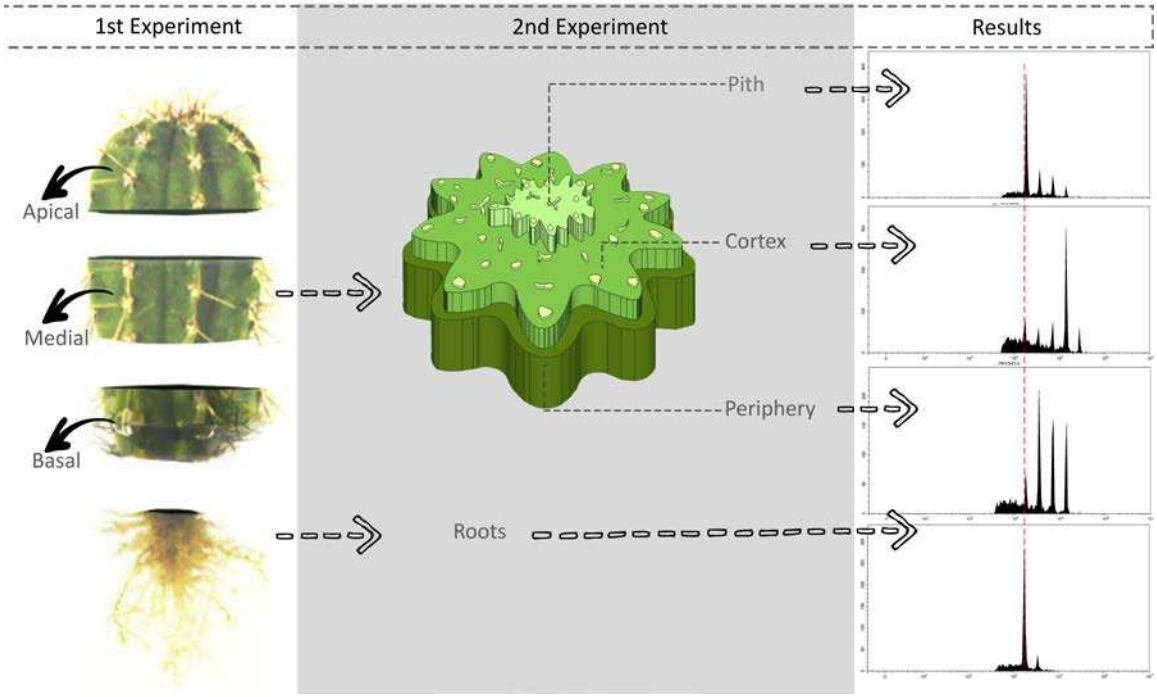

Figure 1. Cladode fragmentation of *Melocactus glaucescens* and flow cytometry analysis. In the first experiment, the cladodes were sectioned transversally producing three topophysical regions (apical, medial and basal). In the second experiment, regions of cladode were manually separated in pith, cortex region and the outermost region of cladode (periphery), as well as root apexes and different ages (ten and four years of culture) were analyzed. Flow cytometry analysis revealed that *M. glaucescens* has the same cell ploidy pattern in ages in all the analyzed ages, and different ploidy throughout the cladode regions, with root apexes diploids and cortex with one more peak of ploidy (~32C).

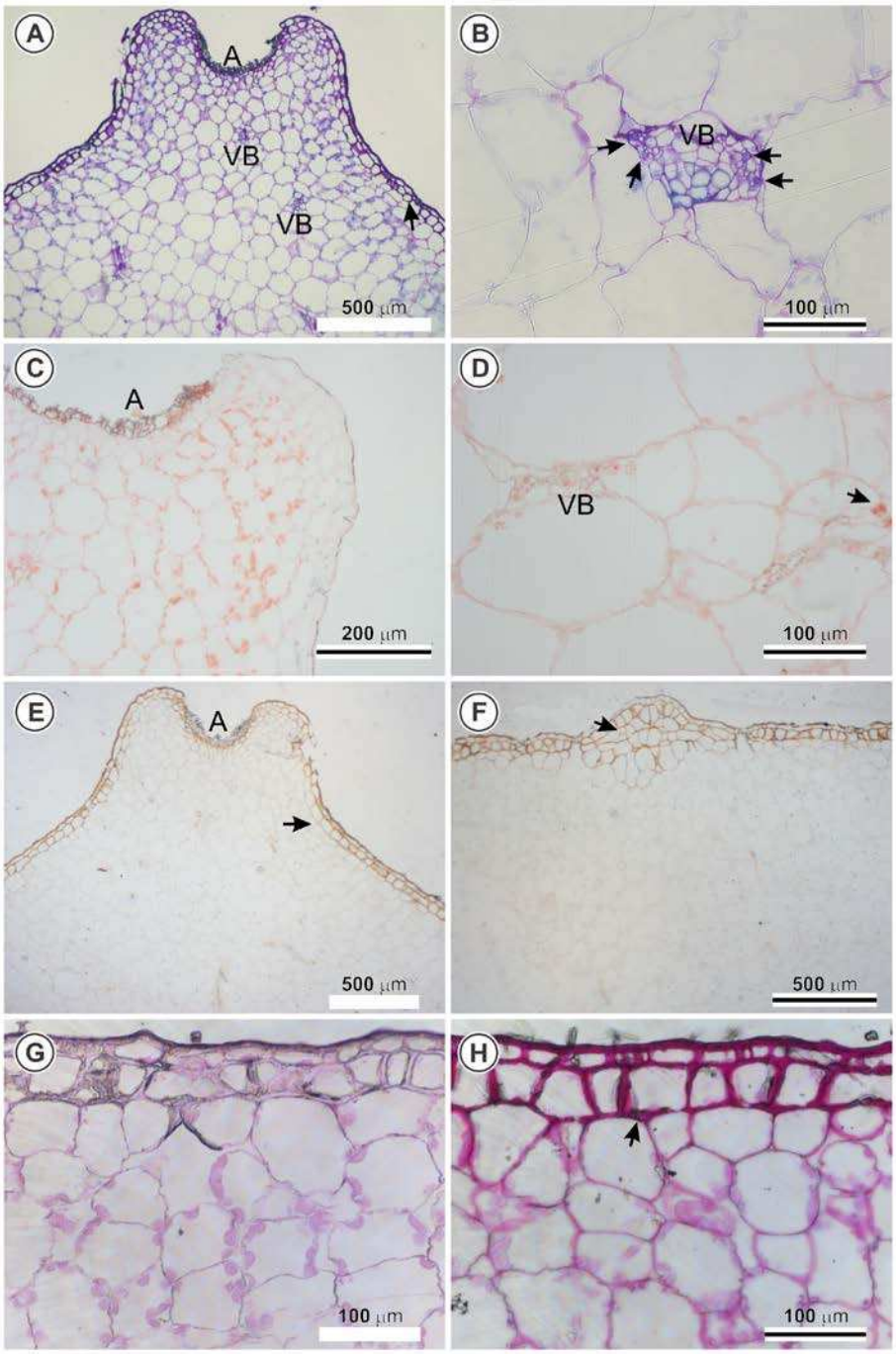

Figure 2. Anatomical characterization of *Melocactus glaucescens* plants cultivated *in vitro.* (**A**) Toluidine blue test of areola region [a] of cladode, and (**B**) aquifer parenchyma with vascular bundles [vb], arrow showing cells with different nucleus size. (**C**) XP test of areola region of cladode, and (**D**) aquifer parenchyma with vascular bundles. (**E**) Ruthenium red test of areola region of cladode, and (**F**) uniseriate epidermis with stomatal cavities. (**G**) Negative and (**H**) positive PAS test in cladode epidermis.

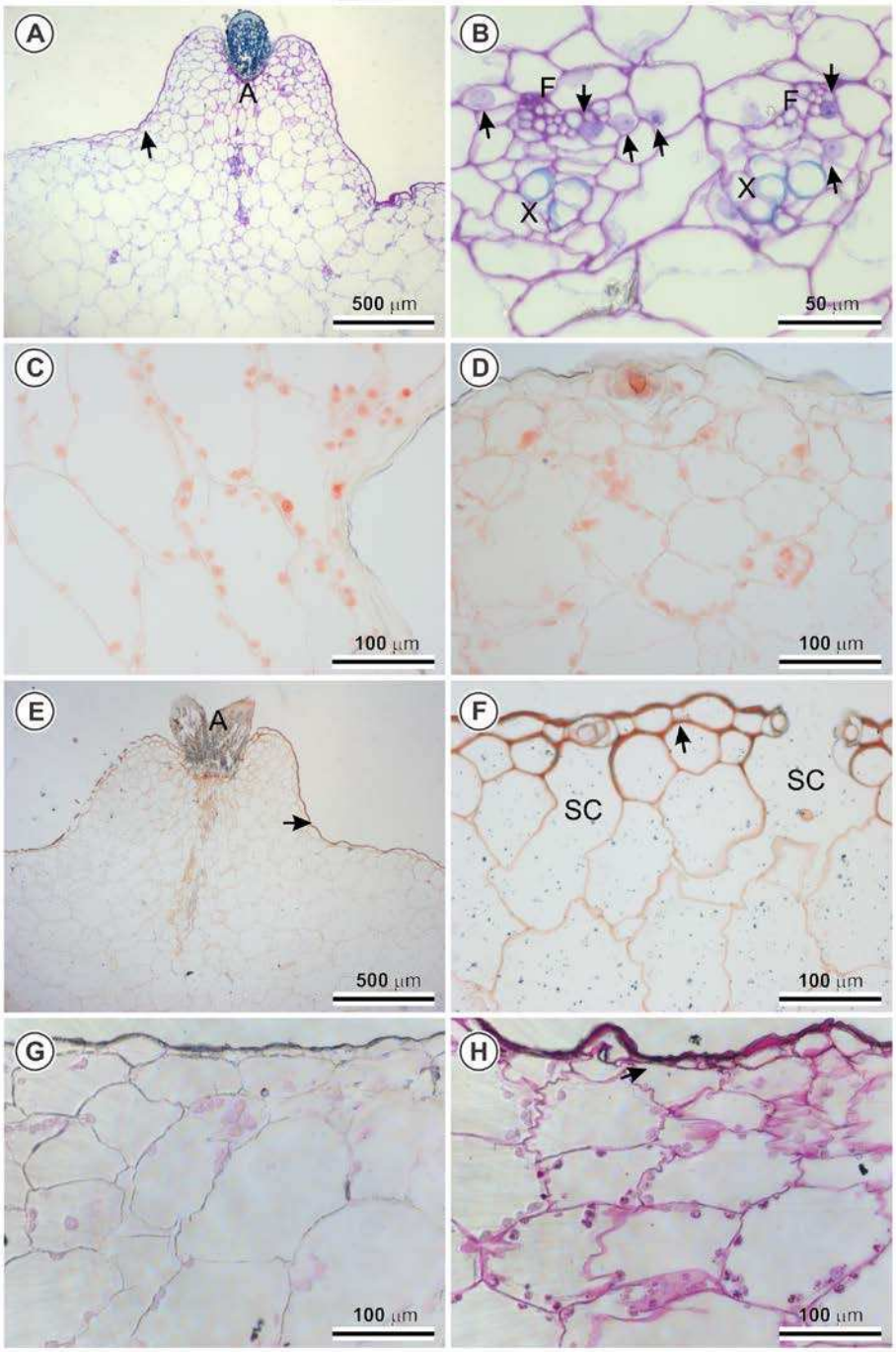

Figure 3. Anatomical characterization of *Melocactus paucispinus* plants cultivated *in vitro*. (**A**) Toluidine blue test of areola region [a] of cladode, and (**B**) vascular system of the pith. (**C**) XP test of epidermis region of cladode, and (**D**) stomata. (**E**) Ruthenium red test of areola region of cladode, and (**F**) uniseriate epidermis with stomatal cavities [sc]. (**G**) Negative and (**H**) positive PAS test in cladode epidermis.

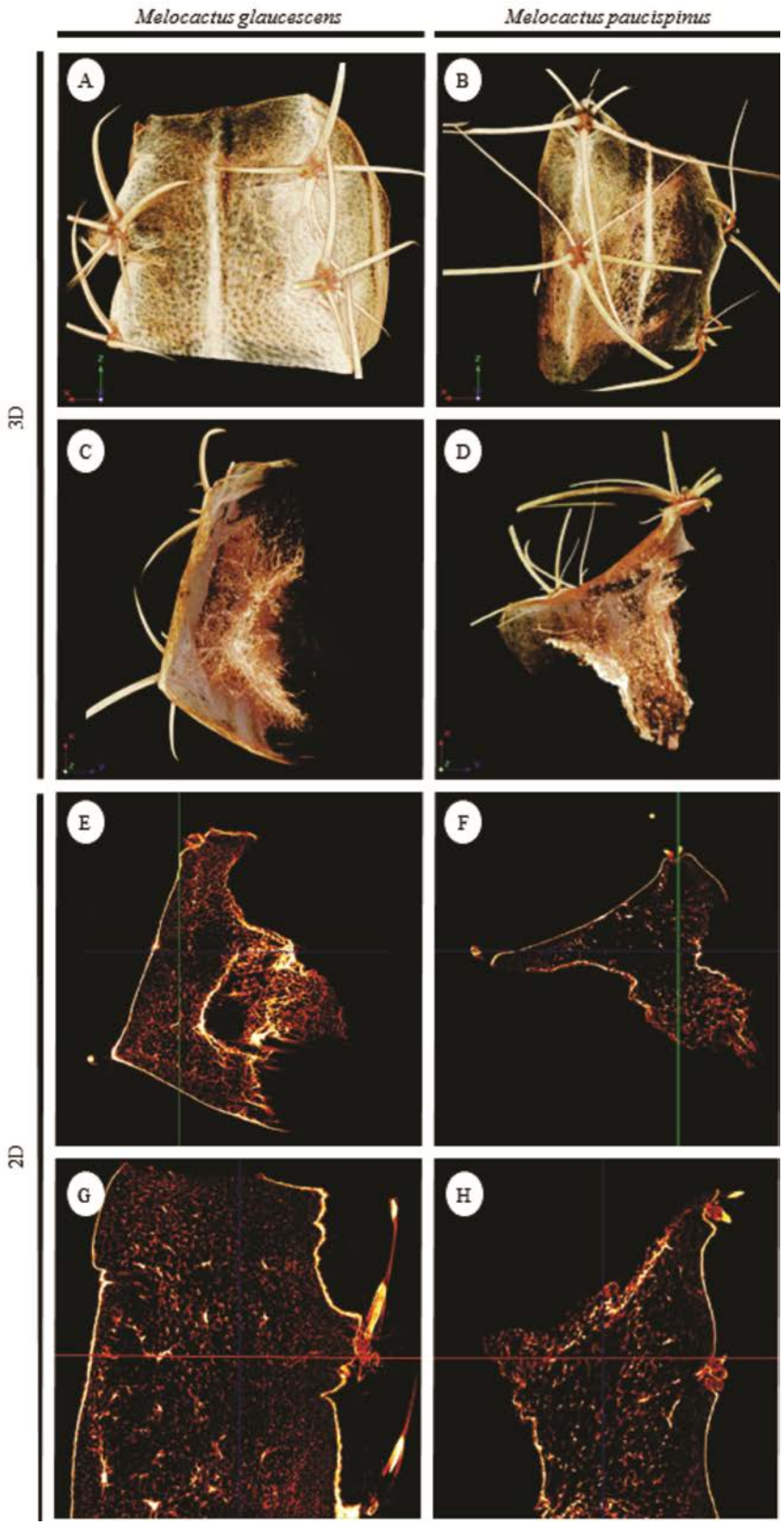

Figure 4. Characterization of *Melocactus glaucescens* and *M. paucispinus* cladodes by X-ray micro-computed tomography.

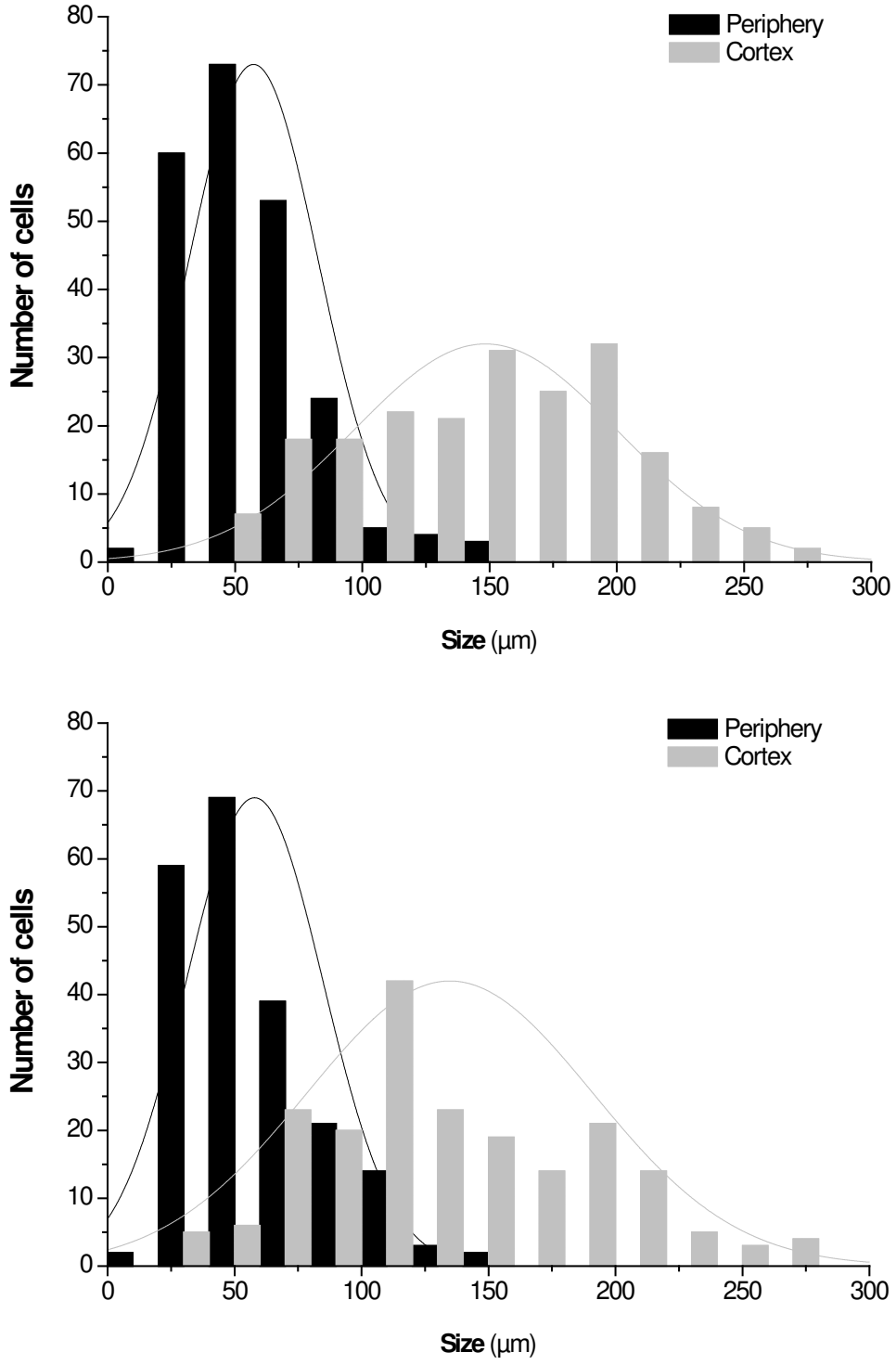

Figure 5. Size cells distribution of *Melocactus glaucescens* (top) and *M. paucispinus* (bottom) in periphery (57 ± 25 and 58 ± 27 µm, respectively) and cortex (150 ± 54 and 135 ± 56 µm, respectively) of cladode. Fittings: normal distribution.

_____CHAPTER 2_____

Unravelling the legend of the areolar activation in cacti by the expression of *Melocactus glaucescens SOMATIC EMBRYOGENESIS RECEPTOR KINASE-LIKE (SERK)* ortholog gene

ABSTRACT

Areolar activation is the most popular *in vitro* propagation method in cacti *in vitro* tissue culture techniques. Even if areolar activation is a relatively simple technique, so far a limited number of cacti species have well established *in vitro* propagation protocols, and rare works explore the anatomical and molecular aspects related to *in vitro* regeneration of cacti. Based on all studies that have been suggesting a link between the acquisition of the cellular-competent state and the expression of *SOMATIC EMBRYOGENESIS RECEPTOR KINASE* (*SERK*) gene during organogenic developmental program in plants, *Melocactus glaucescens* shoot organogenesis (SO) was used to investigate the cell competence acquisition and areolar activation by anatomical studies and the *MgSERK*-like gene expression. This is the first description of a *SERK* gene of a Cactaceae member, as well as the first report of gene expression study in areolar activation process. SO in *M. glaucescens* were investigated by comparing explants submitted to SO-induction in media without plant growth regulator (control), and explants which its areola regions were punctured three times with 0.18 mm needle and submitted to SO-induction in media with 17.76 μM of benzylaminopurine and 1.34 μM of naphthalene acetic acid (treated). Anatomy and *in situ* hybridization analysis showed that SO in *M. glaucescens* occurs by areolar activation and from procambial cells in the cortex of cladode. Additionally, the SO of this species were improved by the punctured with needle in areola region, which activated the axillary bud and amplified the response of the explant, increasing the number of shoots produced. *MgSERK*-like structure isolated in this study is close to others *SERKs* structures and can be considered as a putative SERK, and its expression is associated to SO occurrence in areola and adjacent regions, as well as root organogenesis.

Keywords: Cactaceae, *SERK*, organogenesis, wounding.

1. INTRODUCTION

The interest of ornamental cacti has been increasing each year (Goettsch et al. 2015). In last century, cacti species became more commercially accessible due to the development of efficient methods of propagation, and for this reason the cultivation of this plants increased rapidly in recent decades (Lema-Rumińska and Kulus 2014).

Cacti can be both sexually and vegetatively propagated. Naturally, reproduction via seed is more common, but also lateral branches and adventitious roots allow them to spread (Lema-Rumińska and Kulus 2014). For commercial purpose, conventional propagation may be tricky because: (1) seeds can be difficult to obtain (Godínez–Álvarez et al. 2003); (2) their germination rate may be low (Jenkins 1993); (3) there are some cacti that do not form lateral branches or adventitious roots (Goettsch et al. 2015); or (4) propagation by cuttings is difficult (Rubluo 1997). In the last 50 years, plant tissue culture has been partially solving these difficulties by applying the *in vitro* propagation techniques (Lema-Rumińska and Kulus 2014).

According to recent cacti reviews, its most popular *in vitro* propagation method is axillary bud activation or areolar activation (Pérez-Molphe-Balch et al. 2015, Lema-Rumińska and Kulus 2014). Areola is a highly specialized axillary bud that contains meristematic tissues, and where spines, trichomes and flowers can be developed in Cactaceae (Pérez-Molphe-Balch et al. 2015). This region can also regenerate entire plants by activating meristematic cells via only cutting or by plant growth regulators (PGR) induction (Pérez-Molphe-Balch et al. 2015, Lema-Rumińska and Kulus 2014).

Even if areolar activation is a relatively simple technique, so far a limited number of cacti species have well established *in vitro* propagation protocols, and few works explore the anatomical and molecular aspects related to *in vitro* regeneration of

cacti (Pérez-Molphe-Balch et al. 2015). The phenomena named "areola activation" in cacti can be more complex than the mere acquisition of competence of meristematic cell in the areola region. For example, Sánchez et al. (2015) observed that the floral and shoot morphogenesis in *Echnocereus* occur in internal regions of the buds as a result of the curling and looping of the areola meristem, caused by the periderm layer that seals and disrupts its growth.

It was recently developed an *in vitro* shoot production protocol for *Melocactus glaucescens* Buining & Brederoo: an ornamental, endemic and endangered cactus from eastern Brazil. In this study, it was observed that shoots developed after areola intumescence in the fourth week of cultivation, and a single shoot was developed at each areola. However, some challenges were observed in *M. glaucescens in vitro* propagation (i. e. low number of shoots per explant, high proportion of shoot with morphological alteration, and occurrence of somaclonal variation) and similar difficulties encountered in the *in vitro* cultivation of this species have been previously reported in other works with cactus species (Torres-Silva et al. 2018). Understanding the fundamental molecular events that trigger acquisition of competence in cacti areolar activation could guide the improvement of Cactaceae propagation protocols.

A useful approach to better understand *in vitro* regeneration is the quest of genes that can be markers of acquisition of competence. *SOMATIC EMBRYOGENESIS RECEPTOR-LIKE KINASE* (*SERK*) gene was first isolated from *Daucus carota* cell cultures, where was marking a single somatic cell competent to form embryo (Schimidt et al. 1997). Posteriorly, five SERK proteins were characterized in *Arabidopsis thaliana* (Hecht et al. 2001). Now SERK is considered as a protein family of five homologous

that share only partial functional redundancy (Podio et al. 2014, Aan den Toorn et al. 2015).

Despite ample evidence that reveal the relation between expression of *SERK* genes and the induction of somatic embryogenesis, other studies show a wide developmental role for SERK. First suggestion of a broader role of *SERK* genes in plant morphogenesis was indicated by Baudino et al. (2001) reporting the expression of *ZmSERK1* and *ZmSERK2* in ambryogenic and non-embryogenic callus of *Zea mays*. After that, other reports suggest that SERK may participate to a certain extent in the shoot organogenesis induction process, as by Nolan et al. (2003) in *Medicago truncata*, Thomas et al. (2004) in *Helianthus annuus*, and Singla et al. (2008) in *Triticum aestivum*. Sharma et al. (2008) were the first to propose SERK as a marker of pluripotency rather than embryogenesis.

Recently, studies showed a robust relationship between *SERK* expression and *in vitro* organogenesis. Both *in situ* hybridization studies revealed that *CpSERK1* and *CpSERK2* expression were present in somatic embryogenesis and organogenesis of *Cyclamen persicum*, and *PeSERK1* expression was observed during the organogenic program of *Passiflora edulis* (Savona et al. 2012, Rocha et al. 2016).

Based on all studies that suggest a link between the acquisition of the cellular-competent state and the expression of *SERK* gene during organogenic developmental program in plants, this work aimed to improve the knowledge of cell competence acquisition and areolar activation by studying the role of *SERK*-like gene expression in *Melocactus glaucescens* shoot organogenesis (SO). This is the first description of a *SERK* gene of a Cactaceae member, as well as the first report of gene expression study in the areolar activation process.

2. MATERIALS AND METHODS

Plant material

Plant material for all analysis were obtained from *in vitro* germination of *M. glaucescens* seeds collected from natural populations located in Morro do Chapeu city, Bahia State, eastern Brazil (11°29′38.4′S; 41°20′22.5′W). For establishing the *in vitro* cultures, the seeds were surface-sterilized by immersion in ethanol 96% for 1 min, commercial bleach (SuperGlobo®) at 2% for 10 min, and subsequently washed thrice in sterile water under aseptic conditions. Afterwards, seeds were germinated in flasks containing 50 mL of MS culture medium (Murashige and Skoog 1962) at quarter-strength salt concentration supplemented with 15 g L^{-1} sucrose and solidified with 7 g L^{-1} agar (PhytoTecnology Lab®), with pH was adjusted to 5.7 before autoclaving. The media were autoclaved for 20 min at 120ºC. Cultures were maintained at 25±3°C under two fluorescent lamps with photosynthetically active radiation levels of 60 $\mu mol.m^{-2}.s^{-1}$ and a 16/8-h light/dark photoperiod. After germination, the plants were subcultured periodically in flasks containing 50 mL of MS culture media at half-strength salt concentration until the conduction of *in vitro* shoot organogenesis (SO)-induction experiments.

Shoot organogenesis induction and tissue sampling

In vitro SO-induction was performed according to Torres-Silva et al (2018). Plants after 417 days of *in vitro* germination had their apical cladode segments removed and were sectioned transversely generating explants 3–4 mm of height and placed on horizontal position in glass tubes with 15 mL of MS medium full-strength (Figure 1A).

Explants that were submitted to SO-induction in PGR-free were considered as control. Explants which its areola regions were punctured thrice with 0.18 x 8 mm needles (DBC132, Dong Bang Acupuncture Inc., Chungnam, South Korea) and were placed on MS media full-strength supplemented with 17.76 μM of benzylaminopurine (BA) and 1.34 μM of ∞-naphthalene acetic acid (NAA) were considered as treated. Cultures were maintained at 25±3°C under two fluorescent lamps with photosynthetically active radiation levels of 60 μmol m^{-2} s^{-1} and a 16/8-h light/dark photoperiod for 120 days. After 120 days of culture, the percentage of responsive explants and number of shoots per explant were analyzed.

The material to RNA isolation, gene cloning and probe construction were isolated from treated explants collected with 50 days of cultures. Samples to anatomical analysis and *in situ* hybridization procedures were collected with 0, 10, 20, 30, 40 and 50 days of culture.

Anatomical characterization

For anatomical characterization of *M. glaucescens* SO-induction, five explants of *M. glaucescens* from each treatment were fixed in Karnovsky 0.1M solution (Karnovsky 1965) under -250 mmHg of vacuum for 1 h. After that, the material was dehydrated in ethanol series under -250 mmHg of vacuum. The samples were then embedded in methacrylate resin (Historesina, Leica®). After the inclusion, transversal and longitudinal sections (average 5 μm in thickness) were made with a rotary microtome (RM 2155 - Leica). The sections were disposed in slides and stained with 0.05% (v/v) toluidine blue pH 4.4 for 10 min (O'Brien and McCully 1981).

The material was observed in microscope (AX70TRF, Olympus Optical, Tokyo, Japan). The pictures were made with digital camera (Spot Insightcolour 3.2.0, Diagnostic Instruments Inc.) in the Spot Basic image program. The scales were projected in the same optical conditions.

RNA isolation and cDNA synthesis

Explant tissue was grinded with liquid nitrogen and total RNA was extracted with a Tris®-Reagent (Sigma) method, according to manufacturer's instructions, then 500 µL of Tris®-Reagent and 50 µL of chloroform:isoamyl alcohol (24:1) were added in 500 mg of frozen tissue. The mixture was vortexed and stored in ice for 5 min, then centrifuged in 12,000 x *g* for 15 min, in 4˚C. The aqueous phase was separated in new microtube and added the same volume of isopropanol for RNA precipitation. After incubation of 2h in -20 ˚C, the material was centrifuged again in 12,000 x *g* for 30 min, in 4˚C. The pellet was washed in 1 mL ethanol (70%), dried, and ressuspended in diethylpyrocarbonate treated water (DEPC, Sigma).

The cDNAs single strands were synthetized from of 3.0 µg of total RNA using the kit Super Script TM II, First-Strand Synthesis System (Invitrogen™), according to the manufacturer's recommendations.

Amplification of coding sequence of SERK-*like gene*

Different combinations of degenerated primers (Baudino et al. 2001) were used for the amplification of coding sequence of *SERK*-like gene using as template cDNA of treated explants of *M. glaucescens* submitted to SO-induction with 50 days of culture.

The PCR reaction was conducted in the final volume of 50 μL containing: 2.0 μL of cDNA, 5 μL of buffer 10x, dNTPs (0.2 mM each), 2.0 mM of $MgSO_4$, 200 mM of each primer and 0.2 μL of Taq DNA polymerase Platinum High Fidelity® (Invitrogen™). The reaction was realized in thermocycler C1000™ Touch Thermal Cycle (Bio-Rad) with the program: denaturation at 94 ºC (5 min), followed of 40 cycles at 94ºC (1 min), 50-60 ºC (1 min) as each primer pair used, 68 ºC (1 min), and final extension step at 68 ºC for 5 min.

The amplification fragments were cut out of the gel and purified with the Kit Wizard® SV Gel and PCR clean up (Promega®), according to the manufacturer's recommendations. The fragments were linked at pGEM®-T Easy Vector Systems (Promega®) vector, in proportion of 3:1 (insert:vector), with the T4 DNA ligase (Promega®) enzyme, according to the manufacturer's recommendations.

Recombinant plasmids obtained were introduced into *Escherichia coli* (DH5-alpha) by thermal shock. For transformation, 5 μL of insert and 100 μL of competent cells (1x 108) were used. After incubation at 37 ºC by 1 h the cells were locked in selective solid medium LB (Sambrook and Russel 2001), containing 100 $\mu g\ mL^{-1}$ of ampicillin, 20 $\mu g.mL^{-1}$ of 5-bromo-4-chloro-3-indolyl-β-d-galactopiranoside (X-Gal) and 0.1 mM of isopropyl-beta-D-thiogalactopiranoside (IPTG) and then incubated at 37 ºC overnight.

To confirmation of the insert presence in the vector, the plasmid DNA of the colonies that showed white colors were cleaved with the *Eco*RI restriction enzyme and the fragments were separated by agarose gel electrophoresis at 1.0%. After that, ten positive clones were sequenced using universal M13 primers. The sequences were processed using the PHRED (Ewing et al. 1998) and the CAP3 softwares (Huang and

Madan 1999). The Consensus sequences were compared to public databases at NCBI, Phytozome and TAIR using the BLAST algorithm.

Obtaining the complete sequence of SERK *gene, sequence analysis, and phylogenetic inference*

Beta vulgaris SERK2 gene (*BvSERK2*) was used as query against *M. glaucescens* transcriptome date (*data not published – see chapter 3*) using the BLAST algorithm. The sequence found was aligned to cDNA sequences to assembly of consensus sequence. The ORF (Open reading frame) and protein prediction was made using the ORF Finder (http://www.ncbi.nlm.nih.gov/projects/gorf/). The presence of conserved domains was analyzed by CDD Conserved Domain database (NCBI) (Marchler-Bauer et al. 2015), and the signal peptide was predicted using SignalP 4.1 (Nielsen 2017). Multiple sequence alignments were generated by Clustalw on Bioedit software, and the phylogenetic tree was constructed using neighbor-joining (Saitou and Nei 1987) on MEGA 7 (http://www.megasoftware.net) using as an input 32 sequences of others SERK members (Table 2). Bootstrap values were calculated from 1000 replicates.

Protein structure analysis

For access the conservation status of the protein structure, the conservation scores were determined by the ConSurf webserver (Ashkenazy et al. 2010), which were plotted onto the reported structure of the SERK1 protein extracellular domain (PDB:4LSC; Santiago et al. 2013), and using as an input the same multiple sequence

alignment used above for the distance trees (except the *A. thaliana* NIK1, NIK2, LRR II – RLK1, and LRR II – RLK2 sequences), with *MgSERK*-like as query sequence. The molecular graphics and analysis were performed with PyMOL Viewer version 0.99rc6.

Sense and antisense probe construction

RNA sense and antisense probes were constructed from a cDNA clone from amplification with degenerated primers, and flanked by the T7 and SP6 promoters. The probe fragment was amplified from the plasmid DNA with T7 and SP6 primers. Probes marked with conjugated Digoxyigenin (Dig-UTP) were synthesized by *in vitro* transcription using the DIG RNA Labeling Kit (SP6/T7) (Roche Applied Science), according to the manufacturer's recommendations.

In situ *hybridization*

The samples were fixed in 4 % paraformaldehyde pH 7 at 4˚C for 16 h, and then dehydrated through a series of RNAase free graded ethanol. After that, the samples were included in paraffin (Histosec®, MERCK, Germany) in series of *terc*-butyric alcohol:paraffin at 50˚C. After the inclusion, transversal sections (average 8 µm in thickness) were made in hand microtome (820, Reichert Jung, Germany) and transferred to silanated histological slides Fisherbrand® (FisherScientific, EUA). The slices were deparaffinized in xylol, xylol:ethanol, ethanol, ethanol:DEPC water, and DEPC water washes.

Sense (control) and antisense DIG-labeled *MgSERK*-like RNA probes were used. The hybridization was performed in the mix of 60ng of probe, 60ng of yeast

tRNA, and 100 µL of hybridization buffer (Tris.HCL 10 mM pH 7.5, NaCl 300 mM, formamide 50%, EDTA 1 mM pH 8.0; solution of Denhardt 1x), at 42 ˚C, in a dark moist chamber for 16 h. To visualize the hybridization signal, anti-DIG antibodies (Roche®, diluted 1:2000) conjugated to alkaline phosphatase were applied for 1 h at 37 ˚C and the hybridization signal was detected by reaction with NBT/BCIP (Pierce, USA). The hybridized slides were observed in microscope (AX70TRF, Olympus Optical, Tokyo, Japan), and the pictures were made with digital camera (Spot Insightcolour 3.2.0, Diagnostic Instruments Inc.) in the Spot Basic image program. The scales were projected in the same optical conditions.

Statistical analyses

The data were submitted to analysis of variance (ANOVA) in R statistical software to detect differences between percentage of responsive explants and the number of shoots of control and treated explants after 120 days of culture.

3. RESULTS

Shoot organogenesis induction

Due to the challenges (i. e. low number of shoots per explant, high proportion of shoot with morphological alteration, and occurrence of somaclonal variation) related before to *M. glaucescens in vitro* SO by Torres-Silva et al. (2018), the anatomical characterization and evaluation of the *MgSERK-like* expression were realized to trigger the process of acquisition of competence in the SO of *M. glaucescens*. First, were tested the combination of PGR that showed better results in the later study of this species with the puncture of areola with needle in order to improve the actual protocol of SO of *M. glaucescens*. The SO process was compared between explants that were submitted to SO in PGR-free medium (control), and explants in medium with NAA 1.34 µM, BA 17.76 µM and wounded areolas (treated). In both treatments, a single shoot was visualized emerging from, or close to, the areola region (Figure 1.B). In control explants, it was possible visualize the shoot formation in the fourth week, but in treated explants the shoots started growing in the second week of culture.

The percentage of explants that produced shoots was higher ($P<0.01$) in treated (100%) comparing with control explants (78.1%). The number of shoots per explant was also higher ($P<0.01$) in treated (8.9) than in control explants (2.3). Treated explants showed red coloration after 48h of culture, and shoots with and without morphological variation were observed after 120 days of culture (Figure 1. C-D).

Anatomical characterization

To determine the effects of both conditions on SO-induction at the tissue level, anatomical analyses were carried out of cultured explants collected with 0, 10, 20, 30, 40 and 50 days of culture. After 10 days of culture, control explants did not show any indication of SO (Figure 2A). The shoot formation started from meristematic tissue at areola region with 20 days of culture (Figure 2B), in progressive growth with the formation of an apical meristem and vascular reorganization (Figure 2C). Meristemoids formation was just observed with 50 days of culture in control explant (Figure 2D).

Treated explants showed meristemoid region near the region of epidermis after 10d of culture (Figure 2E), and the number of meristemoids increased during the period of culture (Figure 2F). After 30 days of culture, it was observed explants with an apical meristem developed, differentiation of a juvenile areola, with spines primordia, irrigated by xylem bundles and differentiated phloem (Figure 2G). It was observed shoot formation from meristematic tissue at areola region (Figure 2G), and from the inmost regions of the treated explant (Figure 2H).

Cloning of MgSERK-*like gene*

Given the considerable evidence that *SERK* genes are involved in SO in a number of species (Sharma et al. 2008, Savona et al 2012, Rocha et al 2016), *SERK* transcript accumulation in SO of *M. glaucescens* were analyzed. Given the paucity of genome information for *Melocactus*, degenerate primers were used to clone a *M. glaucescens SERK* from treated explant with 50 days of culture. A fragment of 1,223 bp was generated from the PCR with degenerate primers of *SERK* gene. In addition, three putative sequences corresponding to *SERK* genes were found with BLASTn in the

transcriptome dataset (*data not published – see chapter 3*) using *BvSERK2* as query (clusters number 3493.0; 4472.224, and 4472.225 of transcriptome).

The alignment of all sequences obtained from the sequencing generated a consensus of 2,251 bp (615 amino acids-long) (Figure 3). Due to a lack sequence data from *Melocactus,* the last 12 amino acids are based solely on the sequence of *BvSERK2* (Figure 3).

BLAST searches with this fragment returned several hits matching *SERK* conserved domains, and the assembled sequence was putatively designated as a *Melocactus glaucescens SERK*-like (*MgSERK*-like) fragment (Figure 3). A BLAST search of this sequence resulted in several SERK similarity hits from other plant species, including *Arabidopsis thaliana*, *Spinacia oleracea*, *Carica papaya,* and *B. vulgaris,* being the last the more phylogenetic close species with genome sequenced (Figure 4).

MgSERK *structure and others* SERKs

The *MgSERK*-like deduced protein sequence showed a predicted 27 amino acids-long putative signal peptide, 5 leucine-rich repeats (LRR) domains, a proline-richdomain (SPP), a transmembrane domain and a C-terminal tail (Figure 4). The degree of sequence conservation was not uniform along the deduced MgSERK protein sequence, which the sequence of the signal peptide was the most divergent comparing to other family members (Figure 4).

Phylogenetic analysis based on a multiple sequence alignment of amino acid sequence of *MgSERK*-like with members SERK from other plant species included

MgSERK-like in a clade known as dicots SERK1/SERK2, close to sequences annotated as SERK2 of the species *Chenopodium quinoa*, *B. vulgaris* and *S. oleracea* (Figure 5)

ConSurf algoritm (Ashkenazy et al. 2010) was used to plot the conservation score of the extracellular domain for 17 SERK1 and SERK2 sequences, including MgSERK-like, onto the crystal structure of AtSERK1 (PDB: 4LSC) (Figure 6). Some motifs were consistently conserved, including the residues at the extracellular domain considered essential for the interaction with BRI1 orthologs, which is well conserved among the SERK family members (Aan den Toorn et al. 2015). The concave side (Figure 6A) that interacts with the extracellular domain of BRI1, is more conserved than the convex side (Figure 6B), as shown by the conservation scores.

In situ *hybridization*

In order to evaluate the spatial/temporal distribution of *MgSERK*-like transcripts during SO-induction, a probe with 394 bp was use in explants from both treatements collected with 0, 10, 20, 30, 40 and 50 days of culture. In control explants, was registered a weak hybridization signal in parenchyma cell associated to vascular bundles until the 30th day of culture (Figure 7). From the 40th day of culture on, hybridization signal appeared more intensity in vascular tissue and spine region of newly formed shoots (Figure 7).

The *MgSERK*-like hybridization signal appeared in treated explants in all *in situ* hybridization experiments (Figure 7). After 10 days of culture, the hybridization signal was restricted on structures that were arising from epidermis. From 20th day of culture, hybridization signal was strong in all areola and vascular bundle regions. At 50th of

culture, the hybridization signal was observed at apical meristem of cladode and root of newly formed shoots, as well as along the vascular region of these structures (Figure 7).

4. DISCUSSION

Cactus areoles play three vital roles in the life of cacti: spine clusters, flowers and branches (Anderson 2001, Mauseth 2017). Generally, the initial formation of areole consists in dividing cells to form the shoot apical meristem (SAM) (Boke 1944). After the areole SAM produced the proper number of spines primordia, it becomes dormant. For the *Melocactus* genus in natural habitat, except for the areola that turns into cephalium (reproductive structure), all other areolas remain dormant (Machado 2009, Mauseth 2017).

But the SAM in each dormant areole can become active even though those areoles have been dormant for decades (Mauseth 2017). It is well documented to *Melocactus* genus that, if the SAM is damaged, some areoles below the point of damage become active and produce a branch (Machado 2009). This is possible because the areola is a reservoir of healthy cells capable of growth (Mauseth 2017).

The areolas dormant of *Melocactus* is broken in tissue culture by removing the apical dominancy, by cutting of cladode to form explants, and by adding PGR in the culture media (Retes-Pruneda et al. 2007, Torres-Silva et al. 2018) (Figure 1A). Explants of *M. glaucescens* can produce shoots without PGR addition, but this production (1.3 shoot/explant, with a maximum of 3 shoots/explant) is not viable for commercial purposes (Torres-Silva et al. 2018).

In the actual study, the number of shoots per explant in *M. glaucescens* increased in treated explants (Figure 1D). The treated explants were submitted to the same PGR concentration of the study realized by Torres-Silva et al. (2018), in which were observed an average of 2.5 shoot per explant of *M. glaucescens* after 120 days of culture. This study showed the increase of almost 4x of shoot per explant (8.3

shoots/explant) when the areola region was punctured with needle to stimulate the SAM region. The loss of cell-to-cell communication and disruption of long-distance signaling produced by wounding can generate changes in plasma transmembrane potential, intracellular Ca^{2+} concentration, and H_2O_2 generation (Ikeuchi et al. 2016, Xu 2018). For these reasons, wounding is considered responsible for stimulating the production of phytohormones and is related to both shoot and root organogenesis (Ikeuchi et al. 2016, Xu 2018).

The process of areolar activation of *M. glaucescens* during SO-induction was observed in anatomical analyses (Figure 2). The shoots of *M. glaucescens* can be produced directly from axillary bud of the areola region, as was previously documented by Téllez-Román et al. (2017) to *Mammillaria plumose*. However, SO in *M. glaucescens* occurred near and far from SAM region of areola in both control and treated explants, as suggested before by Sánchez et al. (2015) to *Echnocereus* genus.

Not just the number of shoots, but the time to respond to SO stimuli was different in treated explants. Explants placed on PGR-free media took longer to exhibit SAM activation and meristemoids formation. On the other hand, explants which the areola region was punctured with needle and placed on media with PGR showed meristemoids formation few days after starting *in vitro* cultures (10 days). It was observed the occurrence of meristemoids in the cortex of both control and treated explants of *M. glaucescens* (Figure 2D, E and F). The cortex is the region of *M. glaucescens* cladode that presented cell with the highest level of ploidy (~32C) (*data not published – see chapter 1*).

Controlled endocycles, with discrete periods of S-phase and G-phase, without cytokinesis (endocycle), are responsible to generate cells with a single polyploid

nucleus (Lee et al. 2009, Scholes and Paige 2015). In *M. glaucescens,* cells with more than 15x of DNA content (comparing to 2C) are present surrounding the vascular bundles of cortex region (*data not published – see chapter 1*), the same region where meristemoids were observed. On other hand, for the propitious formation of meristemoids, asymmetric division must occur to adoption of stem-cell identity, and G_2 phase might be of special importance in preparation for this unequal cell division (Jakoby and Schnittger 2004). Therefore, in plant tissue where the cell cycle is modified due to specifications of this tissue (i. e. aquifer parenchyma), the meristemoids may present failings in their formation.

Alterations in meristemoids initial formation can generate shoots with altered morphology, as observed in shoots of *M. glaucescens* derived from treated explants (Figure 1D). Failure to organize the meristemoid may lead to changes in the pattern of expression that confers the differentiation of the new shoot tissues, due the fact that the transcriptional program that determines the cell type-specificity occurs by turning on and off the temporally and spatially expressed genes to fine-tool tissue differentiation (Nagymihályet al. 2017).

The formation of meristemoids, and consequently shoots, in regions where occur variation in cell cycle and ploidy can also be the explanation to the somaclonal variation observed by Torres-Silva et al. (2018) in *in vitro* shoot propagation of *M. glaucescens.* Changes in chromatin environment (caused by endoreduplication process) associated with accelerated cell divisions (induced by the presence of PGRs in culture media) may cause DNA polymerase sliding and consequent pairing mistakes during DNA replication, leading to somaclonal variation occurrence (Aremu et al. 2013, Nagymihályet al. 2017).

The areolar activation in *M. glaucescens* was also investigated by studying the expression of the *MgSERK*-like gene in control and treated explants. The high degree of similarity of the transcript isolated in this study with the transcripts storage in NCBI database suggests that *MgSERK*-like is a functional *SERK* homologue (Figure 4). *SERK* genes comprise the largest sub-family of repeat-receptor-like kinases (RLKs) in plants and are involved in key plant development process (Sharma et al. 2008). The general structure of SERK proteins placed them in the leucine-rich LRR-RLK family (Walker 1994). *SERK* genes belong to the LRR-RLK II group of receptor-like kinases due to the presence of a small extracellular domain consisting of 4.5-5 leucine-rich repeats (LRRs) followed by a serine-proline rich (SPP) domain, a single pass transmembrane (TM) domain, and an intracellular kinase domain (Aan den Toorn et al. 2015). All conserved sequence domain expected to be present in established *SERK* orthologs were observed in *MgSERK*-like (Figures 4 and 5).

The MgSERK-like protein structure presents the conservation scores of both concave and convex sides in agreement to others SERK members (Aan den Toorn et al. 2015, Rocha et al. 2016). The extracellular domain is involved in many different signaling processes and is important for SERK specificity (Aan den Toorn et al. 2015). As observed in MgSERK-like, the concave side is more conserved between SERK members, and presents residues that were reported as having interaction with the BRI1 and FLS2 extracellular domains, playing important roles to elicit biological responses (Aan den Toorn et al. 2015). The convex is not reported to specific interactions, and for this reason may be more susceptible to evolution changes.

The bioinformatic analyses of comparing sequences of transcript and protein (Figures 4 and 5), added with the *in situ* hybridization results allow hypothesize that

MgSERK-like performs a similar role in organogenesis to *CpSERK2* (*Cyclamen persicum*), *PeSERK1* (*Passiflora edulis*), and *BnSERK2* (*Brassica napus*), and this gene family not just mediated embryo-specific signal transduction pathway, but also is involved in organogenic pathway (Savona et al. 2012, Rocha et al. 2016, Ahmadi et al. 2016).

According to the present *in situ* hybridization results, *MgSERK*-like transcripts were observed throughout the *M. glaucescens* organogenic pathway obtained from the *in vitro* culture of control and treated explants. The strong *MgSERK*-like expression was observed in areoles of control and treated explant during the SO process (Figure 7). This fact suggests that the *MgSERK*-like expression is associated with the dormancy breaking of the *M. glaucescens* areolas. A fait *MgSERK*-like hybridization signal was associated to vascular bundles of explants in beginning cultures of control explants (until 30 days of culture). As observed in anatomical analysis, *in situ* hybridization also indicates that the SO occurs in inner regions of explant, in procambial cells, which already exhibit a stem cell capacity, given the correct signals, could acquire a totipotent nature and develop into meristemoids (Podio et al. 2014, Ahmadi et al. 2016). Rocha et al. (2016) also observed fait *PeSERK1* hybridization signal in vascular tissues of *Passiflora edulis* initial hypocotyl explants, and it is suggested that the expression in these tissues was associated to provascular tissue development.

The faster development of shoot in treated explants was observed in anatomical and *in situ* hybridization analyses. *MgSERK*-like hybridization signal was associated to structures arising from epidermis of the treated explants with 10 days of culture (Figure 7). The *MgSERK*-like hybridization signal turned strong in treated explants during SO-induction (50 days of culture), and switched the region of expression from vascular

tissues and SAM of the explant to the vascular tissues, SAM and root apical meristem (RAM) of the new shoot, remaining confined to their meristematic cell populations (Figure 7).

Shoots formed in inner region of treated explants generated roots. The *MgSERK*-like expression was also observed in the RAM of shoot from treated explants after 50 days of culture. These results are consistent with findings of Ahmadi et al. (2016), which observed *BnSERK1* and *BnSERK2* expression in primary and developed shoots and roots of regenerated plants of *Brassica napus.* The results from this study are in agreement with recent studies that suggest a broader view of the actual *SERK* function, which may mark the generation of pluripotent cells, and be capable of developing into several divergent cell types are highly conserved among land plants (Li et al. 2015, Rocha et al. 2016).

5. CONCLUSIONS

Anatomical and *in situ* hybridization analysis showed that shoot organogenesis (SO) in *Melocactus glaucescens* occurs by areolar activation and from parechyma cells in the cortex of cladode. Additionally, the SO of this species were improved by the punction in areola region, which activated the axillary bud and amplified the response of the explant, increasing the number of shoots produced.

MgSERK-like structure isolated in this study is close to others *SERKs* structures and can be considered as putative SERK, and its expression is associated to SO occurrence in areola and adjacent regions, as well as root organogenesis.

6. ACKNOWLEDGEMENTS

We thank Delmar Lopes Alvim for help during field work and Susan Strickler (Boyce Thompson Institute, Ithaca, USA) for helping in the mining data of transcriptome.

7. FUNDING

This work was supported by the Conselho Nacional de Desenvolvimento Científico e Tecnológico (CNPq), Fundação de Amparo à Pesquisa do Estado de Minas Gerais (FAPEMIG), and Coordenação de Aperfeiçoamento de Pessoal de Nível Superior (CAPES).

8. REFERENCES

Aan den Toorn, M.; Albrecht, C.; de Vries, S.C. (2015). On the origin of SERKs: Bioinformatics analysis of the Somatic Embryogenesis Receptor Kinases. Mol Plant, 8:762-782. doi: 10.1016/j.molp.2015.03.015

Ahmadi, B.; Masoomi-Aladizgeh, F.; Shariatpanahi, M.E.; Azadi, P.; Keshavarz-Alizadeh, M. (2016). Molecular characterization and expression analysis of *SERK1* and *SERK2* in *Brassica napus* L.: implication for microspore embryogenesis and plant regeneration. Plant Cell Rep, 35:185-193. doi: 10.1007/s00299-015-1878-6

Anderson, E. F. (2001). The cactus family.Timber Press, Portland, Oregon, p.768.

Aremu, A.O.; Bairu, M.W.; Szüčová, L.; Doležal, K.; Finniea, J.F.; Van Stadena, J. (2013). Genetic fidelity in tissue-cultured 'Williams' bananas – The effect of high concentration of topolins and benzyladenine. Sci Hortic, 161:324-327. doi: 10.1016/j.scienta.2013.07.022

Ashkenazy, H.; Erez, E.; Martz, E.; Pupko, T.; Ben-Tal, N. (2010). ConSurf 2010: calculating evolutionary conservation in sequence and structure of proteins and nucleic acids. Nucleic Acids. Res, 38:W529–W533. doi: 10.1093/nar/gkq399

Baudino, S.; Hansen, S.; Brettschneider, R.; Hecht, V.; Dresselhaus, T.; Lorz, H.; Dumas, C.; Rogowsky, P. (2001). Molecular characterization of two novel maize LRR receptor-like kinases, which belong to the *SERK* gene family. Planta, 213:1-10. doi: 10.1007/s004250000471

Ewing, B.; Hillier, L.; Wendl, M.C.; Green, P. (1998). Base-calling of automated sequencer traces using Phred. I. accuracy assessment. Genome Res, 8:175-185, doi: 10.1101/gr.8.3.175

Goettsch, B., et al. (2015). High proportion of cactus species threatened with extinction. Nat Plants, 1:15142. doi: 10.1038/NPLANTS.2015.142

Godínez-Álvarez, H.; Valverde, T.; Ortega-Baes, P. (2003). Demographic trends in the Cactaceae. Bot Rev, 69 (2): 173-203. doi: 10.1663/0006-8101

Hecht, V.; Vielle-Calzada, J.-P.; Hartog, M.V.; Schmidt, E.D.L.; Boutilier, K.; Grossniklaus, U.; de Vries, S.C. (2001). The *Arabidopsis SOMATIC EMBRYOGENESIS RECEPTOR KINASE 1*gene is expressed in developing ovules and embryos and enhances embryogenic competence in culture. Plant Physiol, 127:803-816. doi: 10.1104/pp.010324

Huang, X.; Madan, A. (1999). CAP3: A DNA sequence assembly program. Genome, 9:868-87710.1101/gr.9.9.868

Ikeuchi, M; Ogawa, Y.; Iwase, A.; Sugimoto, K. (2016). Plant regeneration: cellular origins and molecular mechanisms. Development, 143, 1442-1451. doi:10.1242/dev.134668

Jakoby, M.; Schnittger, A. (2004). Cell cycle and differentiation. Curr Opin Plant Biol, 7(6): 661-669. doi: 10.1016/j.pbi.2004.09.015

Jenkins, M. (1993). The wild plant trade in Europe – results of a traffic Europe survey of European nurseries. Traffic Europe, 3-17.

Karnovsky, M.J. (1965). A formaldehyde-glutaraldehyde fixative of high osmolality for use in electron microscopy. J Cell Biol, 27(2):1–149A.

Lee, H. O.; Davidson, J. M.; Duronio, R. J. (2009). Endoreplication: polyploidy with purpose. Genes Dev, 23:2461–2477. doi: 10.1101/gad.1829209

Lema-Rumińska, J.; Kulus, D. (2014). Micropropagation of cacti – a Review. Haseltonia, 18: 46–63. doi: 10.2985/026.019.0107

Li, W.; Fang, Y-H.; Han, J-D.; Bai, S-N.; Rao, G-Y. (2015). Isolation and characterization of a novel SOMATIC EMBRYOGENESIS RECEPTOR KINASE gene expressed in the fern *Adiantum capillus-veneris* during shoot regeneration *in vitro*. Plant Mol Biol Rep, 33:638–647. doi: 10.1007/s11105-014-0769-2

Machado, M.C. (2009). The genus *Melocactus* in eastern Brazil: part I – an introduction to *Melocactus*. British Cact Succ J, 27:1-16.

Marchler-Bauer, A.; Bo, Y.; Han, L.; He, J.; Lanczycki, C.J.; Lu, S.; Chitsaz, F.; Derbyshire, M.K.; Geer, R.C.; Gonzales, N.R.; Gwadz, M.; Hurwitz, D.I.; Lu, F.; Marchler, G.H.; Song, J.S.; Thanki, N.; Wang, Z.; Yamashita, R.A.; Zhang, D.; Zheng, C.; Geer, L.Y.; Bryant, S.H. (2015). CDD/SPARCLE: functional classification of proteins via subfamily domain architectures Nucleic Acids Res, 45(D1):D200–D203. doi:10.1093/nar/gkw1129

Mauseth, J.D. (2017). An introduction to cactus areoles part II. British Cact Succ J, 89(5):219-229. doi: doi.org/10.2985/015.089.0503

Murashige, T., Skoog, F. (1962). A revised medium for rapid growth and bio assays with tobacco tissue cultures. Physiol Plant, 15:473–497. doi:10.1111/j.13993054.1962.tb08052.x

Nagymihály, M.; Veluchamy, A.; Györgypál, Z.; Ariel, F.; Jégu, T.; Benhamed, M.; Szűcs, A.; Kereszt, A.; Mergaert, P.; Kondorosi, E. (2017). Ploidy-dependent changes in the epigenome of symbiotic cells correlate with specific patterns of gene expression. PNAS, doi: 10.1073/pnas.1704211114

Nielsen, H. (2017). Predicting secretory proteins with SignalP. *In:* Kihara D. (eds) Protein Function Prediction. Methods in Molecular Biology, vol 1611. Humana Press, New York, NY. doi: https://doi.org/10.1007/978-1-4939-7015-5_6

Nolan, K.E.; Irwanto, R.R.; Rose, R.J. (2003). Auxin up-regulates *MtSERK1* expression in both *Medicago truncatula*root-forming and embryogenic cultures. Plant Physiol, 133:218-230. doi: 10.1104/pp.103.020917

O'Brien, T.P.; McCully, M.E. (1981). The study of plant structure: principles and selected methods. Melbourne, Vic., Australia: Termacarphi Pty Ltd.

Pérez-Molphe-Balch, E.; Santos-Díaz, M.S.; Ramírez-Malagón, R.; Ochoa-Alejo, N. (2015). Tissue culture of ornamental cacti. Sci Agric 72(6):540–561. doi: 10.1590/0103-9016-2015-0012

Podio, M.; Felitti, S.A.; Siena, L.A.; Delgado, L.; Mancini, M.; Seijo, J.G.; González, A.M.; Pessino, S.C.; Ortiz, J.P.A. (2014). Characterization and expression analysis of

SOMATIC EMBRYOGENESIS RECEPTOR KINASE (*SERK*) genes in sexual and apomictic *Paspalum notatum*. Plant Mol Biol, 84:479-495. doi: 10.1007/s11103-013-0146-9.

Retes-Pruneda, J.L., Valadez-Aguilar, M.L., Pérez-Reyes, M.E. (2007). Propagación *in vitro* de especies de *Echinocereus, Escontria, Mammillaria, Melocactus* y *Polaskia* (Cactaceae). Bol Soc Bot Méx, 81:9-16. doi: 10.17129/botsci.1761

Rocha, D.I.; Monte-Bello, C.C.; Aizza, L.C.B.; Dornelas, M.C. (2016). A passion fruit putative ortholog of the *SOMATIC EMBRYOGENESIS RECEPTOR KINASE1* gene is expressed throughout the *in vitro de novo* shoot organogenesis developmental program. Plant Cell Tiss Organ Cult, 25(1):107-117. doi: 10.1007/s11240-015-0933-x

Rubluo, A. (1997). Micropropagation of *Mammillaria* species (Cactaceae). In: Bajaj YPS. (ed.) Biotechnology in agriculture and forestry 40. Springer-Verlag, Berlin and Heidelberg, pp. 193-205.

Saitou, N.; Nei, M. (1987). The neighbor-joining method: a new method for reconstructing phylogenetic trees. Mol Biol Evol, 4(4):406-425. doi: 10.1093/oxfordjournals.molbev.a040454

Sambrook, J.; Russell, D.W. (2001). Molecular Cloning, Third ed. Cold Spring Harbor Laboratory Press, Cold Spring Harbor, NY.

Sánchez, D.; Grego-Valencia, D.; Terrazas, T.; Arias, S. (2015). How and why does the areole meristem move in *Echinocereus* (Cactaceae)? Ann Bot, 115: 19-26. doi:10.1093/aob/mcu208

Santiago, J.; Henzler, C.; Hothorn, M. (2013). Molecular mechanism for plant steroid receptor activation by somatic embryogenesis coreceptor kinases. Science, 341:889–892. doi: 10.1126/science.1242468

Savona, M.; Mattioli, R.; Nigro, S.; Falasca, G.; Rovere, F.D.; Costantino, P.; de Vries, S.C.; Ruffoni, B.; Trovato, M.; Altamura, M.M. (2012). Two *SERK* genes are markers of pluripotency in *Cyclamen persicum* Mill. J Exp Bot, 63(1):471-488. doi: 10.1093/jxb/err295

Schmidt, E.D.L.; Guzzo, F.; Toonen, M.A.J.; de Vries, S.C. (1997). A leucine-rich repeat containing receptor-like kinase marks somatic plant cells competent to form embryos. Dev, 124:2049-2062.

Scholes, D.R.; Paige, K.N. (2016). Plasticity in ploidy: a generalized response to stress. Trends Plant Sci, 20(3):165–175. doi: 10.1016/j.tplants.2014.11.007

Sharma, S.K.; Millam, S.; Hein, I.; Bryan, G.J. (2008). Cloning and molecular characterisation of a potato *SERK* gene transcriptionally induced during initiation of somatic embryogenesis. Planta, 228:319-330. doi: 10.1007/s00425-008-0739-8

Singla, B.; Khurana, J.P.; Khurana, P. (2008). Characterization of three somatic embryogenesis receptor kinase genes from wheat, *Triticum aestivum*. Plant Cell Rep, 27:833-843. doi: 10.1007/s00299-008-0505-1

Téllez-Román, J.; López-Peralta, M.C.G.; Hernández-Meneses, E.; Estrada-Luna, A.A. Mancera, H.A.Z.; Muñoz, M.L. (2017). *In vitro* morphogenesis of *Mammillaria plumosa* Weber. Rev Mex Cienc Agric, 8(4):863-876.

Thomas, C.; Meyer, D.; Himber, C.; Steinmetz, A. (2004). Spatial expression of a sunflower *SERK* gene during induction of somaticembryogenesis and shoot organogenesis. Plant Physiol Biochem, 42:35-42. doi:10.1016/j.plaphy.2003.10.008

Torres-Silva, G.; Resende, S.V.; Lima-Brito, A.; Bezerra, H.B.; D, de Santana, J.R.F.; Schnadelbach, A.S. (2018). *In vitro* shoot production, morphological alterations and genetic instability of *Melocactus glaucescens* (Cactaceae), an endangered species endemic to eastern Brazil. S Afri J Bot, 115:100–107. doi: 10.1016/j.sajb.2018.01.001

Walker, J.C. (1994). Structure and function of the receptor-like protein kinases of higher plants. Plant Mol Biol, 26:1599-1609. doi: 10.1007/BF00016492

Xu, L. (2018). *De novo* root regeneration from leaf explants: wounding, auxin, and cell fate transition. Curr Opin Plant Biol, 41:39–45. doi: 10.1016/j.pbi.2017.08.004

9. TABLES, FIGURES AND LEGENDS

Table 1. Degenerated sequences used to amplify the coding sequence of *SERK*-like gene from cDNA of *Melocactus glaucescens* after shoot organogenesis induction.

Primers	Sequence	Structural Domain
Reverse	5' TGTHACRTGGGTRTCCTTGTARTCCAT 3'	Kinase VII
Reverse	5' CGRTGMACWGCCATRCTIATCAT 3'	Kinase III
Foward	5' GTGAAYCCTTGCACATGGTTYCATGT 3'	LRR
Foward	5' CCMTGYCCIGGATCTCCCCCITTT 3'	SPP
Foward	5' ATGTCACTSACYAATATYACWACYCTTCAAG 3'	ZIP

W = A or T; R = A or G; M = A or C; Y = C or T; H = A or C or T; S = C or G; D = A, G or T.

Table 2. SERK members used for the distance tree.

Species	Putative protein	GenBank access
Lactuca sativa	SERK1-like	XP_023770884.1
Beta vulgaris subsp. vulgaris	SERK2 isoform X1	XP_010692604.1
Spinacia oleracea	SERK2	XP_021847294.1
Chenopodium quinoa	SERK2	XP_021714851.1
Vitis vinifera	SERK1	XP_002270847.1
Arabidopsis thaliana	SERK1	NP_177328.1
Arabidopsis thaliana	SERK2	NP_174683.1
Arabidopsis thaliana	SERK3	NP_567920.1
Arabidopsis thaliana	SERK4	NP_178999.2
Arabidopsis thaliana	SERK5	NP_179000.3
Theobroma cacao	SERK1	XP_007020220.1
Theobroma cacao	SERK2	EOY17445.1
Theobroma cacao	SERK3	EOX98956.1
Ricinus communis	SERK1	EEF27892.1
Ricinus communis	SERK3	XP_002520631.1
Carica papaya	SERK	ABS32233.1
Carica papaya	SERK2	XP_021896015.1
Manihot sculenta	SERK2-like isoform X1	XP_021630230.1
Olea europa	SERK2-like isoform X2	XP_022885908.1
Helianthus annuus	SERK1-like isoform X1	XP_021992274.1
Morus notabilis	SERK2	XP_010094829.1
Malus domestica	SERK2	XP_008366148.1
Solanum lycopersicum	SERK1	NP_001233866.1
Glycine soja	SERK1	KHN17066.1
Setaria italica	SERK1-like	XP_004952868.1
Setaria italica	SERK2-like	XP_004972726.1
Brachypodium distachyon	SERK1	XP_003571417.2
Brachypodium distachyon	SERK2	XP_003575217.1
Arabidopsis thaliana	NIK1	NP_197104.1
Arabidopsis thaliana	NIK2	NP_189183.2
Arabidopsis thaliana	LRR II – RLK1	NP_568977.1
Arabidopsis thaliana	LRR II – RLK2	NP_201327.4

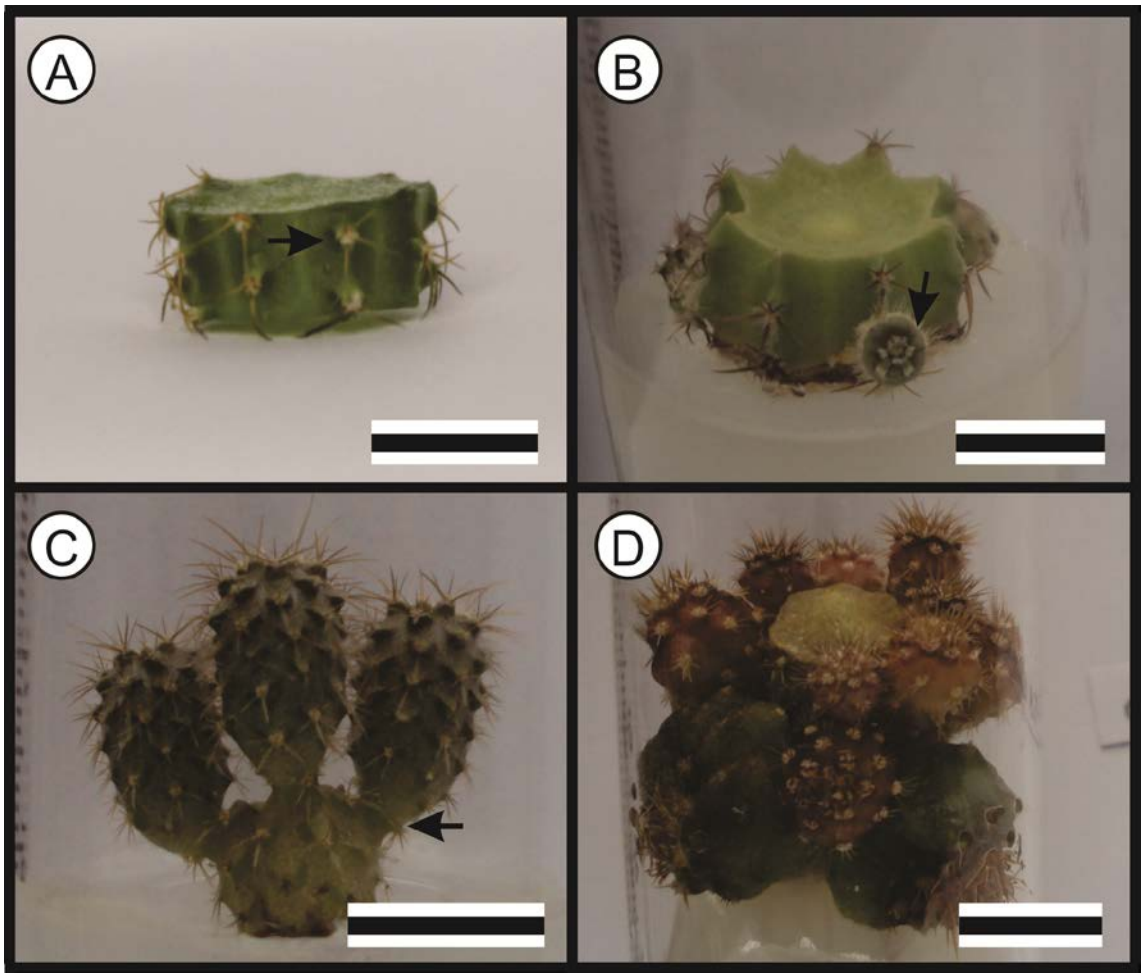

Figure 1. *Melocactus glaucescens in vitro* shoot production. [**A**] 3–4 mm of height explants placed horizontally position in the culture medium, arrow shows areola region. [**B**] Control explant after 30 days of culture showing shoots arising from areole region. [**C**] Control explants after 120 days of culture showing shoot with normal morphology. [**D**] Treated explant after 120 days of culture showing shoots with morphological alteration.

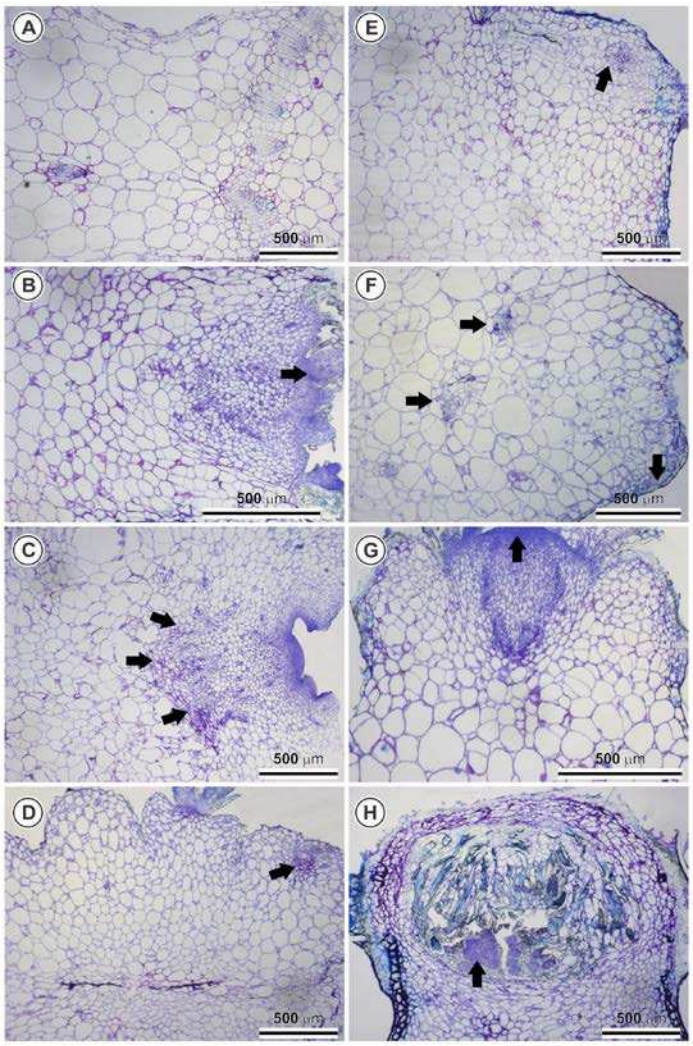

Figure 2. Toluidine blue test of *Melocactus glaucescens* [A to D] explant cultivated in PGR-free media (control) and [E to H] explant with areola region punctured and placed on 17.76 µM of BA and 1.34 µM of NAA (treated). [A] Transversal view of control explant with 10 days of culture. [B] Transversal view of control explant with 20 days of culture, showing axillary bud activation. [C] Longitudinal view of control explant with 50 days of culture, showing vascular reorganization. [D] Transversal view of control explant with 50 days of culture, arrow showing meristemoid. [E] Longitudinal view of treated explant with 10 days of culture, arrow showing meristemoid. [F] Transversal view of treated explant with 20 days of culture, arrow showing meristemoids. [G] Transversal view of treated explant with 30 days of culture, showing shoot initial formation from axillary bud. [H] Transversal view of treated explant with 50 days of culture, showing shoot formation inner part of explant.

.

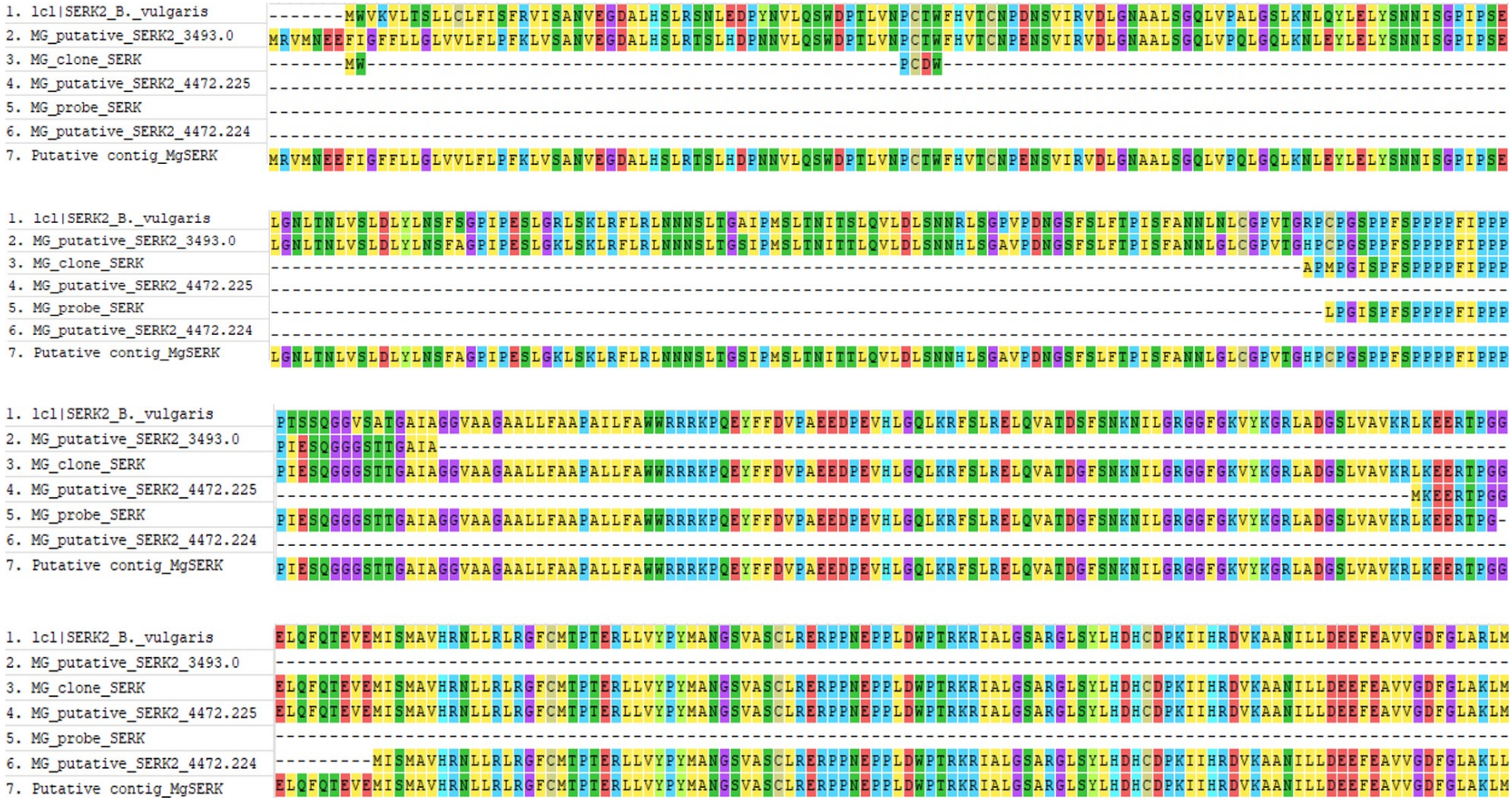
1. lcl|SERK2_B._vulgaris
2. MG_putative_SERK2_3493.0
3. MG_clone_SERK
4. MG_putative_SERK2_4472.225
5. MG_probe_SERK
6. MG_putative_SERK2_4472.224
7. Putative contig_MgSERK

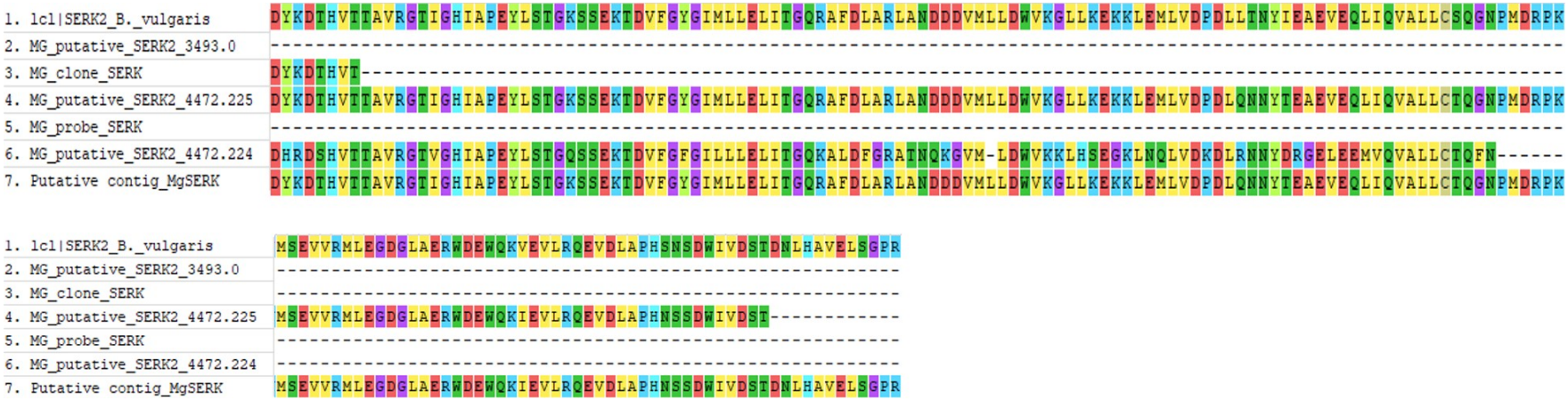

Figure 3. Alignment of *Melocactus glaucescens* nucleotide sequence of *MgSERK*-like reads. Comparison of *Beta vulgaris SERK2* nucleotide sequence with *M. glaucescens* putative *SERK* from transcriptome (clusters 3493.0; 4472.224, and 4472.225), *M. glaucescens* clone from amplification with degenerated primers, *M. glaucescens* probe used to *in situ* hybridization experiments, and the contig of the putative *M. glaucescens SERK-like* sequence.

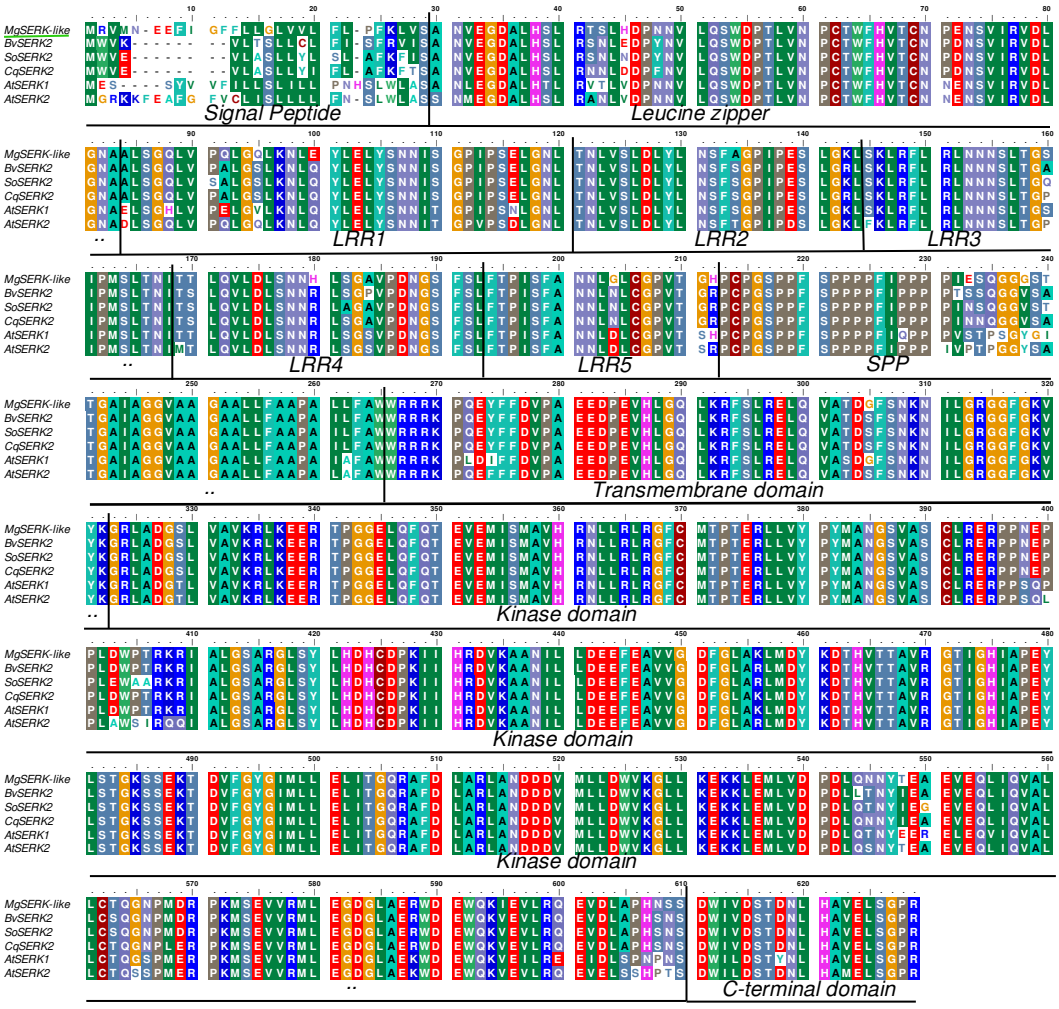

Figure 4. Multiple alignment of predicted *Melocactus glaucescens SERK*-like (*MgSERK*-like) amino acids sequences with *Beta vulgaris SERK2* (*BvSERK2*), *Spinacia oleracea SERK2* (*SoSERK2*), *Carica papaya SERK2* (*CpSERK2*), and *Arabidopsis thaliana SERK1*(*AtSERK1*) and *SERK2* (*AtSERK2*) homologues available in NCBI.

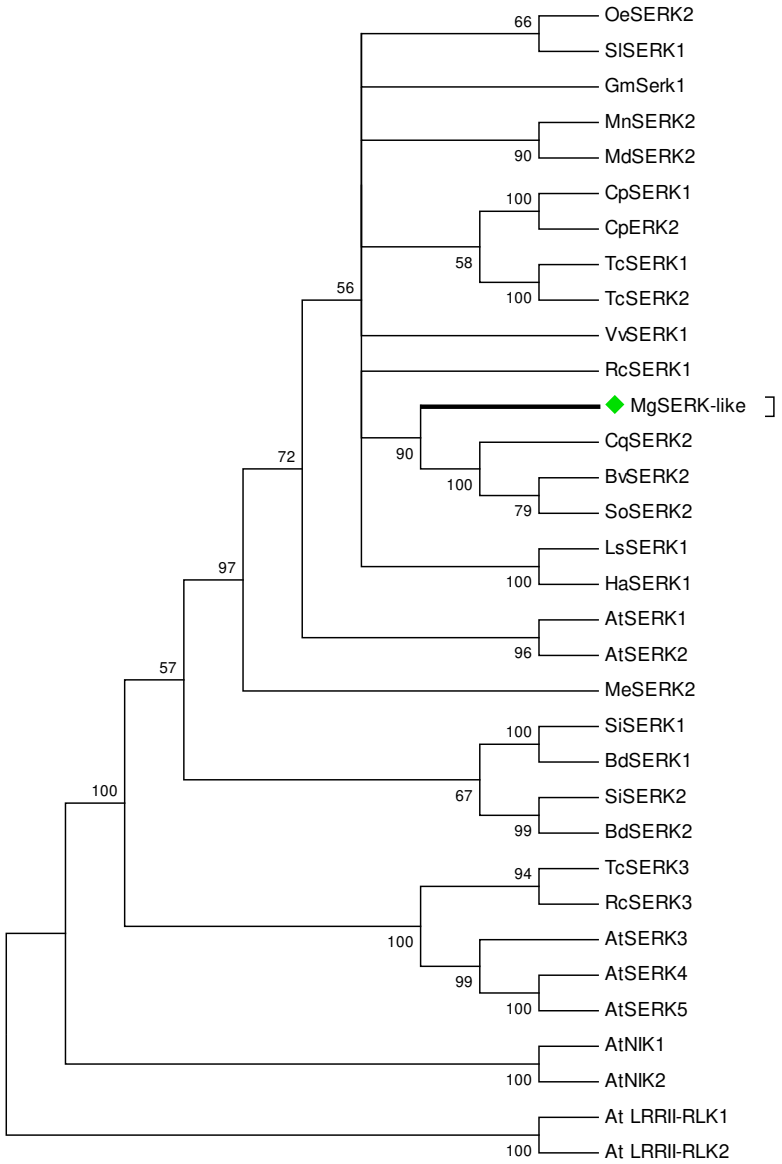

Figure 5. Similarity tree using the using the Neighbor-Joining method. The optimal tree with the sum of branch length = 3.62473858 is shown. The percentage of replicate trees in which the associated taxa clustered together in the bootstrap test (1000 replicates) is shown next to the branches. The evolutionary distances were computed using the JTT matrix-based method and are in the units of the number of amino acid substitutions per site. The rate variation among sites was modeled with a gamma distribution (shape parameter = 1). The analysis involved 33 amino acid sequences. All positions with less than 95% site coverage were eliminated. That is, fewer than 5% alignment gaps, missing data, and ambiguous bases were allowed at any position. There were a total of 574 positions in the final dataset.

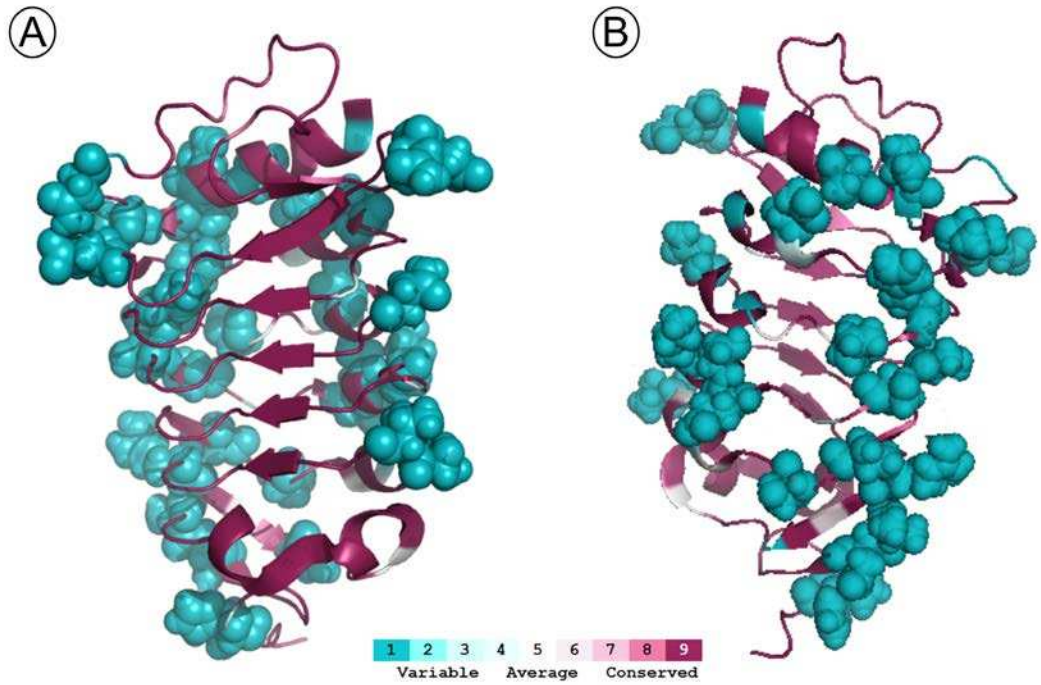

Figure 6. *Melocactus glaucescens* MgSERK-like protein structure showing the amino acid conservation determined by the ConSurf webserver (Ashkenazy et al. 2010), which were plotted onto the reported structure of the SERK1 protein extracellular domain (PDB:4LSC; Santiago et al. 2013), and using as an input 16 multiple sequences of other SERK1 and SERK2 members, with MgSERK-like as query sequence. Highly conserved residues are plotted in magenta, whereas lower scores are depicted by other color shades, with cyan depicting more variable residues, which [A] is the concave or solvent-exposed side, and [B] is the convex side of the MgSERK-like extracellular domain.

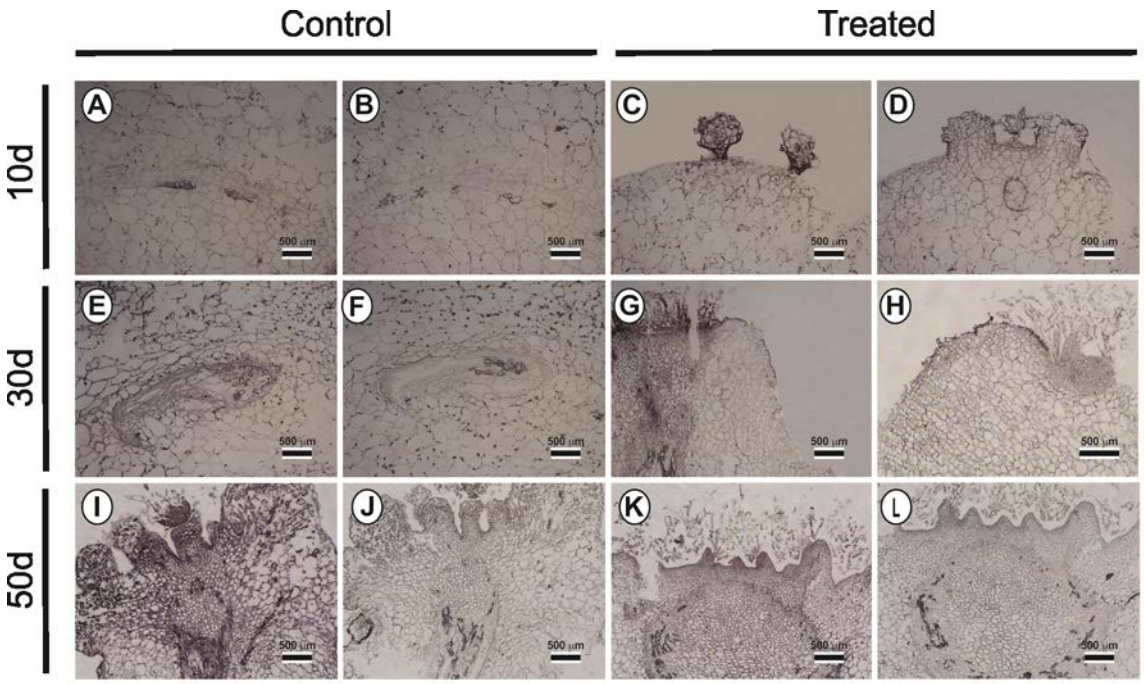

Figure 7. *In situ* hybridization of *Melocactus glaucescens SERK*-like gene expression. [A, B, E, F, I, and J] Explant cultivated in PGR-free media, which [A, E, and I] probe hybridization of *MgSERK*-like, and [B, F, and J] negative control. [C, D, G, H, K, and L] Explant with areola region punctured and placed on 17.76 µM of BA and 1.34 µM of NAA, which [C, G, and K] probe hybridization of *MgSERK*-like, and [D, H, and L] negative control.

CHAPTER 3

A transcriptome analysis of *Melocactus glaucescens* (Cactaceae) reveals changes in the metabolism during *in vitro* shoot organogenesis induction

ABSTRACT

Melocactus glaucescens is an endangered cacti species with ornamental value. *In vitro* culture protocols were previously developed aiming the shoot production of this species as an alternative to its overharvesting. No transcriptome data are available for the regeneration of any Cactaceae member, and *M. glaucescens de novo* transcriptome can be used as a tool to support researches in the molecular regulation of development processes to improve the propagation of these plants. In order to investigate the *in vitro* shoot organogenesis (SO)-induction in *M. glaucescens,* RNA total was extract from explants before (control) and after SO-induction (treated). Libraries were prepared, new generation sequencing was performed using Illumina HiSeq 3000, and *de novo* transcriptome assembly was conducted using pipeline with Timmomatic, FastQC, Trinity, CD-HIT, Salmon, Corset, and STAR programs. Differential expression (DE) analyses were performed using edgeR, and enrichments were conducted in Blast2GO, KEGG, BiNGO and PlantTFDB. A total of 14,478 unigenes (average length = 520 bases) was obtained covering the transcripts in control and treated explants. After normalization, the total of unigenes in *M. glaucescens* transcriptome was 2,058. In pairwise treated vs. control, 1,241 (60.3 %) unigenes had no significant changes in expression, 226 (11 %) were transcripts with DE in control explants, and 591 (28.7%) were transcripts with DE in treated explants. The general view of enrichment analyses indicate that the transcripts with DE in control samples has a disperse pattern in BiNGO graphics, and transcripts with DE in treated samples show a more concentrated pattern. Transcription factors (TFs) content diverged between treatments, which treated samples presented more TFs families and more TFs unigenes among their transcripts. To validate the transcriptome sequences, the *calmodulin* gene expression was assessed, being upregulated in treated, compared to the control. Differences between control and treated transcripts indicate substantial changes in the metabolism of *M. glaucescens* after SO induction. These results bring new data that will benefit researches in molecular genetics and functional genomics for Cactaceae family.

Keywords: Cacti, Next Generation Sequencing, RNA-seq, *Calmodulin*.

1. INTRODUCTION

The remarkable ability to regenerate and form an entire plant body from various tissues or organs, or even from a single somatic cell, is the basis for the application of tissue culture techniques and for the establishment of plant regeneration systems (Rocha et al. 2016, Cervantes-Pérez et al. 2018). Tissue culture techniques allow the *in vitro* propagation of plant material in large scale, with high rates of multiplication in short period, reduced space and free of pathogens, accelerating the growth of the plants (Pérez-Molphe-Balch et al. 2015)

In the case of Cactaceae, *in vitro* methods of regeneration represent an alternative to the conventional propagation of this family, which comprises threatened species with slow growth (Lema-Rumińska and Kulus 2014, Goettsch et al. 2015, Pérez-Molphe-Balch et al. 2015). *Melocactus glaucescens* Buining & Brederoo *in vitro* culture protocols were performed aiming the shoot production as an alternative to its overharvesting (Torres-Silva et al. 2018). This species has high commercial value as ornamental plants and are illegally collected from their natural habitats (Machado 2009). This fact, associated to its natural habitat degradation, included *M. glaucescens* in the Convention on International Trade in Endangered Species of Wild Fauna and Flora (CITES 2018) and in the IUCN Red List of Threatened Species (IUCN 2018).

M. glaucescens reproduces sexually in natural conditions, and do not ramify or produces lateral shoots, unless the plant suffers some injury (Machado 2009). Recent *in vitro* shoot production protocol allowed increase the number of shoots per explant with wounding and use of plant growth regulators (*data not published – see chapter 2*). However, there are still some challenges in *M. glaucescens in vitro* propagation (i. e. high proportion of shoot with morphological and physiological alterations) and the generation of a transcriptome profile will allow the access of molecular studies to better understand the development and the physiology of this species.

Transcriptomic data mining is an efficient way to discover genes or gene families encoding enzymes involved in various physiological pathways (Xiao et al. 2013, Nadiyra et al. 2018). As with many plant physiological and developmental processes, *Arabidopsis thaliana* is the most explored model in plant regeneration and transcriptomic data for callus and callus-mediated regeneration are available (Sugimoto

et al. 2010). This valuable approach to the basic understanding of the process, however, is relatively unexplored for non-model plants such as *M. glaucescens*.

Major challenges for the *de novo* assembly of higher eukaryotic transcriptomes include difficulties associated with handling increasingly large datasets, the wide range in the coverage depth of transcripts, and the identification of alternative splice variants (Xiao et al. 2013). In differential expression analysis, the challenge is related to the few well-characterized model organisms, which may lead to non-characterization of many transcripts from non-model transcriptomes (Brereton et al. 2016)

Genomic analysis of non-model *M. glaucescens* is also limited by the small quantity of publicly available sequence data for cacti, since so far just the transcriptome *Hylocereus polyrhizus* fruits is available (Quingzhu et al. 2016). Despite the many challenges, RNA-seq has been applied to hundreds of non-model plants, and it is a helpful tool to interpret the gene content of an organism where the genome sequence is not available (Garg and Jain 2013, Xiao et al. 2013).

The transcriptome data provide a valuable resource for rapid elucidation of pathways and their mapping through graphical connectivity diagrams along with the identification and subsequent characterization of biosynthesis pathways genes, transcription factor (TFs), microRNAs (miRNAs), transporters and others (Pal et al. 2018). To date, no transcriptome for the regeneration of any Cactaceae member is available. The *M. glaucescens* transcriptome can be used as a tool to support researches in molecular regulation of the development processes to improve the massive propagation of members of this family.

Another well-documented application to the transcriptome dataset is the identification and characterization of transcripts that potentially contribute to the use of the plant to pharmaceutical and food industry purposes (Chakrabarti et al. 2016, Pal et al. 2018). Cactaceae members have been shown many important and desirable biological activities as anti-atherosclerosis (Kwon and Song 2005), anticancer (Yoon et al. 2009a, Yoon et al. 2009b), antibacterial (Lee et al. 2004), antioxidant (Lee et al. 2005a, Park et al. 2005), anti-inflammatory (Lee et al. 2005b), hypoglycemic and hypolipidemic (Kwon and Song 2005). *M. glaucescens* transcriptome may open for

future investigations of how the biotechnological use of genetic resources of this species can be applied to others commercial purpose.

The goal of this study was to characterize the changes in gene expression that follow the organogenic regeneration in the non-model species *M. glaucescens*. The characterization of *M. glaucescens* regulatory networks should provide new insights into the physiological mechanisms that trigger the regeneration in cacti species that do not naturally emit branches. This work also provides useful information to consider others purposes besides ornamental to micropropagated *M. glaucescens*.

2. MATERIALS AND METHODS

Plant material

Plant material for all analysis were obtained from *in vitro* germination of *M. glaucescens* seeds collected from natural populations located in Morro do Chapeu city, Bahia State, eastern Brazil (11°29′38.4′S; 41°20′22.5′W). The seeds were disinfected with 96% ethanol for 1 minute, 2% NaClO (SuperGlobo®) for 10 min, and subsequently washed thrice in deionized and sterile water. Afterwards, seeds were germinated in 500 mL flasks containing 50 mL of MS culture media (Murashige and Skoog 1962) at quarter-strength concentration supplemented with 15 g L^{-1} sucrose and solidified with 7 g L^{-1} agar. Cultures were maintained at 25±3°C under two fluorescent lamps with photosynthetically active radiation levels of 60 $\mu molm^{-2}s^{-1}$ and a 16/8-h light/dark photoperiod.

Shoot organogenesis induction

Plants germinated *in vitro* for 380 days had their apical cladode segments removed and were sectioned transversely generating explants 3–4 mm in height (Torres-Silva et al. 2018). From the same plant, one explant was stocked on liquid nitrogen immediately after excision to be used as the control (Figure 1.aA). Another explant from the same plant had its areola regions punctured thrice with 0.18 x 8 mm needles (DBC132, Dong Bang Acupuncture Inc., Chungnam, South Korea), and was then placed on MS full-strength media supplemented with 17.76 µM of benzylaminopurine (BA) and 1.34 µM of ∞-naphthalene acetic acid (NAA) to induce shoot organogenesis (SO) for 30 days. This explant is referred to as "treated" (Figure 1.aB). Cultures were maintained at 25±3°C under two fluorescent lamps with photosynthetically active radiation levels of 60 $\mu mol\ m^{-2}\ s^{-1}$ and a 16/8-h light/dark photoperiod.

RNA isolation

Tissues from explants of control and treated were grinded with liquid nitrogen and total RNA was extracted with a Tris®-Reagent (Sigma) method, according to

manufacturer's instructions. A volume of 500 µL of Tris®-Reagent and 50 µL of chloroform:isoamyl alcohol (24:1) were added to 500 mg of frozen tissue. The mixture was vortexed and stored in ice for 5 min, then centrifuged at 12,000 xg for 15 min at 4˚C. The aqueous phase was separated in a new microtube and an equal volume of isopropanol for RNA precipitation was added. After incubation of 2h at -20 ˚C, the material was centrifuged again in 12,000 xg for 30 min at 4˚C. The pellet was washed in 1 mL of 70% ethanol, dried, and eluted in diethylpyrocarbonate water (DEPC, Sigma).

Library preparations and sequencing for RNA-seq

From total extracted RNA, mRNA was obtained with Dynabeads Oligo (dT) 25 (Thermo Fisher) and fragmented to approximated 400 nucleotides. The fragmented mRNA was converted to double-stranded DNA using random hexamer primers and appropriate enzymes, which subsequently followed standard DNA library preparation for sequencing. Briefly, cDNA was end-repaired, phosphorylated and adenylated. Common TruSeq adapters containing 8 bp indexes (i5 and i7) suited for Illumina sequencing were ligated to the adenylated molecules and the resulting libraries were amplified with 13 cycles of PCR to enrich the libraries for properly ligated molecules.

The final libraries were quantified using PicoGreen (Thermo Fisher) and equimolarly combined into a single sample, which was then sequenced on an Illumina HiSeq 3000 (Illumina Inc.) machine, to get paired-end reads with an average length of 100bps. Libraries preparation and sequencing was carried out by RAPiD Genomics, LLC (Geinesville, Florida, USA). The raw sequence reads for *M. glaucescens* tissues reported in this study have been deposited in NCBI GEO together with the expression data and *de novo* transcriptome assembly and can be accessed through GEO accession number (XXXXXX).

De novo *transcriptome reference assembling*

RNA-seq reads were processed using Trimmomatic (Bolger et al. 2014) to remove adaptor sequences, short reads, and low quality reads, resulting in paired-end cleaned reads together with unpaired reads that lost their corresponding partner

sequence. FastQC were used before and after cleaning to check quality. Low-quality (with < 20 Phred scores) reads in raw reads were removed with Fastq_clean (Zhang M. et al., 2014) and assessed with FastQC. The clean reads thus obtained were used to assemble a *de novo* transcriptome using Trinity (Grabherr et al. 2011). Additionally, a metric of gene completeness of all these assemblies was determined with BUSCO ver 2.0 (Figure 1b).

Construction of SuperTranscript

In order to analyze the differential expression between control and treated tissues of *M. glaucescens,* a SuperTranscript were made with the representation of all isoforms by a single non-redundant contig. Briefly, all reads from both treatments were collapsed generating a single file using CD-HIT-EST version 4.7 (Li and Godzik 2006) with sequence identity cut-off (-c) 0.98. After, the reads from each treatment were aligned with the cd-hit fasta file and the transcript abundance was quantified by Salmon. The next step was the forming of clusters using shared reads and expression by Corset (version 1.03) (Davidson and Oshlack 2014). Finally, the clusters were transformed in single sequence (SuperTranscript) containing combined information from all isoforms (Davidson et al. 2017). The alignment and quantification of SuperTranscript sequences was made with STAR (Dobin et al. 2013), and it was possible to identify uniquely mapped reads, mismatch rate per base, number of reads mapped to multipleloci, and number of chimeric reads (Figure 1b).

Differential expression analyses

The counts of SuperTrancript clusters generated by STAR were used to perform the differential expression (DE) analyses between control and treated *M. glaucescens* explants in the bioconductor package edgerR (Robinson et al. 2010), with parameter settings fold change (log2) >2 and p value<0.05. edgeR evaluates the genewise dispersions through conditional maximum likelihood, conditioning towards the total count for that gene which enables differential expression analysis for each gene among the samples (Robinson et al. 2010). The control samples were used to compare

the upregulation and downregulation of genes between treated and control *M. glaucescens* explants (Figure 1b).

For the enrichment analysis, BLAST results against NCBI database were imported into Blast2GO and Gene Ontology (GO) annotations and Enzyme Commission (EC) classifications were performed in Blast2GO (Conesa and Götz 2007). Further functional analysis of the transcriptome was performed in the Kyoto Encyclopedia of Genes and Genomes (KEGG) Automatic Annotation Server (KAAS) (http://www.genome.jp/tools/kaas/) to assign KEGG Orthology (KO) terms to the transcripts and also to map them to KEGG pathways (Kanehisa et al. 2007). Interactive graphs of genes expression in both treatments was carried out by BiNGO (Maere et al. 2005) and the result was displayed by Cytoscape 3.4.0 (http://www.cytoscape.org) (Figure 1b).

The enrichment of transcription factors (TFs) was performed with Plant Transcription Factor Database v4.0 (PlantTFDB) (http://planttfdb.cbi.pku.edu.cn/) (Jin et al. 2017). *M. glaucescens* transcripts DE in both treatments were subjected to BLASTx analysis against PlantTFDB of *B. vulgaris*, with scoring matrix BLOSUM62, and expect threshold of 0.1 (Figure 1b).

cDNA synthesis and qPCR validation of DE genes

Total RNA from three plants from each treatment were used to synthesize the cDNAs single strands. For this purpose, total RNA (3.0 µg) was used with the kit Super Script TM II, First- Strand Synthesis System (Invitrogen™), according to the manufacturer's recommendations.

Sequences for *calmodulin* (*CaM*), used as a target, and *glyceraldehyde-3-phosphate dehydrogenase* (*GAPDH*), used as an internal reference, were obtained from the *M. glaucescens* transcriptome. The primers were designed using NCBI Primer-BLAST (http://www.ncbi.nlm.nih.gov/tools/primer-blast/index.cgi?LINK_LOC=BlastHome), with the settings: primer melting temperature, 60 °C; primer GC content, 50–60%; and PCR product size, 100–200 base pairs. Real-time RT-PCR was performed on a CFX96 Touch™ Real-Time PCR Detection System (BIO-RAD), using qPCR-SYBR-Green mix/Rox (Ludwig Biotec®, Alvorada, RS,

Brazil). The qPCR reactions were carried out in duplicate for three biological replicates, in a reaction volume of 10 µL (4 µL SYBR-Green, 1 µL (4 µM) each primer, 3 µL diethylpyrocarbonate-treated water and 1 µL (40 ng) cDNA sample). The amplification conditions were performed using the following steps: 2 min at 50ºC and 10 min at 95ºC, followed by 40 cycles of 95ºC for 16 s and 60ºC for 60 s, and the melting curve performed from 60 to 95°C at 0.1°C/s. The comparative cycle threshold method ($2^{-\Delta\Delta Ct}$) (Livak and Schmittgen 2001) was applied to calculate the fold-change of the target genes.

3. RESULTS

Illumina sequencing and de novo *assembly of the* M. glaucescens *transcriptome*

In order to investigate how the expression changes in SO of *M. glaucescens*, explants no submitted (control) and submitted (treated) to SO were investigated on Illumina HiSeq3000 instrument. The initial processing of these data involved removal of ribosomal RNA-related reads and subsequent demultiplexing and trimming to remove the Illumina adapter sequences, this process altogether generated ~25 million processed reads. In assembly statistics, the percentage of Ns was observed to be minimal, no contigs were observed with reads without a quality value, and STAR did not detect chimeric sequences (Table 2).

A total of 2,231 assembled transcripts with an average length of 527 bp and average GC content of 55% were obtained for control explants (Table 2). The maximum size of transcript amongst the assembled transcript was 7,366 bp while the minimum transcript size obtained was 201 bp long. Differently, for treated explants, a total of 12,247 transcripts were obtained. Similarly with control, treated transcripts showed average length of 513 bp, average GC content of 54%, and the maximum and minimum transcript sizes for the assembled transcripts were 7,403 and 201 bp, respectively.

For developing the differential expression analysis, control (CTL) and treated (TRT) samples were first analyzed separately based on multidimensional scaling with the biological coefficient of variation (BCV). The relationship in the plot indicates that control and treated samples can be separated by the BCV distance 1, and the genotypes can be separated by the BCV distance 2, where control and treated samples from plants 3 and 5 are localized up the plot, and control and treated samples from plants 1, 2 and 4 are localized down the plot (Figure 2).

Differential expression analysis

The *M. glaucescens* transcriptome was functionally annotated using Blast2GO (Conesa et al. 2005). The output of a BLASTx comparison of the *M. glaucescens* contigs against the NCBI database was imported in Blast2GO to carry out GO mapping and functional characterization. Transcripts were grouped into three main GO categories: molecular function, biological processes, and cellular component. In the

molecular function category, catalytic activity and binding are the most highly represented groups. In the biological process category, cellular process is the most abundant groups, followed by regulation of biological process, metabolic process, biological regulation and response to stimulus. In the cellular component category, cell, cell part, and organelle are the most highly represented groups.

Utilizing RNA-seq data, the differential expression profile of control and treated *M. glaucescens* explants were constructed. To quantify the gene expression levels, total mapped reads corresponding to each gene were calculated and normalized the reads to compare the gene expression level between the two samples and allowed the identification of upregulated and downregulated unigenes in both control and treated *M. glaucescens*. After normalization the total of unigenes in *M. glaucescens* transcriptome were 2,058. In pairwise treated vs. control, 1,241 (60.3 %) unigenes have no significant changes in expression, 226 (11 %) were downregulated, and 591 (28.7%) were upregulated in treated explants.

On further analysis, the unigenes were categorized into 44 functional classes, where the most frequent functional groups in the molecular function category were catalytic activity (247 unigenes) and binding (223 unigenes). The most highly represented group in the biological process category was cellular process (255 unigenes). In the cellular component category, cell (229 unigenes) and cell part (227 unigenes) were the most highly represented groups. Functional profile comparing control and treated samples reveled that treated has more unigenes expressed in all GO groups in all GO categories, except in nucleoid group, which control has two unigenes and treated has no unigenes (Figure 5).

Pathway mapping using KEGG and BiNGO

KEGG automatic annotation server (KAAS) was employed to map transcripts onto their biological pathways. Bi-directional best hit scheme was employed for KEGG orthology (KO) assignments with default BHR (> 0.95). KEGG pathway mapping of *M. glaucescens* genes overexpressed in control and treated explants resulted in 748 unigenes assigned to 233 KEGG pathways (Table 3). Transcripts downregulated (i. e. transcripts DE in control samples) do not were categorized in the same KEGG pathways

than transcripts DE in treated samples, which indicate that SO-induction plays a distinct role in the cacti metabolism.

Some KEGG pathways were observed in both treatments but the transcripts were not the same (indicated with *) (i. e. KEGG pathways related to amino acids metabolism and ribosome), which indicate that these pathways were redirected to attend to SO metabolic demands. Few KEGG pathways were observed only in control samples (i. e. photosynthesis and antenna proteins), indicating photoautotrophic growth of control samples. DE transcripts from treated samples presented some KEGG pathways related to transcription demands, signaling, cell cycle, cytoskeletal rearrangement, cell differentiation, and mitochondrial dysfunction (Table 3).

BiNGO analysis of the GO categories assigned to *M. glaucescens* transcriptome identified three major categories of GOs that were statistically overrepresented in treated compared to control samples (Figure 6). The general view of BiNGO analyses was that the unigenes expressed exclusively in control has a disperse pattern, with smaller bubbles and in higher number than in the treated. Treated analysis showed a pattern more concentrated in certain categories, such as metabolic metabolism, cellular metabolism, and macromolecule metabolic processes for biological process category. For cellular compound, the most abundant groups were cell wall, extracellular region, ribosome and vacuole. In the molecular function category, catalytic activity (lyase and hydrolase activities) and enzyme regulator activity are the most highly represented groups.

Analysis of transcription factors (TFs)

A transcription factor represents multigene family which plays significant roles in gene expression regulation during various stages of plant development and other metabolic processes. BLASTx of DE unigenes from control and treated samples against *Beta vulgaris* TF database allowed identifying 177 TFs representing 39 families. The most abundant family observed was C3H (20) followed by LBD (16), C2H2 (11), WRKY (10), HB-other (9), ERF (9), HSF (8), and bHLH (7). Remarkable differential expression of TFs was observed between the control and treated explants of *M.*

glaucescens due to the occurrence of six TRs family members only in control samples, and 14 only in treated samples (Table 4).

Validation of the expression profile of Calmodulin by real time qPCR

To validate the candidate genes obtained from the comparative transcriptome analysis, the real time PCR were performed with *CaM* (target) and *GAPDH* (internal reference) genes in control and treated explants. The results revealed by real time qPCR (Figure 7) show that the expression patterns of *CaM* were consistent with the obtained by transcriptome analysis, indicating the reliability of the transcriptome data in this study.

4. DISCUSSION

This study is the first application of RNA-seq data to explore the transcript expression levels of the non-model plant *M. glaucescens* aiming to detect the genes participating in the SO pathways. One of the major challenges in annotating transcriptomes of non-model species is that many nonmodel-transcripts can still be characterized as such, were not annotated, or were very divergent from models species to be recognized (Brereton et al. 2016), as observed by the unspecificity in many KEGG pathways of this study (Table 3).

M. glaucescens transcript profile was performed comparing explant before (control) and after (treated) SO-induction, aiming at highlighting the differences occurred in metabolism caused by *in vitro* shoot organogenesis. The biological coefficients of variation "treatment" (dimension 1) as well as "genotype" (dimension 2) clearly separate control and treated samples (Figure 2), which indicate that not just the growth conditions, but also the genotype plays an important role on SO-induction response in *M. glaucescens*. This is in line with Torres-Silva et al. (2018) that reported the absence of relationship between morphological alterations and somaclonal variation occurred in the *in vitro* shoot production of *M. glaucescens*.

The changes in GO categories reflect the large reorganization that treated explants were undergoing during regeneration. Genes related to mitochondria, cell wall, ER, cell organization, and biogenesis were highly upregulated during SO-induction. This is a likely consequence of increased protein synthesis to support cell division and wall formation during regeneration (Bao et al. 2009). Conversely, chloroplast/plastid genes were strongly downregulated during SO-induction, which likely corresponds to the transition from photoautotrophy to photoheterotrophy at this developmental modification. The same pattern of expression was also observed in the regeneration of *Populus* and *Agave salmiana*, indicating that the cellular changes during regeneration is conserved among these species (Bao et al. 2009, Cervantes-Pérez et al. 2018).

The general view of DE enrichment analyses also indicates substantial changes in the metabolism of *M. glaucescens* explants for the occurrence of SO. The presence of common genes in control and treated transcriptomes (60.3%) infers the common function of genes in various physio-biological processes in *M. glaucescens,* which may

be responsible for fundamental processes as well as defense responses to *in vitro* conditions.

The unique genes present in treated (and/or control) transcriptomes might be due the metabolism modification occurred in *M. glaucescens* explants during SO-inductions, which is consider to promote remarkable changes in the gene expression pattern (Zhao et al. 2008). Changes in cell fate occurs by a new balance established between euchromatin and heterochromatin, implicating in dynamic changes in chromatin structure (Zhao et al. 2008), which was observed with the presence of histone-encoding among the transcripts with DE in treated samples.

TFs content diverged between control and treated explants, which treated samples presented more TFs families and higher number of TFs unigenes among its transcripts (Table 4). Transcription factors and regulators act either as expression of activators or repressors resulting in increased or decreased mRNA accumulation depending on the tissue type or changes in environment (Nadiyra et al. 2018). The higher abundance of TFs in treated samples indicates that many metabolic pathways are activated during SO-induction. TFs families upregulated in treated samples (i. e. NF-Y, MYB, ERF, E2F, LBD, and NAC) showed similarity with others studies of plant organogenesis, confirming the acting of these TFs in plant regeneration (Cheong et al. 2002, Bao et al. 2009, Cervantes-Pérez et al. 2018, Nadiyra et al. 2018, Pal et al. 2018).

Control samples metabolism is involved in photoautotrophy and apical dominance

Control samples represent the metabolism of *M. glaucescens* during *in vitro* culture growth before SO-induction. The expression of genes downregulated in treated explants (i.e. transcripts with DE in control explants) related to the control were lower than the upregulated, corroborating with the low growth rate observed in cacti cultures (Lema-Rumińska and Kulus 2014, Pérez-Molphe-Balch et al. 2015). Analysis of transcripts with DE in control samples in GO annotation, KEGG, BiNGO and PlantTFDB showed that its expression profile is largely involved with the primary metabolism. Transcripts DE in control samples presented 15 unigenes related to photosynthesis and 5 related to antenna proteins in KEGG pathways (Table 3), as well as a large numbers of photosynthesis-related bubbles in BiNGO graphs.

In vitro plant tissue cultures are established in closed culture vessels to control microbial contamination, which creates a limitation on the CO_2 availability and an exogenous carbon source (i. e. sucrose) in the culture medium is required (Batista et al. 2018). As observed before to *Euphorbia characia,* when sucrose is no longer available, photosynthetic carbon fixation is reestablished, which confers a photoautotrophic growth to the cultures and is considered a physiological adaptation of cultures to changes in the environment (Hardy et al. 1987). Possibly the explants metabolism changed to the photoheterotrophy when submitted to SO, when the metabolism was directed to the organogenesis.

Few TFs were observed only in DE transcripts from control samples. Teosinte branched1/Cycloidea/Proliferating cell factor (TCP) family was the TF family present in more abundance (5 unigenes) and exclusively in transcripts DE in control samples. TCPs were largely studied to determine strong apical dominance in domesticated maize (Martín-Trillo and Cubas 2010). Thus, TCP may plays a significant role determining the no-branch in *M. glaucescens,* and can be an important target to future studies improving the SO-induction in cacti that naturally do not emit lateral branches.

SO-changes in plant hormone signal transduction

Plant hormone signal transduction pathways were changed during SO in *M. glaucescens.* Treated samples presented 9 upregulated unigenes related to auxins (auxin response protein IAA, auxin responsive GH3 gene family, and small auxin upregulated RNAs family), gibberellins (DELLA protein), abscisic acid (abscisic acid receptor PYR/PYL family), ethylene (EIN3-binding F-box protein and ethylene-insensitive protein 3), and brassinosteroids (BR-signaling kinase and protein brassinosteroid insensitive 2) in KEGG analysis, which indicates that stem growth, cell elongation, and cell division pathways were significantly activated during SO-induction (Ikeuchi et al. 2019).

Different unigenes belonging to *SMALL AUXIN UPREGULATED RNAs* (*SAUR*) family were observed in both transcripts DE in control and treated samples. *SAUR* are small transcripts that rapidly responded to auxin, and its proteins are related to auxin-induced cell elongation that occurs according to the acid growth theory

(Stortenbeker and Bemer 2018). Most higher plant species contain between 60 and 140 *SAUR* genes in their genomes (Stortenbeker and Bemer 2018), and different members of this family were observed in *M. glaucescens* explants before (control) and after (treated) SO-induction. This fact indicates that auxin-responses to promote cell elongation and growth may occur differently during or not SO-induction. The occurrence of TFs that promotes cell elongation exclusively in control samples (i. e. ARF and GRF) also supports this hypothesis.

WIND1 *was upregulated in treated samples*

WOUND INDUCED DEDIFFERENTIATION1 (*WIND1*) was upregulated in *M. glaucescens* treated explants. *WIND1* expression is related to acquisition of regeneration competency in the culture system and its transcripts are observed at the wound site of *A. thaliana* root explants, indicating that one role of the wounding step is to increase the expression of key factors such as *WIND1* (Iwase et al. 2015).

Wound signals act immediately after occur the damage (Xu et al. 2018). The first changes are quick physical and chemical responses to wounding, probably involving alterations in plasma transmembrane potential and intracellular Ca^{2+} concentration, and H_2O_2 generation. Side effects are reported as changes in the production of plant hormones, but the pathways that connect wound signaling, *WIND1* expression, and the production of plant hormones to promote organogenesis are still unclear (Iwase et al. 2015, Xu et al. 2018).

PEROXIDASE 9 and *PEROXIDASE 12*, and calcium (Ca^{2+}) sensor protein (*CaM*) was present among the transcripts DE in treated samples, which indicate that metabolism was modulated by the wounding stimulus. *WIND1* was present among transcripts DE in treated samples after 30 days of SO-induction, indicating that *WIND1* might be related to long-term responses to wounding and is involved in *M. glaucescens* SO.

CaM *expression pattern validated the* M. glaucescens *transcriptome*

CaM was upregulated in *M. glaucescens* treated explants after 30 days of SO-induction, and its expression profile was validated by real time RT-qPCR (Figure 7). Plants have adopted Ca^{2+} as a versatile second messenger in various responses to abiotic and biotic stimuli (i. e. light, temperature, mechanical disturbance, drought, osmotic stresses, plant hormones and pathogen elicitors), and CaM is one of the main type of Ca^{2+} sensor proteins in plants (Hashimoto and Kudla 2011, Zeng et al. 2015). CaM decodes specific signals to generate specific or overlapping responses to increased cellular Ca^{2+} concentration (Zeng et al. 2015).

In *Arabidopsis*, seven genes encode four *CaM* isoforms (CaM1/4; CaM2/3/5; CaM6; CaM7), and the differences between them can account for a differential interaction/activation of CaM target by diverse CaM isoforms and CaM-related proteins (Ranty et al. 2006, Kushwaha et al. 2008). In SO-induction of *M. glaucescens*, CaM was related to 16% of the KEGG pathways, linked to immune system, signaling, senescence, phototransduction, and secretion (Table 3 and Figure 5). These results are in agreement with the large repertoire of CaM target proteins that are known to act in ions homeostasis, metabolism, hormone biosynthesis, and gene expression, and in general promote plant growth, development, stress response and defense (Ranty et al. 2006).

CaM is also associated to WRKY family of TF, which was observed 10 unigenes upregulated in treated samples (Table 4), indicating a large role of this Ca^{2+} sensor protein in morphogenesis of *M. glaucescens.*

Potential for the production of secondary metabolites

There has been an increase in the number of studies that explore the advantages of the *in vitro* culture method for the production of secondary metabolites (Batista et al. 2018). *In vitro* tissue culture is well-known to increase the activity of metabolic pathways by improving the nutrition, PGRs, light-inducing, and using elicitors for the target metabolic pathway (Batista et al. 2018). Some cacti are *in vitro* cultured to the production of alkaloids and betalain-type pigments, indicating the potential of these family members to produce bioactive compounds with use in the pharmaceutical and food industries (Vázquez-Flota and Loyola-Vargas 2003, Pérez-Molphe-Balch et al. 2015).

SO-induction affected positively the biosynthetic pathways of phenylpropanoids, flavonoid, flavones and flavonol in *M. glaucescens* (Table 3), and treated samples also exhibited upregulation of many TFs associated with secondary metabolite biosynthesis (i. e. bHLH, MYB, NAC, and WRKY) (Table 4). The biosynthetic pathways that were activated during SO-induction of *M. glaucescens* indicate that this species has potential to producing bioactive compound with a wide range of functions, which can improve the micropropagation of *M. glaucescens* not just to ornamental, but for other commercial purposes.

5. CONCLUSION

In the present study, was described the construction and functional annotation of a *de novo* transcriptome assembly for *M. glaucescens*, a non-model plant with ornamental and medicinal potential. This assembly was used to study tissue-enriched gene expression and it was possible to identify genes related to shoot organogenesis, as well as a large number of genes that encode putative transcription factors. This will benefit future essays on regulation of gene expression in *M. glaucescens*. Altogether, this study expands the existing genomic resources for cacti and provides a new platform for further genetic and biotechnological improvement of cacti for different commercial purposes.

6. ACKNOWLEDGEMENTS

We thank Delmar Lopes Alvim for help during field work, the Boyce Thompson Institute (Ithaca, USA) for providing the server to perform the *de novo* transcriptome assembly, and Specht Lab (Cornell University) for providing the facilities to perform the differential expression analysis.

7. FUNDING

This work was supported by the Conselho Nacional de Desenvolvimento Científico e Tecnológico (CNPq), Fundação de Amparo à Pesquisa do Estado de Minas Gerais (FAPEMIG), and Coordenação de Aperfeiçoamento de Pessoal de Nível Superior (CAPES).

8. REFERENCES

Andrews S. (2010). FastQC: A quality control tool for high throughput sequence data [Internet]. http://www.bioinformatics.babraham.ac.uk/projects/fastqc/

Batista, D.S.; Felipe, S.H.S.; Silva, T.D. et al. (2018). Light quality in plant tissue culture: does it matter? In Vitro Cell Dev Biol Plant, 54(3):195-215. doi: 10.1007/s11627-018-9902-5

Bao, Y.; Dharmawardhana, P.; Mockler, T.C.; Strauss, S.H. (2009). Genome scale transcriptome analysis of shoot organogenesis in *Populus*. BMC Plant Biol, 9:132. doi: 10.1186/1471-2229-9-132

Bolger, A.M.; Lohse, M.; Usadel, B. (2011). Trimmomatic: a flexible trimmer for Illumina sequence data. Bioinformatics, 30(15):2114-2120. doi:10.1093/bioinformatics/btu170

Brereton, N.J.B.; Gonzalez, E.; Marleau, J.; Nissim, W.G.; Labrecque, M.; Joly, S.; Pitre, F.E. (2016). Comparative transcriptomic approaches exploring contamination stress tolerance in *Salix* sp. reveal the importance for a metaorganismal *de novo* assembly approach for nonmodel plants. Plant Physiol, 171:3–24. doi: 10.1104/pp.16.00090

Cervantes-Pérez, S.A.; Espinal-Centeno, A.;Oropeza-Aburto, A.;Caballero-Pérez, J.; Falcon, F.; Aragón-Raygoza, A.; Sánchez-Segura, L.; Herrera-Estrella, L.; Cruz-Hernández, A.; Cruz-Ramírez, A. (2018). Transcriptional profiling of the CAM plant *Agave salmiana* reveals conservation of a genetic program for regeneration. Dev Biol, 442(1):28-39. doi: 10.1016/j.ydbio.2018.04.018

Chakrabarti, M.; Dinkins, R.D.; Hunt, A.G. (2016). *De novo* transcriptome assembly and dynamic spatial gene expression analysis in red clover. Plant Genome, 9(2):1-12. doi: 10.3835/plantgenome2015.06.0048

Cheong, Y.H.; Chang, H.-S.; Gupta, R.; Wang, X.; Zhu, T.; Luan, S. (2002). Transcriptional profiling reveals novel interactions between wounding, pathogen, abiotic stress, and hormonal responses in *Arabidopsis*. Plant Physiol, 129:661-677. doi: 10.1104/pp.002857

CITES (2018).Convention on international trade in endangered species of wild fauna and flora. Apêndice 1. [on line] URL, http: //www.cites.org/eng/app/index.shtml. Accessed in December 20th, 2018.

Conesa, A.; Götz, S. (2007). Blast2GO: A comprehensive suite for functional analysis in plant genomics. Int J Plant Genomics, 2008:619832. doi:10.1155/2008/619832

Davidson, N.; Oshlack, A. (2014). Corset: enabling differential gene expression analysis for *de novo* assembled transcriptomes. Genome Biol, 15:410. doi: 10.1186/s13059-014-0410-6

Dobin, A.; Davis, C.A.; Schlesinger, F.; Drenkow, J.; Zaleski, C.; Jha, S.; Batut, P.; Chaisson, M.; Gingeras, T.R. (2013). STAR: ultrafast universal RNA-seq aligner. Bioinformatics, 29(1):15-21. doi: 10.1093/bioinformatics/bts635

Duclercq, J.; Sangwan-Norreel, B.; Catterou, M.; Sangwan, R.S. (2011). *De novo* shoot organogenesis: from art to science. Trends Plant Sci, 16(11):597-606. doi: 10.1016/j.tplants.2011.08.004

Garg, R.; Jain, M. (2013). RNA-Seq for transcriptome analysis in non-model plants. Methods Mol Biol, 1069:43–58. doi:10.1007/978-1-62703-613-9_4

Goettsch, B., et al. (2015). High proportion of cactus species threatened with extinction. Nat Plants. doi: 10.1038/NPLANTS.2015.142

Grabherr, M. G.; Haas, B.J.; Yassour, M. et al. (2011). Full-length transcriptome assembly from RNA-Seq data without a reference genome. Nature Biotechnol, 29, pages 644-652. doi: 10.1038/nbt.1883

Hardy, T.; Chaumont, D.; Wessinges, M.E.; Bournat, T. (1987). Photoautotrophic suspension cultures II - transition from photoheterotrophic to photoautotrophic growth. J Plant Physiol, 130:351-361. doi: 10.1016/S0176-1617(87)80201-8

Hashimoto, K.; Kudla, J. (2011). Calcium decoding mechanisms in plants. Biochimie 93:2054-2059. doi: 10.1016/j.biochi.2011.05.019

Ikeuchi, M.; Ogawa, Y.; Iwase, A.; Sugimoto, K. (2016). Plant regeneration: cellular origins and molecular mechanisms. Development, 143:1442-1451. doi:10.1242/dev.134668

IUCN (2018).IUCN Red List of Threatened Species.Version 2013.2. [on line] URL, http://www.iucnredlist.org. Accessed in December 20th, 2018.

Iwase, A.; Mita, K; Nonaka, S.; Ikeuchi, M.; Koizuka, C.; Ohnuma, M.; Ezura, H.; Imamura, J.; Sugimot, K. (2015). *WIND1*-based acquisition of regeneration competency in *Arabidopsis* and rapeseed. J Plant Res, 128(3): 389-397. doi: 10.1007/s10265-015-0714-y

Jin, J.P.; Tian, F.; Yang, D.C.; Meng, Y.Q.; Kong, L.; Luo, J.; Gao, G. (2017). PlantTFDB 4.0: toward a central hub for transcription factors and regulatory interactions in plants. Nucleic Acids Res, 45(D1):D1040-D1045. doi: 10.1093/nar/gkw982

Kanehisa, M.; Araki, M.; Goto, S.; Hattori, M.; Hirakawa, M.; Itoh, M.; Katayama, T.; Kawashima, S.; Okuda, S.; Tokimatsu, T.; Yamanishi, Y. (2008). KEGG for linking genomes to life and the environment. Nucleic Acids Res, 36:D480-D484. doi:10.1093/nar/gkm882

Kushwaha, R.; Singh, A.; Chattopadhyay, S. (2008). Calmodulin7 plays an important role as transcriptional regulator in Arabidopsis seedling development. Plant Cell, 20: 1747-1759. doi: 10.1105/tpc.107.057612

Kwon, D.K.; Song, Y.J. (2005) Effect of *Opuntia humifusa* supplementation on endurance exercise performance in rats fed a high-fat diet. Korean J Exer Nutr, 9:183–8.

Lee K.S.; Oh, C.S.; Lee, K.Y. (2005a) Antioxidative effect of the fractions extracted from a cactus Chounyouncho (*Opuntia humifusa*). J Korean Soc Food Sci Nutr, 37:474–8.

Lee, J.L.; Kim, A.; Kopelovich, L.; Bickers. D.R.; Athar. M. (2005b) Differential expression of E prostanoid receptors in murine and human non-melanoma skin cancer. J Invest Dermatol, 125:818–25. doi: 10.1111/j.0022-202X.2005.23829.x

Lee, K.S.; Kim, M.G.; Lee, K.Y. (2004). Antimicrobial effects of the extracts of cactus Cheonnyuncho (*Opuntia humifusa*) against food borne pathogens. J Korean Soc Food Sci Nutr, 33:1268–72.

Lema-Rumińska, J.,Kulus, D. (2014). Micropropagation of cacti – a Review. Haseltonia, 18: 46-63. doi: 10.2985/026.019.0107

Li, W.; Godzik, A. (2006). Cd-hit: a fast program for clustering and comparing large sets of protein or nucleotide sequences. Bioinformatics, 22(13):1658-1659. doi: 10.1093/bioinformatics/btl158

Livak, K.J.; Schmittgen, T.D. (2001). Analysis of relative gene expression data using real-time quantitative PCR and the $2^{-\Delta\Delta CT}$ method. Methods, 25(4):402-408. doi: 10.1006/meth.2001.1262

Machado, M.C. (2009). The genus *Melocactus* in eastern Brazil: part I - an introduction to *Melocactus*. British Cact Succ J, 27:1-16.

Maere, S.; Heymans, K.; Kuiper, M. (2005). BiNGO: a Cytoscape plugin to assess overrepresentation of Gene Ontology categories in Biological Networks. Bioinformatics, 21(16):3448-3449. doi:10.1093/bioinformatics/bti551

Martín-Trillo, Mar.; Cubas, P. (2010). TCP genes: a family snapshot ten years later. Trends Plant Sci, 15(1):31-39. doi: 10.1016/j.tplants.2009.11.003

Murashige, T.; Skoog, F. (1962). A revised medium for rapid growth and bio assays with tobacco tissue cultures. Physiol Plant, 15:473–497. doi:10.1111/j.13993054.1962.tb08052.x

Nadiya, F.; Anjali, N.; Thomas, J.; Gangaprasad, A.; Sabu, K.K. (2018). Genome-wide differential expression profiling in wild and cultivar genotypes of cardamom reveals regulation of key pathways in plant growth and development. Agri Gene, 8:18-27. doi: 10.1016/j.aggene.2018.03.002

Pal, T.; Padhan, J.K.; Kumar, P.; Sood, H.; Chauhan, R.S. (2018). Comparative transcriptomics uncovers differences in photoautotrophic versus photoheterotrophic modes of nutrition in relation to secondary metabolites biosynthesis in *Swertia chirayita*. ol Biol Rep, 45:77–98. doi: nb10.1007/s11033-017-4135-y

Park, M.K.; Lee, Y.J.; Kang, E.S. (2005). Physiological activity/nutrition: hepatoprotective effect of cheonnyuncho (*Opuntia humifusa*) extract in rats treated carbon tetrachloride. Korea J Food Sci Technol, 27:822–6.

Pérez-Molphe-Balch, E.; Santos-Díaz, M.S.; Ramírez-Malagón, R.; Ochoa-Alejo, N. (2015). Tissue culture of ornamental cacti. Sci Agric, 72(6):540–561. doi: 10.1590/0103-9016-2015-0012

Qingzhu, H.; Chengjie, C.; Zhe, C.; Pengkun, C.; Yuewen, M.; Jingyu, W.; Jian, Z.; Guibing, Hu.; Jietang, Z.; Yonghua, Q. (2016). Transcriptomic analysis reveals key genes related to betalain biosynthesis in pulp coloration of *Hylocereus polyrhizus*. Front Plant Sci, 6:1179. doi: 10.3389/fpls.2015.01179

Ranty, B.; Aldon, D.; Galaud, J-P. (2006). Plant calmodulins and calmodulin-related proteins: multifaceted relays to decode calcium signals. Plant Signal Behav, 1(3):96-104. doi: 10.4161/psb.1.3.2998

Robinson, M.D. McCarthy, D.J.; Smyth, G.K. (2010). edgeR: a Bioconductor package for differential expression analysis of digital gene expression data. Bioinformatics, 26(1):139-140: doi:10.1093/bioinformatics/btp616

Rocha, D.I.; Monte-Bello, C.C.; Aizza, L.C.B.; Dornelas, M.C. (2016). A passion fruit putative ortholog of the *SOMATIC EMBRYOGENESIS RECEPTOR KINASE1* gene is expressed throughout the *in vitro de novo* shoot organogenesis developmental program. Plant Cell Tiss Organ Cult, 25(1):107-117. doi: 10.1007/s11240-015-0933-x

Stortenbeker, N.; Bemer, M. (2018). The SAUR gene family: the plant's toolbox for adaptation of growth and development. J Exp Bot, 70(1):17–27. doi:10.1093/jxb/ery332

Sugimoto, K.; Jiao, Y.; Meyerowitz, E.M. (2010). *Arabidopsis* regeneration from multiple tissues occurs via a root development pathway. Dev Cell, 18(3):463-471. doi: 10.1016/j.devcel.2010.02.004

Torres-Silva, G.; Resende, S.V.; Lima-Brito, A.; Bezerra, H.B.; D, de Santana, J.R.F.; Schnadelbach, A.S. (2018). *In vitro* shoot production, morphological alterations and genetic instability of *Melocactus glaucescens* (Cactaceae), an endangered species endemic to eastern Brazil. S Afri J Bot, 115:100–107. doi: 10.1016/j.sajb.2018.01.001

Vázquez-Flota, F.; Loyola-Vargas, V.M. (2003). *In vitro* plant cell cultures as basis for the development of a Research Institute in Mexico: Centro de Investigación Científica de Yacatán. In Vitro Cell Dev Biol Plant, 39:250-258. doi: 10.1079/IVP2002398

Xiao, M.; Zhanga, Y.;Chenc. X.; Lee, E-J. et al. (2013). Transcriptome analysis based on next-generation sequencing of non-model plants producing specialized metabolites of biotechnological interest. J Biotechnol, 166(3):122-134. doi: 10.1016/j.jbiotec.2013.04.004

Xu, L. (2018). *De novo* root organogenesis from leaf explants: wounding, auxin, and cell fate transition. Curr Opin Plant Biol, 41:39-45. doi: 10.1016/j.pbi.2017.08.004

Yoon, J.A.; Hahm, S.; Son, Y.S (2009a). Nutrients contents in different parts of prickly pear (*Opuntia humifusa*) and possible anti-breast cancer effect. Korean J Food Nutr, 22:485–91.

Yoon, J.A.; Hahm, S.W.; Son, Y.S. (2009b) Total polyphenol and flavonoid of fruit extract of *Opuntia humifusa* and its inhibitory effect on the growth of MCF-7 human breast cancer cells. J Korean Soc Food Sci Nutr, 38:1679–84.

Zeng, H.; Xu, L.; Singh, A.; Wang, H.; Du, L.; Poovaiah, B.W. (2015). Involvement of calmodulin and calmodulin-like proteins in plant responses to abiotic stresses. Front Plant Sci, 6:600. doi: 10.3389/fpls.2015.00600

Zhao, X.Y.; Su, Y.H.; Cheng, Z.J.; Zhang, X.S. (2008). Cell fate switch during in vitro plant organogenesis. J Integr Plant Biol, 50(7):816-824. doi: 10.1111/j.1744-7909.2008.00701.x

9. TABLES, FIGURES AND LEGENDS

Table 1. Sequences of the primers used to validate the differential expression of *Melocactus glaucescens* transcriptome.

Primers	Sequence
Glyceraldehyde-3-phosphate dehydrogenase	
Foward	5'- AAGGTCCAAGTAGCAAGGGC– 3'
Reverse	5' - TGCACCGATGTCTCTTCCAC– 3'
Calmodulin	
Foward	5'- AAGGGTGGACAAAGGCGAAT– 3'
Reverse	5' - CCTCCAGGTACATCGGAAACC– 3'

Table 2. Raw data and assembly statistics for transcriptomes from *Melocactus glaucescens* explants before (control) and after (treated) shoot organogenesis induction.

Description	**Control**	**Treated**
Raw data statistics		
Total number of raw reads	11,778,019	13,371,985
Clean Reads	4,712,559	5,433,394
Clean Bases (Mb)	1.18	6.63
Assembly statistics		
Number of transcripts	2,231	12,247
Total transcript length (bp)	1,180,871	6,626,929
Transcript N50	527	513
Max transcript size (bp)	7,366	7,403
Mean transcript size (bp)	527	513
Min transcript size (bp)	201	201
GC content (%)	55	54
Unigenes with significant BLAST hits	1,447	1,796
Unigenes without significant BLAST hits	20	36

Table 3. KEGG metabolic pathways categories in differential expressed unigenes of *Melocactus glaucescens* explants before (control) and after (treated) shoot organogenesis induction. *indicates the same transcript in both treatments.

Metabolic pathway	Treated	Control	Unigene shared in the pathway
Glycolysis / Gluconeogenesis	6	1	Fructose-bisphosphate aldolase, class I
Citrate cycle (TCA cycle)	3		
Pentose phosphate pathway	1	1	Fructose-bisphosphate aldolase, class I
Pentose and glucuronate interconversions	3	1*	
Fructose and mannose metabolism	2	1* and 1	Fructose-bisphosphate aldolase, class I
Galactose metabolism	1		
Ascorbate and aldarate metabolism	3		
Fatty acid biosynthesis	1	1	Acetyl-CoA carboxylase / biotin carboxylase 1
Fatty acid elongation	1		
Fatty acid degradation	5		
Steroid biosynthesis	4		
Ubiquinone and other terpenoid-quinone biosynthesis	1		
Oxidative phosphorylation	9	1* and 5	F-type H^+-transporting ATPase subunit a
Photosynthesis		15	
Photosynthesis - antenna proteins		5	
Arginine biosynthesis	1		
Purine metabolism	3		
Pyrimidine metabolism	1	1*	
Alanine, aspartate and glutamate metabolism	1	1*	
Glycine, serine and threonine metabolism	4	3*	
Cysteine and methionine metabolism	4		
Valine, leucine and isoleucine degradation	3		
Lysine degradation	1		
Arginine and proline metabolism	2		
Histidine metabolism	2		
Tyrosine metabolism	1	1*	

Phenylalanine metabolism	2	1*	
Tryptophan metabolism	2	1*	
Phenylalanine, tyrosine and tryptophan biosynthesis	2		
beta-Alanine metabolism	2		
Selenocompound metabolism	1		
Cyanoamino acid metabolism	1		
D-Glutamine and D-glutamate metabolism	1		
Glutathione metabolism	5	1	Glutathione S-transferase
Starch and sucrose metabolism	5		
Amino sugar and nucleotide sugar metabolism	5		
Streptomycin biosynthesis	1		
Glycerolipid metabolism	1	1*	
Inositol phosphate metabolism	3		
Glycerophospholipid metabolism	2	1*	
Ether lipid metabolism	2	1*	
Arachidonic acid metabolism		1	
Linoleic acid metabolism		1	
alpha-Linolenic acid metabolism	4	1*	
Sphingolipid metabolism	2		
Pyruvate metabolism	6	1	Acetyl-CoA carboxylase / biotin carboxylase 1
Chloroalkane and chloroalkene degradation	1		
Glyoxylate and dicarboxylate metabolism	3	1* and 3	Glycine dehydrogenase
Propanoate metabolism	3	1	Acetyl-CoA carboxylase / biotin carboxylase 1
One carbon pool by folate	1	1*	
Methane metabolism	3	1* and 1	Fructose-bisphosphate aldolase, class I
Carbon fixation in photosynthetic organisms	3	1* and 1	Fructose-bisphosphate aldolase, class I
Carbon fixation pathways in prokaryotes	5	1	Acetyl-CoA carboxylase / biotin carboxylase 1
Riboflavin metabolism	1		
Vitamin B6 metabolism	1		
Folate biosynthesis		1	

Limonene and pinene degradation	1		
Sesquiterpenoid and triterpenoid biosynthesis	1		
Nitrogen metabolism	3		
Sulfur metabolism	2		
Phenylpropanoid biosynthesis	6		
Flavonoid biosynthesis	3		
Flavone and flavonol biosynthesis	1		
Stilbenoid, diarylheptanoid and gingerol biosynthesis	1		
Metabolism of xenobiotics by cytochrome P450	1	1	Glutathione S-transferase
Insect hormone biosynthesis	1		
Drug metabolism - cytochrome P450	2	1	Glutathione S-transferase
Drug metabolism - other enzymes	2	1	Glutathione S-transferase
Biosynthesis of unsaturated fatty acids	2		
EGFR tyrosine kinase inhibitor resistance	3		
Antifolate resistance	1		
Platinum drug resistance	2	2	Solute carrier family 31 and Glutathione S-transferase
Quorum sensing	3		
Biofilm formation - Escherichia coli	1		
Ribosome	15	5*	
RNA transport	9		
mRNA surveillance pathway	2		
RNA degradation	1		
Spliceosome	10		
Proteasome	6		
Protein export	2		
PPAR signaling pathway	3		
MAPK signaling pathway	1		
MAPK signaling pathway - yeast	3		
MAPK signaling pathway - fly	1		
Ras signaling pathway	4	1*	

Rap1 signaling pathway	1		
MAPK signaling pathway - plant	8		
Calcium signaling pathway	2		
cGMP-PKG signaling pathway	2		
cAMP signaling pathway	3		
Chemokine signaling pathway	1		
HIF-1 signaling pathway	2		
FoxO signaling pathway	5		
Phosphatidylinositol signaling system	2		
Sphingolipid signaling pathway	4		
Phospholipase D signaling pathway	1	1*	
Plant hormone signal transduction	9	1	Small auxin upregulated RNAs
Cell cycle	3		
Cell cycle - yeast	2		
Meiosis - yeast	1		
Oocyte meiosis	4		
p53 signaling pathway	2		
Ubiquitin mediated proteolysis	5	1*	
Sulfur relay system	1		
Autophagy - animal	2		
Protein processing in endoplasmic reticulum	11	2*	
Lysosome	6	1	ATPeV
Endocytosis	5	1*	
Phagosome	9	2* and 1	v-ATPase and Tubulin alpha
Peroxisome	5	1* and 1	Superoxide dismutase
mTOR signaling pathway	7		
PI3K-Akt signaling pathway	8		
AMPK signaling pathway	2		
Apoptosis	4	1	Tubulin alpha
Longevity regulating pathway	3		

Longevity regulating pathway - worm	3		
Longevity regulating pathway - multiple species	3	1	Superoxide dismutase
Necroptosis	6		
Cellular senescence	4		
Cardiac muscle contraction		2	
Adrenergic signaling in cardiomyocytes	2		
Vascular smooth muscle contraction	1	1*	
Wnt signaling pathway		1	
Notch signaling pathway	1	1*	
TGF-beta signaling pathway	1		
Axon guidance	2		
Apelin signaling pathway	3		
Osteoclast differentiation	1		
Hippo signaling pathway	1		
Hippo signaling pathway - fly	3		
Hippo signaling pathway - multiple species	1		
Focal adhesion	1		
Tight junction	2	1	Tubulin alpha
Gap junction	1	1	Tubulin alpha
Antigen processing and presentation	6		
NOD-like receptor signaling pathway	2		
C-type lectin receptor signaling pathway	1		
Plant-pathogen interaction	4	1	Calmodulin
IL-17 signaling pathway	1		
Th17 cell differentiation	1		
Fc gamma R-mediated phagocytosis	2		
Circadian rhythm - plant	3	1*	
Circadian entrainment	2		
Thermogenesis	5	2	NADH-ubiquinone oxidoreductase chain 1
Long-term potentiation	1		

Synaptic vesicle cycle	4	2	ATPase
Neurotrophin signaling pathway	2	1*	
Retrograde endocannabinoid signaling	4		
Glutamatergic synapse	2		
Cholinergic synapse	1		
Serotonergic synapse	1		
GABAergic synapse	1		
Dopaminergic synapse	3		
Long-term depression	1		
Olfactory transduction	2		
Phototransduction	2		
Phototransduction - fly	1		
Inflammatory mediator regulation of TRP channels	1		
Regulation of actin cytoskeleton	2		
Insulin signaling pathway	3		
GnRH signaling pathway	2		
Progesterone-mediated oocyte maturation	2		
Estrogen signaling pathway	3		
Melanogenesis	1		
Thyroid hormone synthesis	1		
Thyroid hormone signaling pathway	1		
Oxytocin signaling pathway	2		
Glucagon signaling pathway	2		
Renin secretion	2		
Aldosterone synthesis and secretion	1		
Relaxin signaling pathway	1		
Parathyroid hormone synthesis, secretion and action	1		
Type II diabetes mellitus	1		
Insulin resistance	1		
Non-alcoholic fatty liver disease (NAFLD)	3	2*	

Cushing syndrome	1		
Vasopressin-regulated water reabsorption	1		
Proximal tubule bicarbonate reclamation	1		
Collecting duct acid secretion	4	2	ATPase
Salivary secretion	1		
Gastric acid secretion	1		
Pancreatic secretion		1	
Fat digestion and absorption		1	
Mineral absorption	2	1	Solute carrier family 31
Alzheimer disease	5	3*	
Parkinson disease	6	3*	
Amyotrophic lateral sclerosis (ALS)	1		
Huntington disease	6	3*	
Prion diseases		1	
Amphetamine addiction	1		
Morphine addiction	1		
Alcoholism	5		
Vibrio cholerae infection	5	1* and 2	ATPeV
Epithelial cell signaling in Helicobacter pylori infection	4	2	ATPeV
Pathogenic Escherichia coli infection	2	1	Tubulin alpha
Pertussis	2		
Legionellosis	3	1*	
Chagas disease (American trypanosomiasis)	2		
Toxoplasmosis	2		
Amoebiasis	1		
Tuberculosis	3	1	v-ATPase
Hepatitis C	3		
Hepatitis B	2		
Measles	2		

Human cytomegalovirus infection	3		
Influenza A	1		
Human papillomavirus infection	8	1* and 2	v-ATPase
Human T-cell leukemia virus 1 infection	6		
Kaposi sarcoma-associated herpesvirus infection	2		
Herpes simplex infection	4		
Epstein-Barr virus infection	7		
Human immunodeficiency virus 1 infection	4		
Pathways in cancer	7	1	Glutathione S-transferase
Transcriptional misregulation in cancer	2		
Viral carcinogenesis	9		
Chemical carcinogenesis	1	1	Glutathione S-transferase
Proteoglycans in cancer	2		
MicroRNAs in cancer	1		
Endometrial cancer	1		
Glioma	2		
Prostate cancer	3		
Melanoma	1		
Small cell lung cancer	3		
Breast cancer	1		
Hepatocellular carcinoma	2	1	Glutathione S-transferase
Gastric cancer	1		
Choline metabolism in cancer	1		
Systemic lupus erythematosus	3		
Rheumatoid arthritis	5	1* and 1	ATPase
Viral myocarditis	1		
Fluid shear stress and atherosclerosis	3	1	Glutathione S-transferase
Central carbon metabolism in cancer	2		

Table 4. Transcription factors families in differential expressed unigenes of *Melocactus glaucescens* explants before (control) and after (treated) shoot organogenesis induction.

Transcription factor family	Domain	No. of unigenes	
		Control	Treated
ERF family protein	AP2	2	7
AP2 family protein	AP2	1	0
Dof family protein	zf-Dof	0	4
LBD family protein	DUF260	5	11
ARF family protein	B3 and auxin response	1	5
B3 family protein	B3	0	2
LSD family protein	zf-LSD1	2	2
G2-like family protein	G2-like	2	3
GRAS family protein	GRAS	1	3
HD-ZIP family protein	Homeobox	0	1
HB-other family protein	Homeobox	4	5
TALE family protein	Homeobox	0	3
C3H family protein	zf-CCCH	3	17
NAC family protein	NAM	1	5
bZIP family protein	bZIP_1	4	2
WRKY family protein	WRKY	0	10
MYB family protein	Myb_DNA-binding	1	4
MYB_related family protein	Myb_DNA-binding	0	4
bHLH family protein	HLH	4	3
EIL family protein	EIN3	0	2
HSF family protein	HSF_DNA-bind	1	7
C2H2 family protein	zf-C2H2	3	8
Trihelix family protein	Trihelix	0	5
GATA family protein	GATA	0	2
E2F/DP family protein	E2F_TDP	0	2
CAMTA family protein	CG-1	0	1
NF-YC family protein	NF-YC	0	1
NF-YA family protein	CBFB_NFYA	1	0
NF-X1 family protein	zf-NF-X1	3	1
ZF-HD family protein	ZF-HD_dimer	1	0
SBP family protein	SBP	0	1
YABBY family protein	YABBY	0	1
FAR1 family protein	FAR1	0	1
CO-like family protein	zf-B_box and CCT	1	1
MIKC_MADS family protein	SRF-TF and K-box	0	1
GRF family protein	WRC and QLQ	1	0
S1Fa-like family protein	S1FA	1	0
TCP family protein	TCP	5	0
DBB family protein	zf-B_box	1	0

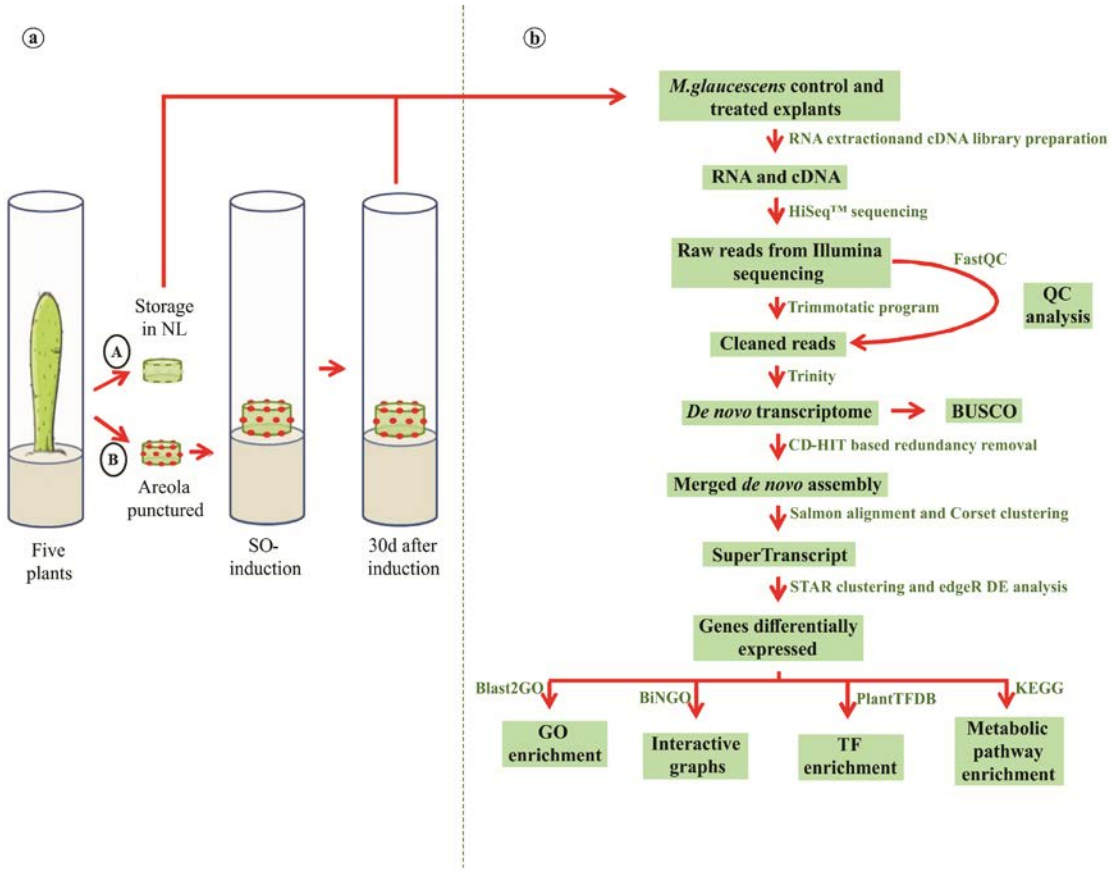

Figure 1. *Melocactus glaucescens* tissues used for transcriptome analysis and work flow of transcriptome assembly and characterization. **a.** Five tissues of *M. glaucescens* used for the RNA extraction, cDNA libraries preparation, and RNA-sequencing; (**A**) the explant was stocked on liquid nitrogen immediately after excision (control); (**B**) the explant wich had its areola regions punctured three times with 0.18 x 8 mm needles was placed on MS full-strength media supplemented with 17.76 µM of benzyladenine and 1.34 µM of ∞-naphthalene acetic acid to shoot organogenesis (SO)-induction for 30 days (treated). **b.** Transcriptome analyzes pipeline and strategy used for *de novo* transcriptome assembly and characterization.

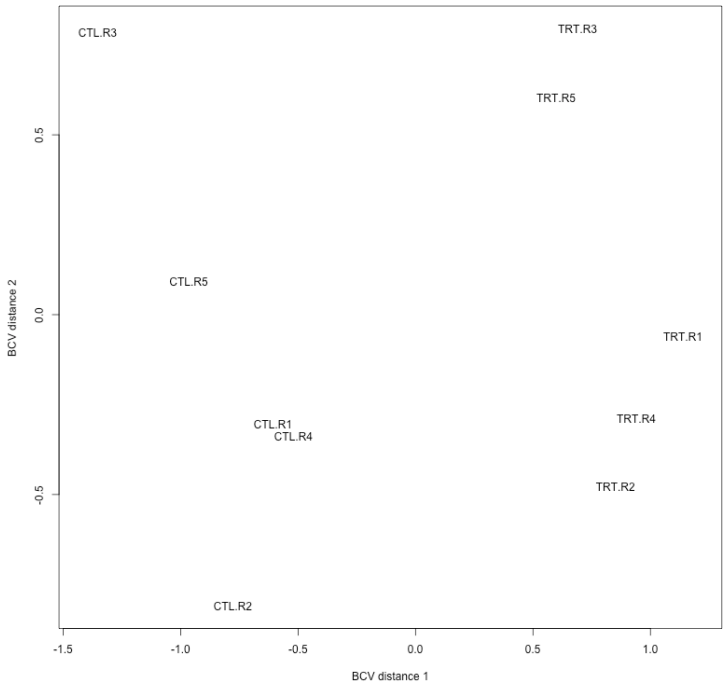

Figure 2. Relationship between *Melocactus glaucescens* explants before (CTL) and after (TRT) shoot organogenesis induction on multidimensional scaling. In the plot, the biological coefficient of variation (BCV) dimension 1 separates control and treated samples. BVC dimension 2 separates the genotypes, where control and treated samples from plants 3 and 5 are localized up, and control and treated samples from plants 1, 2 and 4 are localized down the plot.

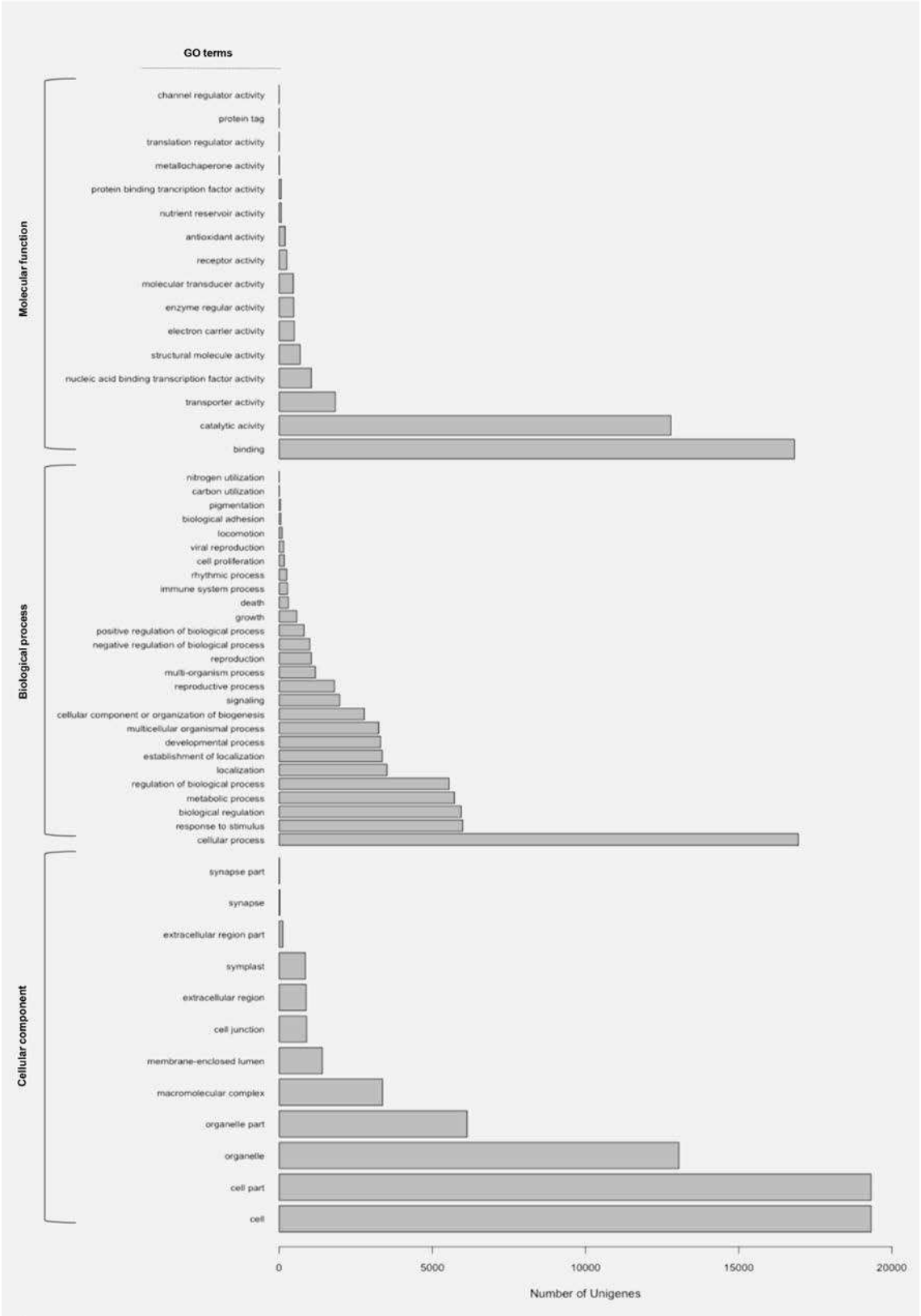

Figure 3. Gene Ontology annotation for all assembled unigenes in the *Melocactus glaucescens* transcriptome.

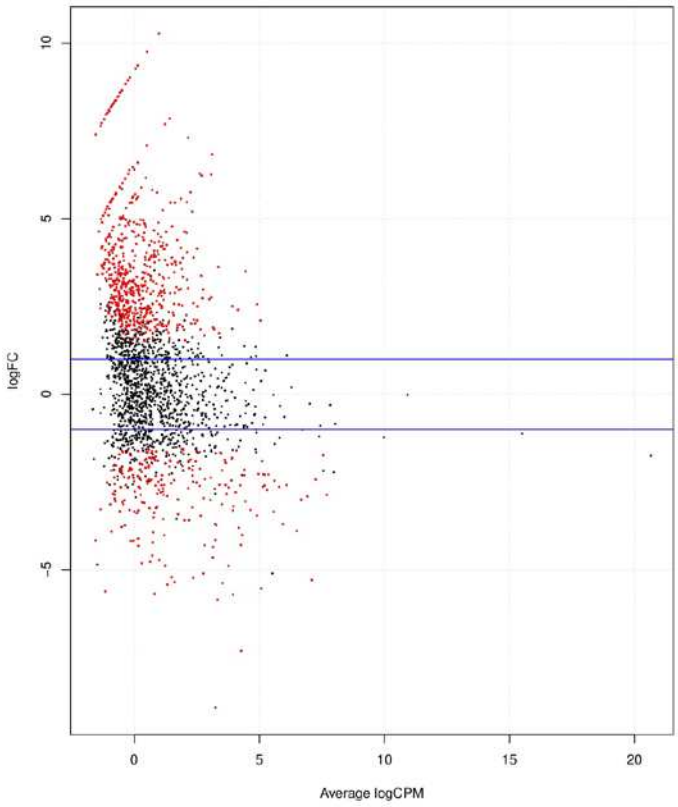

Figure 4. Differentially expressed genes in the pairwise *Melocactus glaucescens* explants after shoot organogenesis (SO)-induction (treated) vs. before SO-induction (control). Blue lines indicate genes with no significant changes in expression; red points indicate genes with a significantly different expression at a false discovery rate (FDR) of $P<0.001$. FC, fold change; CPM, counts per million mapped reads.

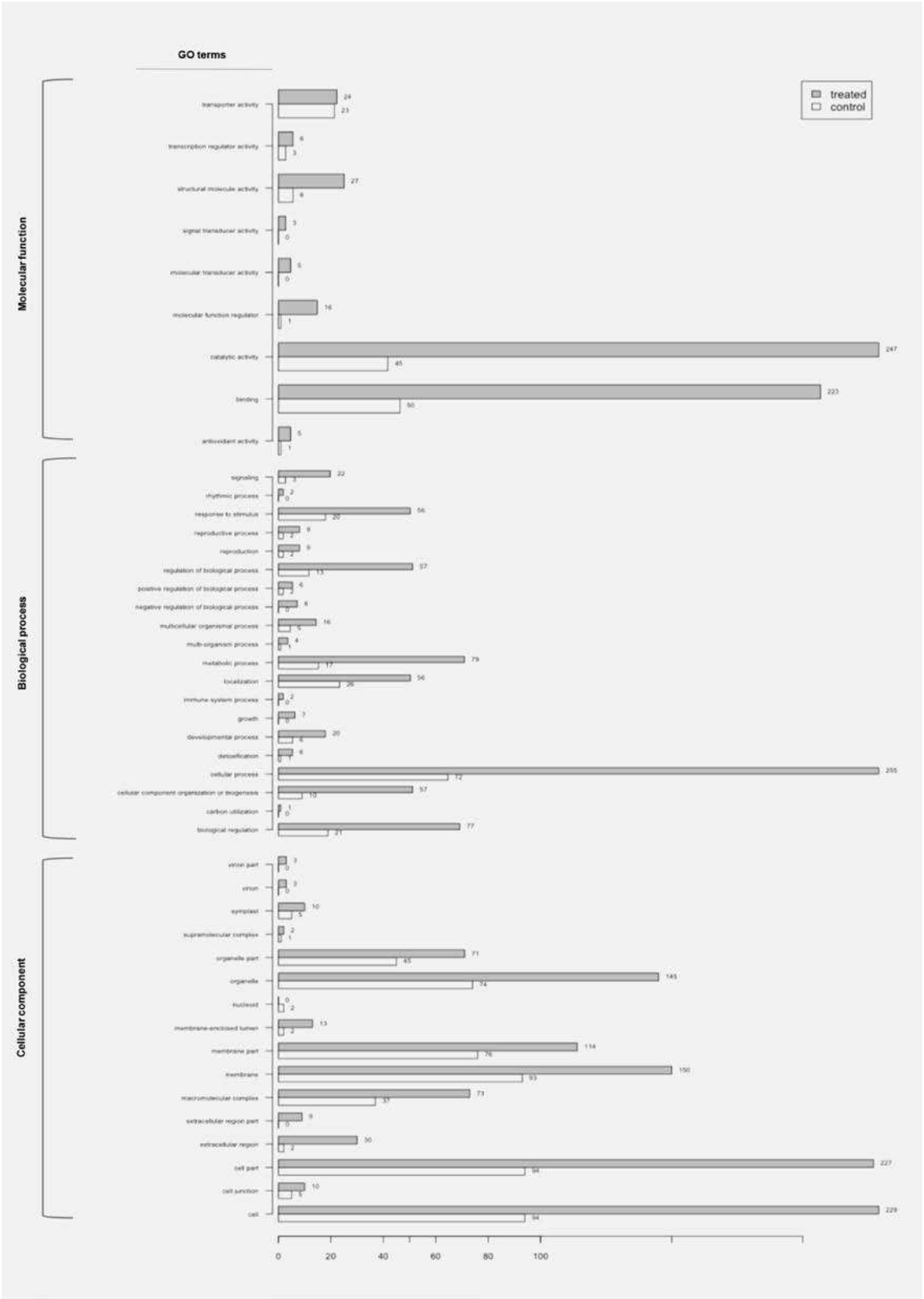

Figure 5. Gene Ontology functional profile comparing transcripts of *Melocactus glaucescens* explants before (control) and after (treated) shoot organogenesis induction.

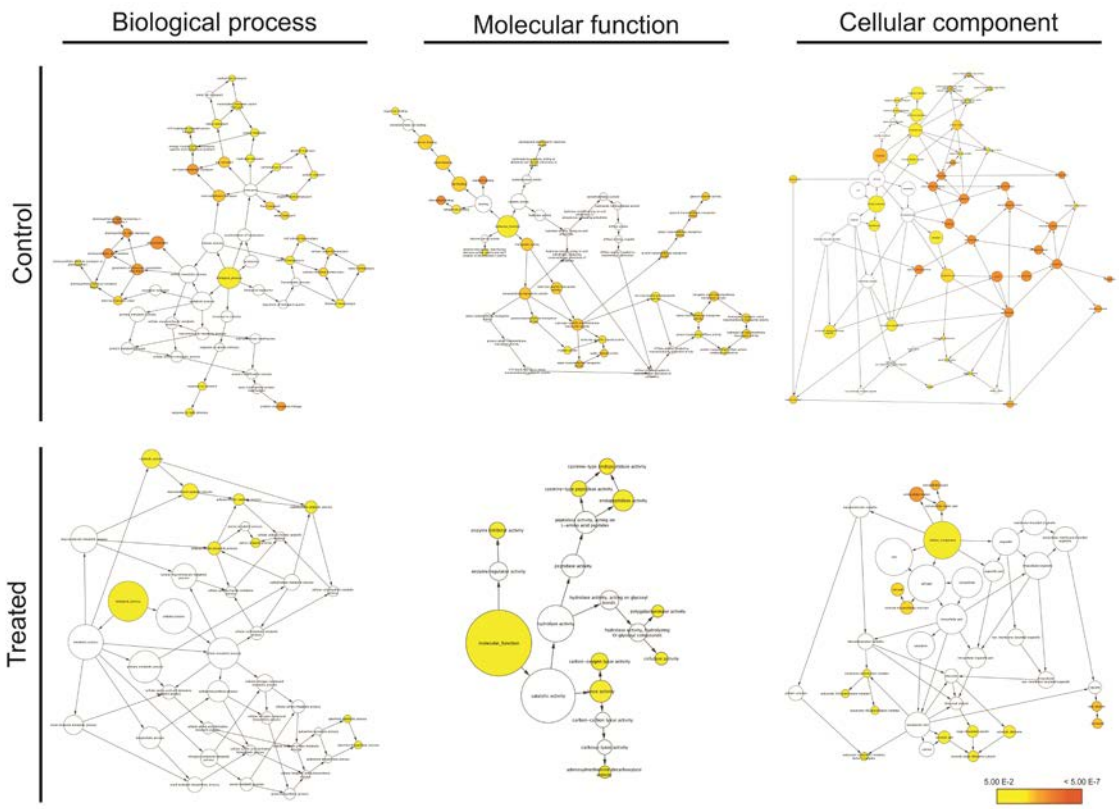

Figure 6. Gene networks developed using the Gene Ontology (GO) categories in BiNGO for differentially expressed genes of *Melocactus glaucescens* explants before (control) and after (treated) shoot organogenesis induction. Bubble size and color indicate the frequency of the GO term and the P value, respectively.

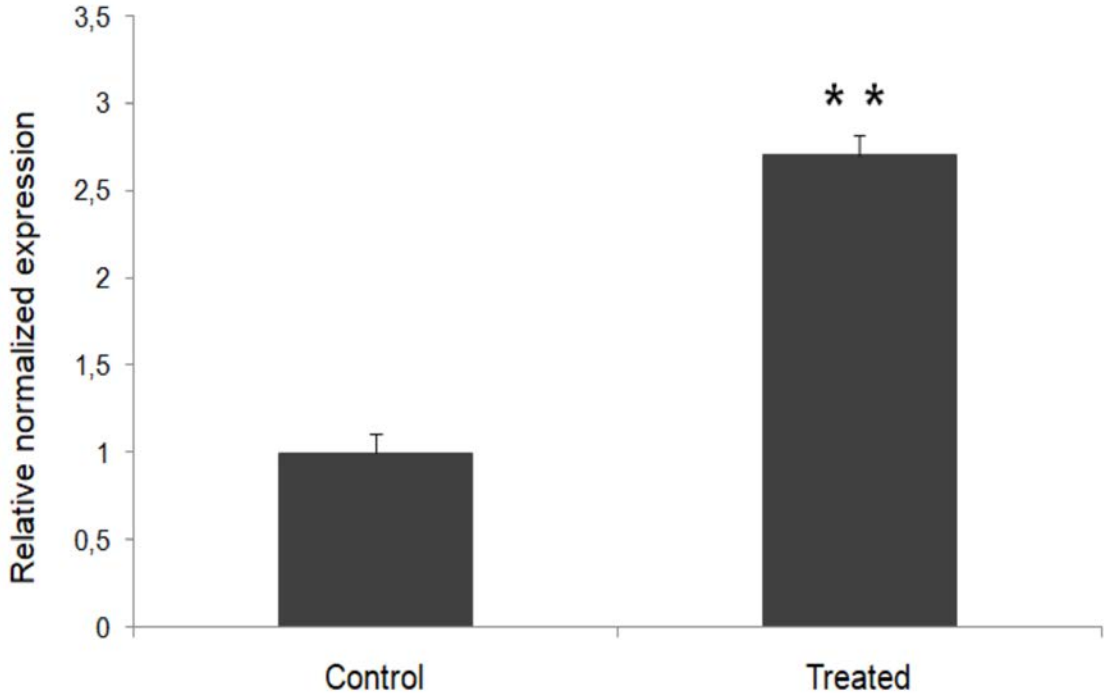

Figure 7. Expression profile obtained by real time RT-qPCR of *calmodulin* gene in *Melocactus glaucescens* explants before (control) and after (treated) shoot organogenesis induction.

CONCLUSÕES GERAIS

1. Os cladódios de *Melocactus glaucescens* e *M. paucispinus* são mixoploides;
2. A mixoploidia dos cladódios é atribuida ao programa de formação dos diferentes tecidos que compõem o organismo, os quais possuem uma das principais funções para a sobrevivência dessas plantas, o armazenamento de água;
3. Em *M. glaucescens,* a formação dos brotos ocorre oriunda da ativação da região meristemática das aréolas, bem como de regiões internas do cladódio;
4. O aumento de quase 4x do número de brotos por explante é possível com a adição de regulador de crescimento no meio de cultura e ferimento da região da aréola;
5. Esta é a primeira descrição do gene *SERK* de um membro da família Cactaceae, e a expressão de *MgSERK*-like está relacionada à organogênese de brotos e raízes;
6. Este é o primeiro transcriptoma que explora as mudanças ocorridas na regeneração *in vitro* de um membro da família Cactaceae;
7. O transcriptoma de *M. glaucescens* é uma nova plataforma para futuros trabalhos com o objetivo de melhorar programas genéticos e biotecnológicos de cactos com diferentes finalidades comerciais.